

Stz. (36)

DEC 22 1994 (67)

ENGINEERING DATA TRANSMITTAL

Page 1 of 1  
1. EDT 605514

2. To: (Receiving Organization) Distribution	3. From: (Originating Organization) Thermal & Fluid Mechanics Engineering	4. Related EDT No.: N/A
5. Proj./Prog./Dept./Div.: MWTF	6. Cog. Engr.: B. A. Crea	7. Purchase Order No.: N/A
8. Originator Remarks:		9. Equip./Component No.: N/A
		10. System/Bldg./Facility: N/A
11. Receiver Remarks:		12. Major Assm. Dwg. No.: N/A
		13. Permit/Permit Application No.: N/A
		14. Required Response Date: October 21, 1994

15. DATA TRANSMITTED					(F)	(G)	(H)	(I)
(A) Item No.	(B) Document/Drawing No.	(C) Sheet No.	(D) Rev. No.	(E) Title or Description of Data Transmitted	Impact Level	Reason for Trans- mittal	Orig- inator Dispo- sition	Receiv- er Dispo- sition
1	WHC-SD-W236A-ER-009		0	Results from Evaporation Tests to Support the MWTF Heat Removal System Design	Q	1		

16. KEY		
Impact Level (F)	Reason for Transmittal (G)	Disposition (H) & (I)
1, 2, 3, or 4 (see MRP 5.43)	1. Approval 2. Release 3. Information 4. Review 5. Post-Review 6. Dist. (Receipt Acknow. Required)	1. Approved 2. Approved w/comment 3. Disapproved w/comment 4. Reviewed no/comment 5. Reviewed w/comment 6. Receipt acknowledged

17. SIGNATURE/DISTRIBUTION (See Impact Level for required signatures)													
(G)	(H)	(J) Name (K) Signature (L) Date (M) MSIN				(J) Name (K) Signature (L) Date (M) MSIN				(G)	(H)		
Reason	Disp.	(J) Name		(K) Signature	(L) Date	(M) MSIN	(J) Name		(K) Signature	(L) Date	(M) MSIN	Reason	Disp.
1	1	Cog. Eng. B. A. Crea		<i>B. A. Crea</i>	10/21/94		Central Files (2)		<i>T. B. McCall</i>	10/24/94		18-04	
1	1	Cog. Mgr. T. B. McCall		<i>T. B. McCall</i>	10/24/94		OSTI (2)		<i>A. K. Sharma</i>	11/30/94		18-07	
1	1	QA A. K. Sharma		<i>A. K. Sharma</i>	11/30/94								
		Safety											
		Env.											
1		S. K. Farnworth		<i>S. K. Farnworth</i>	12/20/94								
1		M. D. Stine		<i>M. D. Stine</i>	12/15/94								

18. Signature of EDT Originator <i>B. A. Crea</i> Date: 10/21/94	19. Authorized Representative for Receiving Organization <i>J. M. V. [Signature]</i> Date: 12-20-94	20. Cognizant/Project Engineer's Manager <i>T. B. McCall</i> Date: 10/24/94	21. DOE APPROVAL (if required) Ltr. No. <input type="checkbox"/> Approved <input type="checkbox"/> Approved w/comments <input type="checkbox"/> Disapproved w/comments
--	---	---	--

BD-7400-172-2 (07/91) GEF097

## **DISCLAIMER**

**Portions of this document may be illegible in electronic image products. Images are produced from the best available original document.**

## RELEASE AUTHORIZATION

**Document Number:** WHC-SD-W236A-ER-009, Rev. 0

**Document Title:** Results from Evaporation Tests to Support the MWTF Heat Removal System Design

**Release Date:** 12/21/94

This document was reviewed following the procedures described in WHC-CM-3-4 and is:

**APPROVED FOR PUBLIC RELEASE**

**WHC Information Release Administration Specialist:**

*V. L. Birkland*

12/21/94

V. L. Birkland

TRADEMARK DISCLAIMER. Reference herein to any specific commercial product, process, or service by trade name, trademark, manufacturer, or otherwise, does not necessarily constitute or imply its endorsement, recommendation, or favoring by the United States Government or any agency thereof or its contractors or subcontractors.

This report has been reproduced from the best available copy. Available in paper copy and microfiche. Printed in the United States of America. Available to the U.S. Department of Energy and its contractors from:

U.S. Department of Energy  
Office of Scientific and Technical Information (OSTI)  
P.O. Box 62  
Oak Ridge, TN 37831  
Telephone: (615) 576-8401


Available to the public from: U.S. Department of Commerce  
National Technical Information Service (NTIS)  
5285 Port Royal Road  
Springfield, VA 22161  
Telephone: (703) 487-4650

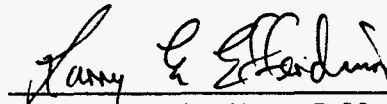
SUPPORTING DOCUMENT		1. Total Pages 101
2. Title Results from Evaporation Tests to Support the MWTF Heat Removal System Design	3. Number WHC-SD-W236A-ER-009	4. Rev No. 0
5. Key Words evaporation, cooling, waste tank, MWTF, test, ventilation system	6. Author Name: B. A. Crea <i>B. A. Crea</i> Signature Organization/Charge Code 71410/DTTC6	
7. Abstract An experimental test program was conducted to measure the evaporative heat removal from the surface of a tank of simulated waste. The results contained in this report constitute definition design data for the latest heat removal function of the MWTF primary ventilation system.  <p style="text-align: center;"><b>DISCLAIMER</b></p> <p>This report was prepared as an account of work sponsored by an agency of the United States Government. Neither the United States Government nor any agency thereof, nor any of their employees, makes any warranty, express or implied, or assumes any legal liability or responsibility for the accuracy, completeness, or usefulness of any information, apparatus, product, or process disclosed, or represents that its use would not infringe privately owned rights. Reference herein to any specific commercial product, process, or service by trade name, trademark, manufacturer, or otherwise does not necessarily constitute or imply its endorsement, recommendation, or favoring by the United States Government or any agency thereof. The views and opinions of authors expressed herein do not necessarily state or reflect those of the United States Government or any agency thereof.</p>		
		8. RELEASE STAMP <div style="border: 1px solid black; padding: 5px; text-align: center;"><p>OFFICIAL RELEASE BY W-236A IMT DEC 22 1994 DATE STATION (36) CLERK (67)</p></div>




**RESULTS FROM EVAPORATION TESTS TO SUPPORT THE MWTF  
HEAT REMOVAL SYSTEM DESIGN**

November 23, 1994

Prepared by:   
Blaine A. Crea, Principal Engineer  
Thermal & Fluid Mechanics Engineering

Reviewed by:   
Larry E. Efferding, Fellow Engineer  
Thermal & Fluid Mechanics Engineering

Approved by:   
T. B. McCall, Manager  
Thermal & Fluid Mechanics Engineering

Issued by  
WESTINGHOUSE HANFORD COMPANY  
for the

U.S. DEPARTMENT OF ENERGY  
RICHLAND FIELD OFFICE  
RICHLAND, WASHINGTON

**Table of Contents**

1.0	Introduction . . . . .	1
1.1	Scope . . . . .	1
1.2	Background . . . . .	1
2.0	Conclusion . . . . .	1
3.0	System Description . . . . .	2
3.1	Test Tank . . . . .	2
3.2	Instrumentation and Control System . . . . .	4
3.3	Makeup Water Control and Measurement System . . . . .	5
3.4	Test Fluids . . . . .	7
4.0	Test Procedure . . . . .	8
5.0	Results . . . . .	10

**List of Figures**

Figure 1.	Fabrication Sketch of Tank . . . . .	3
Figure 2.	Test Tank prior to Installation in Test Facility. . . . .	4
Figure 3.	Schematic Diagram of Test Facility. . . . .	5
Figure 4.	Solution Vapor Pressures . . . . .	8
Figure 5.	Test Results Compared to Correlations . . . . .	12
Figure 6.	Recommended Design Values for MWTF . . . . .	13

**List of Tables**

Table 1.	Original Test Matrix . . . . .	9
Table 2.	Test Results in Chronological Order. . . . .	14

**Appendices**

A.	Vapor Pressure Measurements of Test Solutions . . . . .	A-i
B.	Instrument List . . . . .	B-i
C.	Test Data . . . . .	C-i
D.	Vapor Pressure Experiment on MWTF Surrogate Solution . . . . .	D-i
E.	Literature Review . . . . .	E-i
F.	Scaling Discussion . . . . .	F-i

RESULTS FROM EVAPORATION TESTS TO SUPPORT THE MWTF  
HEAT REMOVAL SYSTEM DESIGN

## 1.0 Introduction

### 1.1 Scope

The objective of this test program was to provide design data for the Multi-Function Waste Tank Facility (MWTF) vapor space heat removal system. These tests will also provide reliable data for evaporation evaluation for a wide range of waste temperature and air flows. This investigation was conducted based on a test plan prepared as impact level Q (Reference 1) and the results contained herein have been assigned the same impact level.

### 1.2 Background

The current design of the MWTF primary tank ventilation system includes a continuous flow of air through the vapor space above the liquid waste. This flow of air has multiple uses. One use is to maintain a negative pressure in the dome space so that any vapors or aerosols that are derived from the waste can be passed through a filter bank before they are released to the environment. Another use of this airflow is a net removal of sensible heat from the dome space if the temperature of the waste exceeds the mean inlet air temperature. In addition, this air flow will remove potentially harmful (explosive or corrosive) vapors from the vapor space which also ensures that any water vapor evolved from the waste through evaporation will be swept out also. The removal of this water vapor is an important part of the cooling process for the tank.

A dependable calculation of the evaporative heat removal in the vapor space has proven to be an elusive item. Several calculational methodologies based on the approach recommended in Reference 6 as well as the results in Appendix A and B of Reference 7 have been used, but the answers provided via these means have significant discrepancies between them. A review of the literature associated with this subject has shown that there is no directly applicable test data in existence. A summary of that review is included as Appendix E. Therefore, a scale test to determine the evaporative heat removal was a necessary and cost-effective task to accurately specify the heat removal system requirements for the MWTF design.

The test has been designed so that when a scale factor of unity is applied to the heat flux results the design data will be conservative for the full-scale MWTF. Appendix F contains a detailed discussion of the scaling issues associated with transferring the test data to the full size MWTF.

## 2.0 Conclusion

The evaporative heat removal function of the vapor space ventilation system for the MWTF is capable of removing 547,000 Btu/hr at the flow rate of 500 scfm, with design basis inlet conditions (77 °F inlet temperature and .004 lbm H<sub>2</sub>O/lbm air) when the waste temperature is 190 °F. This value is based on the results

presented in Figure 6. Data has been developed to predict evaporation heat removal rates for the waste temperature range of 90 - 200 °F and air flow rates of 300 - 1000 scfm.

### 3.0 System Description

The MWTF heat removal system has three independent heat removal mechanisms. There is a ventilation system for the tank annulus that removes only sensible heat. There is a ventilation system for the dome that removes both sensible and latent heat from the waste. This test system is a model of the dome space ventilation system, with special emphasis placed on evaluating the latent heat removal capabilities of this ventilation system. Because the depth of the liquid is irrelevant to the test, only a minimal liquid depth was used for practical requirements of facility operation. One test with water was conducted with a liquid depth scaled to the maximum freeboard value for MWTF to evaluate whether there was any significant change in heat removal capabilities at the minimum allowable headspace.

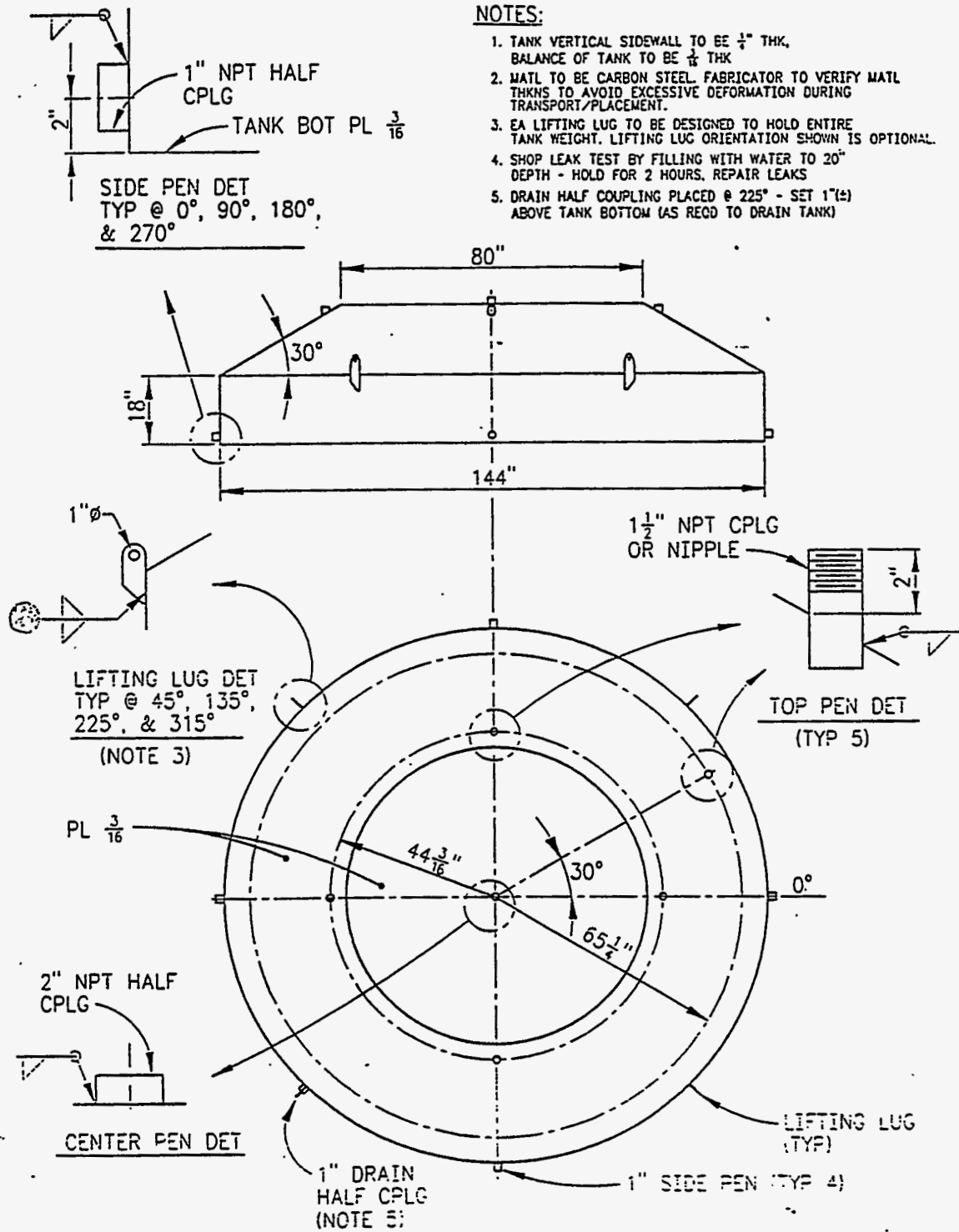
#### 3.1 Test Tank

The test article itself is a welded steel tank. Figure 1 is a dimensioned sketch of the tank. The tank has a shallow truncated cone top designed to be as geometrically similar as possible to the ellipsoidal section head that the MWTF will utilize. It is designed to give a scaled dome similar to the MWTF at the 1,000,000 gallon level when filled with 6 inches of simulated waste. Figure 2 is a photo of the tank prior to installation.

When installed the tank was placed on a 1 1/2" thick layer of styrofoam insulation and covered with a 1 inch thick layer of flexible rubber insulation. The insulation had two functions. The most important function was to act as a guard so that the temperature of exterior surface of the vessel was reduced below the point where it would burn someone who inadvertently came into contact with it. The other function was to reduce heat loss to the environment. The test setup had a loss to the environment of 2 - 3 Kw when operating at 190 °F exclusive of the heat removal that resulted from the ventilation flow.

The tank has air inlet and exhaust ports at locations that are geometrically similar (azimuthally identical and scaled radially) to the locations of the Title I Design for the MWTF dome space ventilation system inlet and outlet. The test tank is 12 feet in diameter which has a 1:6.25 linear scale ratio to the actual tank which is 75 feet in diameter.

Figure 1. Fabrication Sketch of Tank.



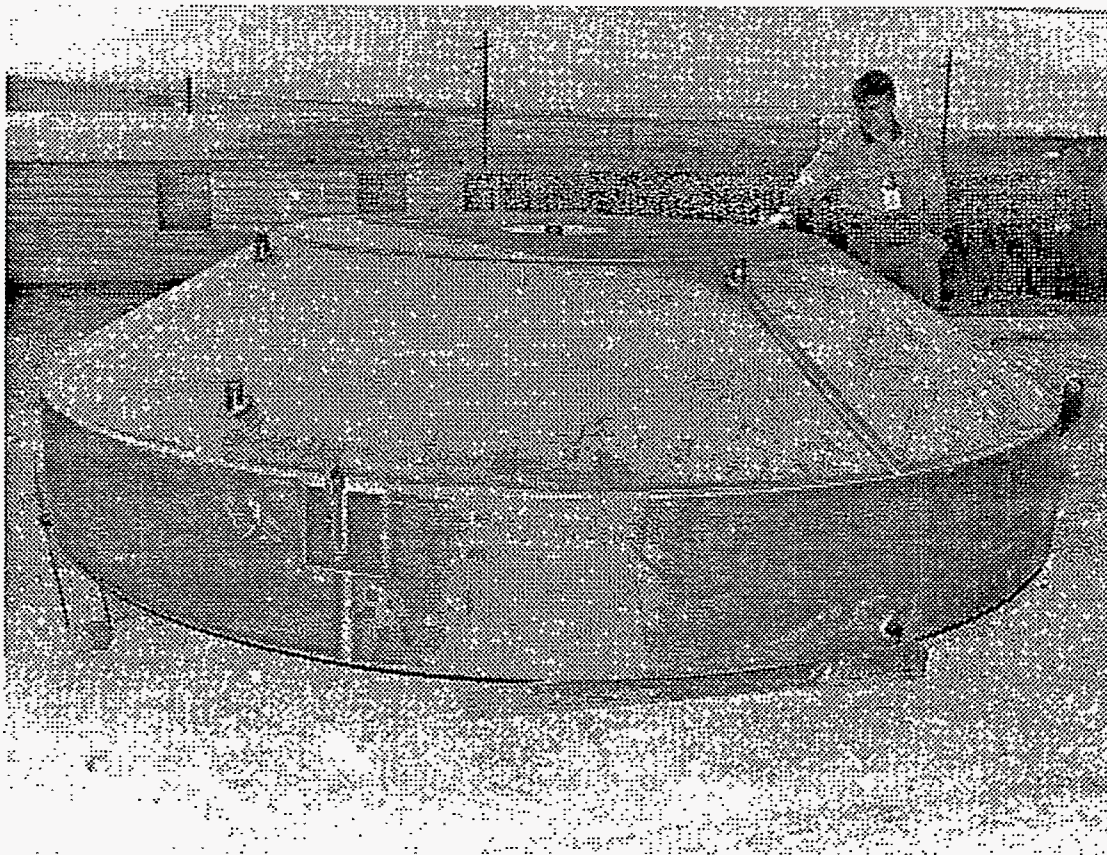


Figure 2. Test Tank prior to Installation in Test Facility.

### 3.2 Instrumentation and Control System

The tank inlet port has a heat exchanger attached to a temperature controlled water loop to stabilize the inlet temperature. It also has flow, temperature, and relative humidity monitoring instrumentation. The outlet port is connected to the suction of a centrifugal blower. The volumetric flowrate of the blower is controlled with a variable speed drive and a suction bypass valve. Monitoring of the exhaust conditions from the tank is accomplished by an integrated temperature/relative humidity probe installed in the outlet. The outlet flow is also monitored through the use of a calibrated pitot/static test section placed directly downstream of the temperature/relative humidity monitoring instrumentation. Appendix B contains a list of the instruments used to monitor the test. Included in that table are the WHC Standards lab code number for the calibration of the instruments and the manufacturers accuracy specification for the instrument. All instruments except the thermocouples were calibrated by the



WHC standards lab. The thermocouples were purchased to "special limits of accuracy" and used in the as received condition.

The temperature of the simulated waste solution in the tank is controlled through the use of an external circulation loop with an in-line 12 KW circulation heater. The heater power is controlled by a thermocouple in the heater outlet, although the solution temperature for determining the proper setpoint for the heater is monitored by thermocouples in the tank itself. Figure 3 is a schematic diagram of the essential elements of the system. The circulation pump runs at about 10 gpm. This produces a mixed solution in the tank without excessive agitation.

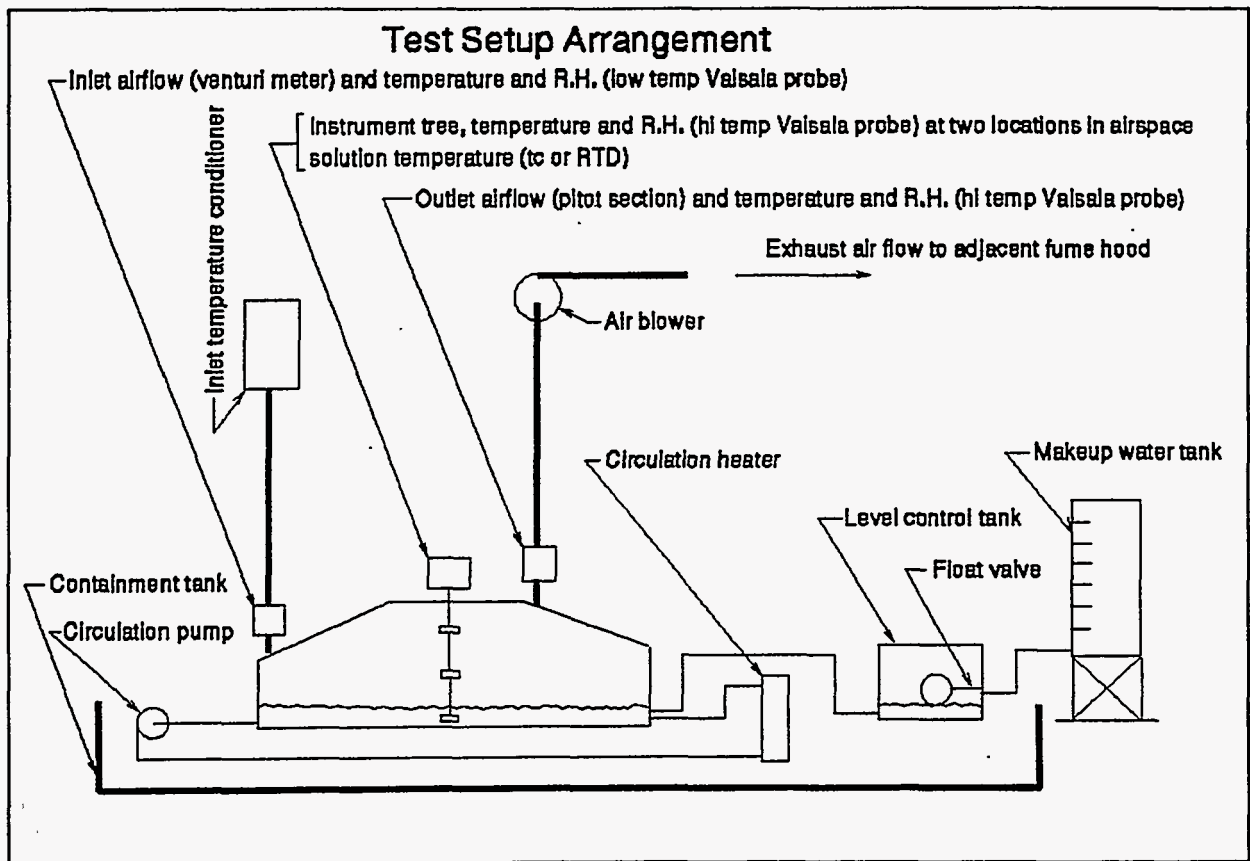


Figure 3. Schematic Diagram of Test Facility.

### 3.3 Makeup Water Control and Measurement System

An automatic makeup water system to replace that lost by evaporation is part of the facility. As water is evaporated from the simulant in the tank it needs to be replaced for several reasons. If the level drops too low the circulation pump will cavitate. In addition, the geometric conditions of the system would then change during the test. But most important, if water is evaporated over the duration of a test the concentration of the simulant solution will change and so

will the vapor pressure of the solution at the test temperature. In addition to these practical reasons, it was desirable to accurately record the makeup water as a reality check for the test instrumentation. For these reasons a makeup system with level control was included. The source of the makeup water was a supply tank with a calibrated sight glass on the exterior of the tank so that changes in makeup level could be accurately recorded.

This system went through several major design iterations as the test program progressed. The initial design was a small external tank with an easily removed lid. The subsequent changes made to this system in an effort to reduce uncertainty in the measured water consumption are described in the following paragraphs.

1. The first four tests, conducted with water in the tank, used the original system which consisted of a "toilet bowl" float and valve mounted in the rectangular polyethylene float tank. Because of force required to actuate the float valve this system had a level uncertainty of about  $\pm 0.25$  in. (18 gallons)
2. Between tests 4 and 5 (the first NaOH test), the manual valve was replaced with an electric solenoid valve that was activated by a micro-switch mounted to the float stand. The float continued to be used to activate the micro-switch. Also, the small poly tube connecting the float tank to the test tank was lengthened and coiled to minimize back-flow into the float tank. This change improved the level control to the point that the uncertainty was reduced to about  $\pm 0.1$  in. (7 gallons)
3. Between tests 8 and 11, a sight glass was added to the test tank at the drain valve that allowed external measurement of the test tank level. This allowed a better measurement, reducing the uncertainty to approximately  $\pm 0.05$  in. (3.5 gallons)
4. Between tests 12 and 10-10R, a hole was drilled into the test tank and make-up water was plumbed to feed directly into the tank. The coiled poly tubing from the float tank to the test tank was replaced with a short one inch iron pipe. The water was removed from the float tank and replaced with the same NaOH solution as the test tank. The float/microswitch in the float tank was used for Test 10R to control make-up water addition. This change made the system operate with less operator attention, but didn't increase the accuracy.
5. Between tests 10-10R and 17, a conductivity level probe was installed in the test tank and the float tank was taken out of service. The conductivity probe signaled the solenoid valve for water addition. This system was used for Test 17 and for all tests that followed. This gave a dead band of about 0.09 in (6.4 gallons)
6. After test 20 the end of the conductivity probe was rounded to provide added sensitivity. This reduced the deadband by about a factor of 4 so the uncertainty with this system was about  $\pm 0.8$  gallons. Tests 5R, 6R, 9, 21, 13, 22 used this make-up water system.



### 3.4 Test Fluids

The test fluid for tests 1-4 was de-ionized water. The balance of the tests were run with a solution of sodium hydroxide. The sodium hydroxide solution was prepared to simulate the vapor pressure curve of waste simulants that had been previously tested to determine their vapor pressure (Appendix D). Rather than use the simulant for the previous small-scale experiments to determine the worst vapor pressure reduction for the wastes, a simple solution of NaOH was used to give the desired vapor pressure reduction. Based on the information in Appendix D, a solution of NaOH was used that would have a vapor pressure that was 55% of pure water at the boiling point. Table 3-27 in reference 3 provides a tabulation of the equilibrium vapor pressure of aqueous solutions of NaOH as a function of wt% NaOH. Table 68 in Reference 4 provides a tabulation of specific gravity of NaOH solutions at 20 °C as a function of concentration. The solution specific gravity of the target concentration is 1.335.

The NaOH solution specific gravity was measured on a regular basis for all tests. The recorded values range from a high of 1.342 to a low of 1.318. The mean for all tests was 1.331. In addition to regular monitoring of the solution specific gravity a series equilibrium vapor pressure measurements on samples of the test solution were made. The reason for making these measurements was to provide an independent verification that the solutions used for the tests had been mixed correctly, and also to make sure that no unknown ingredients which might affect the results (such as a surfactant) had been introduced into the system. The results of these measurements are presented in Appendix A.

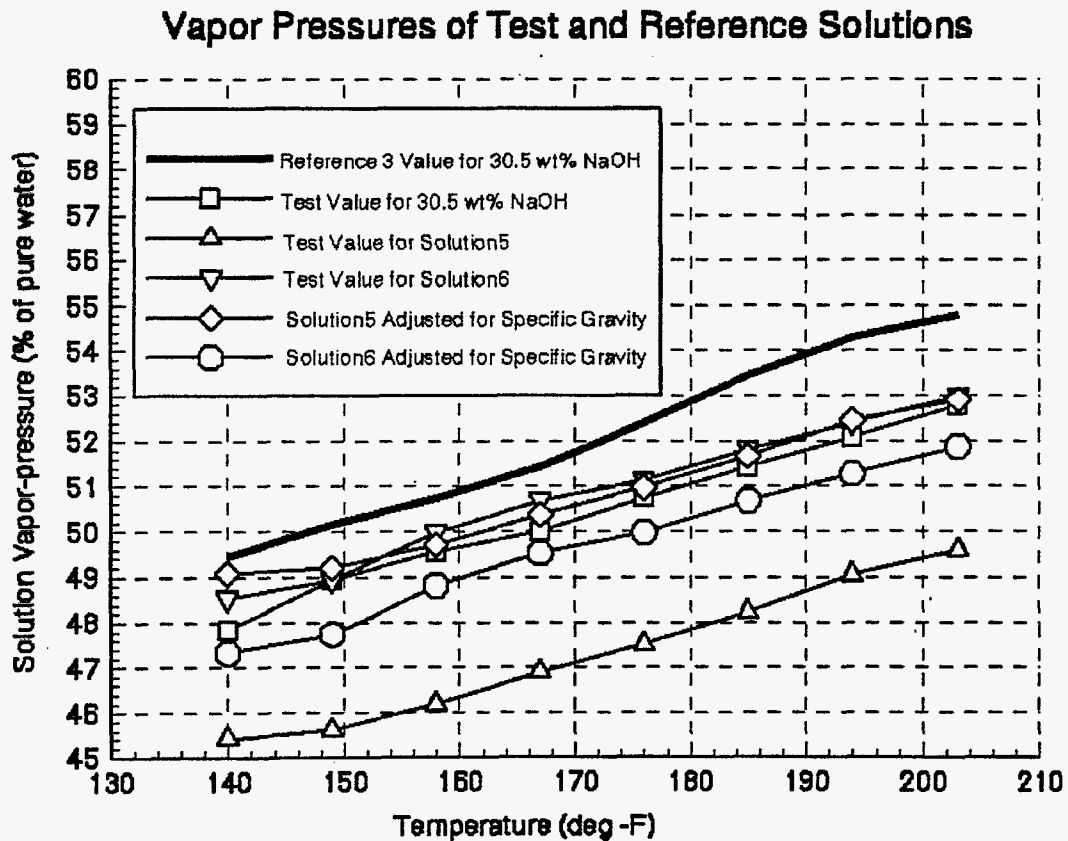
Figure 4 shows vapor pressure data from the measurements reported in Appendix A and from Reference 3. From this figure and the discussion in Appendix A it is apparent that the Cottrell Apparatus that was used to measure the vapor pressure of the solutions wasn't able to exactly reproduce the values from Reference 3. The data is quite consistent and implies that the vapor pressure of a 30.5 wt% NaOH solution is 1.5-2.0% less with respect to the vapor pressure of water than the handbook value from Reference 3. Based on the test/calibration runs performed with deionized water as discussed in Appendix A it isn't reasonable to attribute a deviation of this magnitude to instrumentation error. It is possible to draw the conclusion that the Cottrell Apparatus, while giving vapor pressure values for the solutions that are closer to the Reference 3 values than simply boiling the solution in a flask, still produces biased data values.

The reported values in Appendix A show that solution 6 has an NaOH concentration (based on specific gravity measurement) that is slightly less than the target value, although within the variation that was measured over the course of the testing program. Solution 5 has an NaOH concentration (based on specific gravity measurement) that is more than the target value, and is also slightly outside the range of values that was measured over the course of the testing program (1.350 vs a max of 1.342 measured during the testing). Since it has been around 6 months since the samples were drawn from the evaporation test setup, and they have been run through several different types of apparatus in an attempt to measure their vapor pressure it is not unrealistic to expect that a small amount of water has been lost from one of them. For purposes of determining the appropriate vapor pressure suppression to use as a basis for reducing the data from this test series, the data from Appendix A has been corrected/adjusted to the nominal value of specific gravity. Those adjustments make the data

reported in Appendix A lie in a fairly narrow band, which is consistently suppressed about 2% from the handbook values contained in Reference 3.

The original reason for making these measurements was to verify that the test fluid had been mixed properly and also that it hadn't been adulterated by some unknown constituent. The data in Appendix A clearly show this to be the case since the vapor pressure curves for solutions 5 and 6 agree within 1% with the vapor pressure curves for a 30.5 wt% solution of NaOH mixed as a "calibration sample" in the lab when corrected for specific gravity variation. The "bias" that exists between the data in Reference 3 and the data reported in Appendix A will be attributed to apparatus bias. The curve in Figure 4 that comes from Reference 3 will be used as the vapor pressure of the test solution for purposes of reducing the test data.

Figure 4. Solution Vapor Pressures.



#### 4.0 Test Procedure

The tests were run under the control of a detailed test procedure (Reference 2). The basic idea behind each test was to get the system set up at a desired condition, and let it run long enough so that the measured and calculated values of water usage were relatively large with respect to the uncertainties in those

values. Table 1 shows the test matrix as excerpted from the test plan. Tests 14, 15, 16, 18, and 19 weren't run. Tests 14, 15, and 16 weren't run because of limitations of the test apparatus. Tests 18 and 19 weren't run because as the test program progressed additional tests, defined as 20, 21, and 22 were run which would be more desirable than 18 and 19.

Table 1. Original Test Matrix.

Test No.	Solution Temp. Deg. F	Inlet Air Flow SCFM	Inlet Air Temp. Deg.F	Approximate Test Duration hours	Solution Level inches	Vapor Pressure Suppression %
1	100	7.7	53	24	6	0
2	full KW*	7.7	53	24	6	0
3	full KW*	25.6	53	6	6	0
4	full KW*	7.7	53	24	15.3	0
5	190	25.6	77	24	6	45
6	190	7.7	77	6	6	45
7	190	38.4	77	24	6	45
8	200	15	53	24	6	45
9	190	15	53	6	6	45
10	170	15	53	6	6	45
11	190	25.6	77	24	6	45
12	135	15	53	6	6	45
13	100	15	53	6	6	45
14	full KW*	15	53	24	6	45
15	full KW*	25.6	53	24	6	45
16	200	7.7	77	6	6	45
17	150	7.7	77	6	6	45
18	100	7.7	77	6	6	45
19	190	15	77	6	6	45

\* full KW refers to full power operation of the heater and will be achieved by setting the temperature controller unachievably high

## 5.0 Results

A total of nineteen tests were run of which 15 were with simulated waste. The conditions and results are shown in Table 2. The lab notebook containing the raw data is Reference 8. The two different inlet temperatures used caused no appreciable difference in latent heat removal. The heat flux shown in Figure 4 is plotted in two temperature ranges to give better resolution. The curves referred to as "Boelter" curves are derived from the relationship presented in Reference 5. The relationship is:

$$e = 0.067 (P_{vs} - P_{vb})^{1.22}$$

where:  $e$  = unit evaporation rate (lb/ft<sup>2</sup>-hr)  
 $P_{vs}$  = Vapor pressure of water at the surface (inches Hg)  
 $P_{vb}$  = Vapor pressure of water in the bulk phase (inches Hg)

The curves referred to as "similarity" are based on the development presented in Reference 6. The basic correlation is:

$$Sh = .14 (Gr_m S_c)^{1/3}$$

where:  $Sh$  is the Sherwood number  
 $S_c$  is the Schmidt number  
 $Gr_m$  is the mass transport Grashof number

Uncertainties were assigned based on the inherent error in the measuring devices for both the measured and the calculated water usage. The principal contributor to the uncertainty associated with the measured water usage was the measurement of the water/solution level in the tank. The principal uncertainty associated with the calculated water usage is the uncertainty in the differential pressure transducer used on the inlet flow transducer, however, the uncertainties quoted in Table 2 result from consideration of propagation of all instrument errors involved. The "Value Assigned" column is based on a weighted average of the calculated and measured values of water used. The weighing function that was used attributes a weight inversely proportional to the percent uncertainty in a measurement except that negative values of water usage are set to zero. The "Value Assigned" column was then used as a basis for constructing the curves shown in Figure 4. The curves are based on a least squares fit of the data in Table 2 with three constraints levied upon the data.

The first constraint is that the driving force to transfer mass/evaporate water has the same shape as the saturation pressure of water as a function of temperature. The second constraint is that a single node lumped parameter model of the following form is a valid approximation to the behavior of the system being tested:

$$H_m * A * (E_s - E_b) = W (E_{out} - E_{in})$$

Where:

$H_m$	Mass transport coefficient
$A$	Area available for evaporation
$E_s$	Surface moisture ratio
$E_b$	Bulk moisture ratio
$W$	Airflow through dome space
$E_{out}$	Outlet moisture ratio

$E_{in}$  inlet moisture ratio

$E_b = E_{out}$  is also applied as a condition to this equation.

The detailed results shown in Appendix C support this assumption, since the moisture ratio measured at the tank exit is the same as that measured by the transducers internal to the tank.

The third constraint is that the mass transport coefficient is proportional to the 1/3 power of the density difference.

$$H_m \propto (\rho_b - \rho_s)^{1/3}$$

where:  $\rho_s$  = Surface mixture density  
 $\rho_b$  = Bulk mixture density

The experimental results shown in Figure 5 have been "scaled up" to the full size (75-foot diameter) tank and plotted in Figure 6. These heat removal curves form the design basis for evaporative heat removal from the MWTF. The scaling was done based on the ratio of waste surface area to volumetric flow rate. Appendix F contains a discussion of the issues associated with this scaling. Tests 2 and 4 were done to find out whether reduced headspace caused by filling the tank to the maximum allowable level will have an effect on the heat removal capabilities. Test 2 was run with a solution depth of 6 inches and Test 4 was run with a solution depth of 15.3 inches as shown in Table 1. When the heat removal values are normalized to the same flow value (7.7 scfm) the latent heat removal are 130.6 Btu/hr-ft<sup>2</sup> and 115.6 Btu/hr-ft<sup>2</sup> for tests 4 and 2, respectively. From this it can be seen that filling the tank to the maximum level will have no deleterious effect on latent heat removal.

Figure 5. Test Results Compared to Correlations.

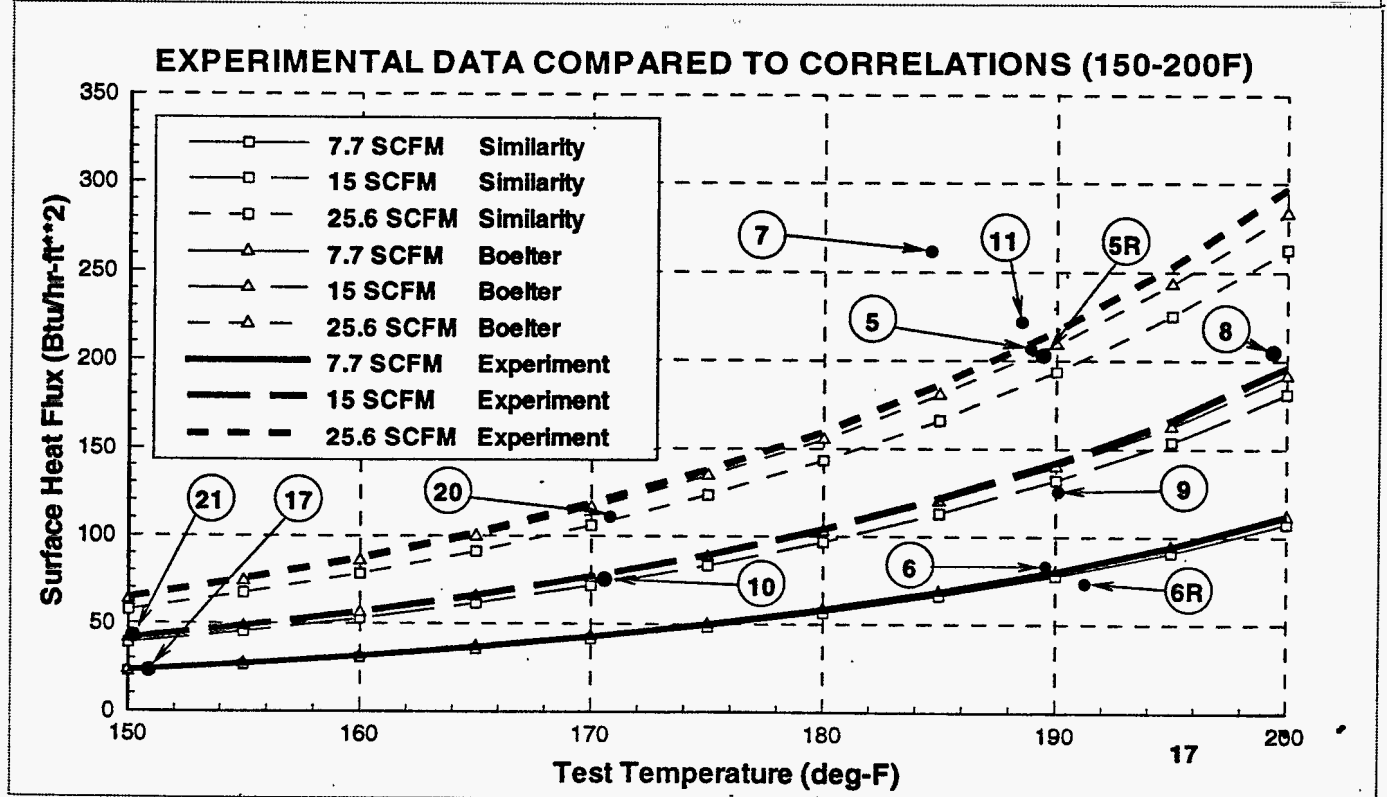
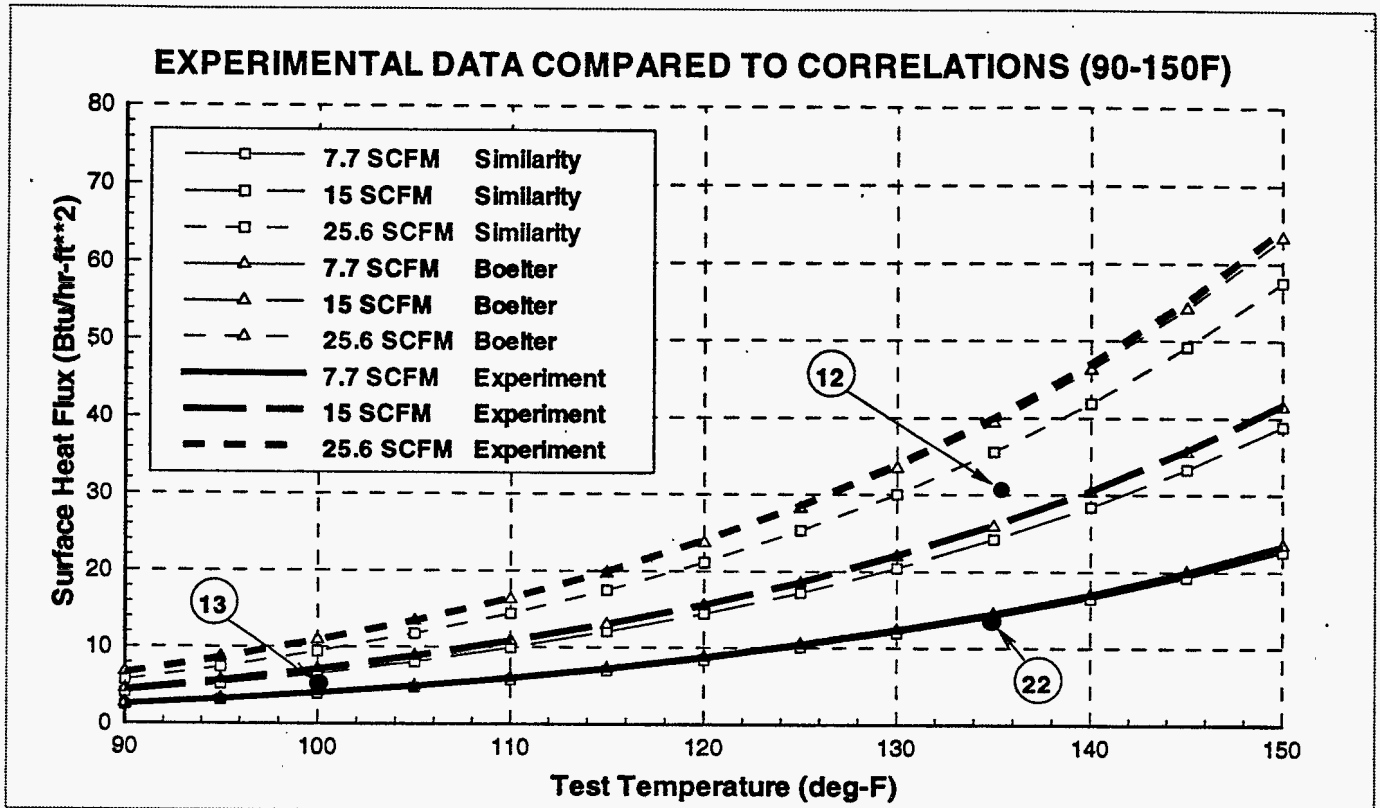


Figure 6. Recommended Design Values for MWTf.

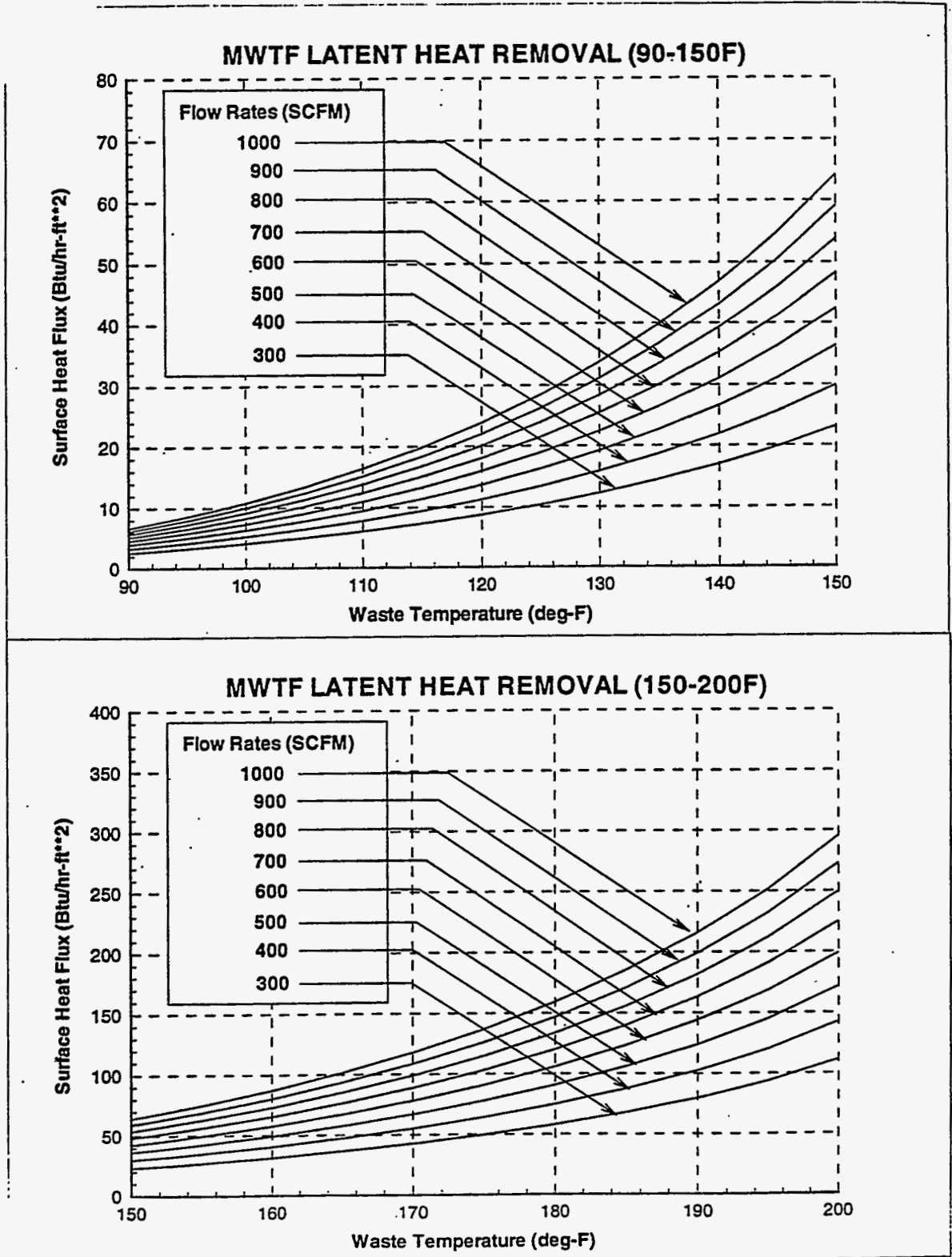


Table 2. Test Results in Chronological Order.

Test #	Date (1994)	Inlet Air Moisture Ratio	Outlet Air Moisture Ratio	Inlet Air Temperature (deg F)	Dome Air Temperature (deg F)	Solution Temperature (deg F)	Flowrate (SCFM)	Calculated Water Used <sup>a</sup> (gallons)	Measured Water Used <sup>b</sup> (gallons)	Value Assigned Water Used (gallons)	Test Duration (hours)	Latent Heat Removal (Btu/hr-ft <sup>2</sup> )
1	2/3	.0026	.039	53.3	98.8	100.2	7.35	3.2 ± .1	.6 ± 18	3.23	22.46	11.1
2	2/5	.0026	.426	52.5	170.1	173.4	8.67	89.2 ± 10.5	47.0 ± 18	79.56	44.93	130.2
3	2/7	.0017	.240	53.1	154.4	162.3	26.85	21.3 ± .26	37.5 ± 18	21.50	6.17	258.7
4	2/9	.0028	.429	54.0	171.7	173.8	6.78	26.4 ± 5.2	17.7 ± 18	26.05	17.05	115.0
5	2/21-22	.0029	.217	77.0	167.2	188.8	25.05	67.0 ± .9	66.5 ± 7	66.70	23.17	208.8
7	2/22	.0031	.181	77.5	163.6	184.6	38.31	22.9 ± .13	20.8 ± 7	22.70	6.25	264.1
6	2/23	.0039	.293	77.6	167.3	189.8	7.51	7.2 ± .11	no data	7.20	6.13	85.1
8	2/24-25	.0029	.375	52.5	172.2	199.9	14.89	70.8 ± 2.8	63.5 ± 7	68.10	23.67	207.3
11	3/2-4	.0068	.239	77.1	172.2	188.5	24.77	50.0 ± .72	no data	50.00	16.15	224.6
12	3/7-9	.0022	.055	52.9	126.2	135.5	14.75	20.3 ± .82	20.0 ± 3.5	20.25	47.98	31.6
10-10R	3/11-14	.0041	.147	52.6	155.3	170.5	14.49	73.3 ± 3.1	63.9 ± 3.5	68.60	65.57	76.73
17	3-16-21	.0038	.079	77.2	141.1	150.9	7.84	36.5 ± 5.2	34.4 ± 3.2	35.40	114.44	23.0
20	3/21-23	.0026	.115	52.4	154.2	170.4	25.52	61.2 ± .82	55.9 ± 3.2	59.95	39.45	111.5
5R	3/23-25	.0024	.198	76.7	170.9	189.8	25.3	68.3 ± .9	76.0 ± .8	72.10	25.63	203.9
6R	3/29-31	.0043	.252	76.6	174.3	191.3	7.22	46.4 ± 7.8	51.3 ± .8	48.87	48.00	73.8
9	5/11-13	.0065	.225	53.1	155.3	190.1	15.21	90.7 ± 3.4	87.4 ± .8	88.33	50.50	126.8
21	5/16-17	.0063	.071	76.8	140.1	150.2	15.07	10.6 ± 5.0	11.9 ± .8	11.76	19.90	43.9
13	5/26-6/6	.0059	.016	52.0	95.6	100.2	15.19	23.3 ± .9	21.6 ± .8	22.45	262.83	6.5
22	6/10-13	.0076	.049	76.3	127.4	135.0	7.40	12.0 ± 2.1	13.7 ± .8	13.21	71.93	13.7

<sup>a</sup> Calculated based on flowmeters and temp/humidity probes

<sup>b</sup> Measured based on makeup water tanks



## 6.0 References

1. B. A. Crea, January 1994, *Test Plan and Specification for Multifunction Waste Tank Facility (MWTF) Evaporative Heat Removal Tests*, WHC-SD-W236A-TP-004, Westinghouse Hanford Company, Richland, Washington.
2. E. R. Cramer, February 1994, *Test Procedure for Multifunction Waste Tank Facility (MWTF) Evaporative Heat Removal Tests*, WHC-SD-W236A-TC-001, Westinghouse Hanford Company, Richland, Washington.
3. Perry, Robert H. and Don Green, *Perry's Chemical Engineers' Handbook*, Sixth Edition, McGraw-Hill, Inc., dated 1984.
4. *Handbook of Chemistry and Physics*, 55th Edition, CRC Press, 1974.
5. Boelter, L. M. K., et. al., *Free Evaporation into air of water from a Free Horizontal Quiet Surface*, Ind. Eng. Chem., Vol. 38, pp 596, 1946.
6. Shah, M. M., *Estimating Evaporation from Horizontal Surfaces*, ASHRAE Trans., Vol. 87, Pt. 1, pp.35, 1981.
7. Cramer, E. R., *Multi-Function Waste Tank Facility Thermal Hydraulic Analysis for Title I Design*, WHC-SD-W236A-ER-006, Rev. 0, Westinghouse Hanford Company, Richland, Washington.
8. Crea, B. A., 1994, *MWTF Evaporation Test Lab Notebook*, WHC-SD-W236A-TL-001, Rev. 0, Westinghouse Hanford Company, Richland, Washington.

**Appendix A. Vapor Pressure Measurements of Test Solutions.**

Westinghouse  
Hanford Company

Internal  
Memo

From: Chemical Engineering Laboratory 8A400-94-039  
Phone: 373-5434 S4-25  
Date: November 22, 1994  
Subject: VAPOR PRESSURE MEASUREMENTS ON CAUSTIC/SURROGATE WASTE SOLUTIONS  
WITH COTTRELL BOILING POINT APPARATUS

To: T. B. McCall H0-33

cc: B. A. Crea H0-33  
M. J. Duchsherer S4-25  
C. A. Hinman H0-33  
M. J. Kupfer H5-46  
M. J. Schliebe S4-25  
J. P. Sloughter T6-07  
CJB File/LB

- References: (1) Internal Memo 8E130-94-058, C. J. Berglund to C. A. Hinman, "Vapor Pressure Measurements on Caustic/Surrogate Waste Solutions with Enhanced Test Apparatus", dated June 30, 1994.
- (2) Experimental Physical Chemistry; Daniels, Williams, Bender, Alberty and Cornwell; McGraw-Hill Book Company, Inc., 1962.

In an effort to improve on the results reported in reference 1 additional vapor pressure measurements were performed on the same test solutions, employing a more sophisticated glassware setup. The Cottrell boiling point apparatus described in reference 2 was designed to eliminate the effect of superheating when measuring the boiling points of solutions. This assembly is a catalog item from Fisher Scientific but they were out of stock and were having difficulty getting resupplied, so a set of dimensioned sketches were prepared based on the catalog illustration and the Westinghouse glass shop fabricated the apparatus. Figure 1 in the Attachment is a fairly literal schematic diagram of the resulting assembly. As an indication of scale, the heating vessel is 50-millimeter glass tubing.

In use the apparatus is supported by a ring stand and clamps, with the heating vessel resting in a small heating mantle which is regulated by a variable transformer. The vacuum pump and digital electronic pressure gauge ("electronic manometer") are connected as shown in Figure 1 with flexible tubing. The heating vessel is filled with the test liquid to the level indicated in the figure. There are three small holes (approximately 5 millimeters in diameter) spaced around the circumference of the inner shroud and located about 3 centimeters above its lower rim; this equalizes pressures within the apparatus. A bleed valve on the vacuum pump was adjusted to yield the desired indicated absolute pressure in the apparatus, which typically fluctuated several tenths of a millimeter of mercury (mm Hg). The solution was heated and when it reached the boiling point vapor bubbles rising in the

T. B. McCall  
 Page 2  
 November 22, 1994

recirculation risers capture small volumes of solution, resulting in a stream of vapor and solution impinging on the RTD temperature element. Presumably the boiling liquid will flash to equilibrium with the ambient pressure in the apparatus, thus subjecting the temperature element to the corresponding boiling temperature. This is obviously a dynamic situation and it is necessary that the flow of solution impinging on the temperature element be sustained, since the ambient temperature in the apparatus is dictated by solvent condensation (pure water, in this case) at that pressure. Thus there is potential for heat loss from the sensing portion of the temperature element to that area which is exposed to the ambient temperature, so the impinging solution must provide enough heat to the sensing portion to maintain the proper temperature. When a satisfactory recirculation flow was being maintained and the indicated temperature had stabilized the data were recorded and the internal pressure adjusted to the next desired value.

Several test runs were made with deionized (DI) water at intervals during this test effort to provide an ongoing informal verification of the pressure and temperature instrumentation calibrations. Interestingly, the performance of this apparatus with DI water at the lowest pressures (ergo, the lowest temperatures) was somewhat unsatisfactory, in that recirculation flow was quite erratic. The water would apparently superheat and finally vaporize too vigorously to develop good recirculation flow, and then the cycle would repeat. Nothing that was utilized as a "boiling chip" resulted in any improvement. As the pressure (and thus the boiling temperature) was increased the boiling did become more benign and recirculation was maintained. It seems likely that the viscosity and surface tension properties of water at the lower temperatures, in conjunction with the dimensions of the apparatus, were not conducive to yielding stable recirculation flow. Inasmuch as only the solvent was involved here the benefit of recirculation is not really required; the measured temperatures would be valid so long as enough vapor is generated to adequately heat the temperature element. The data from these runs are shown in Table 1 of the Attachment.

The test solutions displayed this phenomenon to a lesser degree so it was possible to achieve recirculation, albeit somewhat sluggish, at the lower pressures. This was probably due in part to the fact that the solutions, of course, boil at higher temperatures for a given pressure. Initially the test runs were started at the lowest absolute pressure desired (usually 65 mm Hg), but an alternative technique was employed for some of the tests in which the run was started at a higher boiling temperature (70-80°C) to achieve a sustained recirculation flow, and then slowly reducing the pressure to the desired lower values so that boiling did not have to be initiated at a lower temperature. This procedure was marginally successful in improving boiling and recirculation performance.

Table 2 in the Attachment shows the vapor pressure/temperature data obtained with the Cottrell apparatus on the solutions that were employed for the work reported in reference 1; namely, a 30.5-percent sodium hydroxide (NaOH) solution, Test Solutions 5 and 6 (samples of 30.5-percent NaOH solution that had been used in tests by another engineering organization) and cc:waste (complexant concentrate) surrogate. In addition, a newly-prepared 10-molar NaOH solution (30.1 percent, 43 gms NaOH/100 gms water) was tested to offer a

T. B. McCall  
Page 3  
November 22, 1994

known reference solution. As seen from Table 2 the data from this fresh solution is quite consistent with the data from the 30.5 percent solution and Test Solution 6, while the Test Solution 5 results are displaced a degree or two high. The current specific gravities (SpG) of two of the test solutions were measured, weighing the amount of solution in a 250-milliliter volumetric flask and comparing it with the weight of DI water the flask held. Test Solution 5 gave a SpG of 1.350 and the SpG of Test Solution 6 was 1.330.

In an effort to obtain additional insight into the quality of data generated with this apparatus a set of solutions was prepared to provide direct comparison with sodium hydroxide solution vapor pressure data in the Chemical Engineer's Handbook. Solutions were made up containing 20, 40 and 70 grams of sodium hydroxide per 100 milliliters of DI water. The boiling temperatures of these solutions were measured in the Cottrell apparatus at internal pressures matching the data in the reference handbook. Table 3 in the Attachment lists the values obtained along with the corresponding reference data. The temperatures for the 20 and 40 gram solutions are higher than the reference data by one degree Celsius or less; the two lower temperatures for the 70 gram solution are slightly lower than the reference values, probably because the recirculation flows with this higher concentration solution were irregular and sluggish due to the higher viscosity and did not adequately heat the temperature element.

As noted previously, the data from the 10-molar solution, the 30.5 percent solution, and Test Solution 6 are in quite good agreement, while Test Solution 5 routinely yielded temperatures between one and two degrees Celsius higher. This is consistent with Test Solution 5 showing a slightly higher SpG, which suggests a higher solution concentration. This same relationship was observed in the work reported in reference 1, but these latest temperatures are all about one degree lower. This would be consistent with temperature measurement in the Cottrell apparatus being less prone to sense solution superheat. In general the temperatures recorded were judged to be the result of good recirculation impingement on the temperature element and the DI water runs certainly indicate good instrument accuracy. Thus the relatively larger disparity (compared with the DI water results) between the reference data and the observed results with the specifically-matching test solutions is somewhat disconcerting. And the apparent high-bias of the temperatures suggests superheating, which seems inconceivable in the Cottrell apparatus. Hopefully the potential uncertainty in this vapor pressure data does not significantly impact the ultimate application of this information.



C. J. Berglund, Principal Engineer  
Chemical Engineering Laboratory

cjb

Attachment

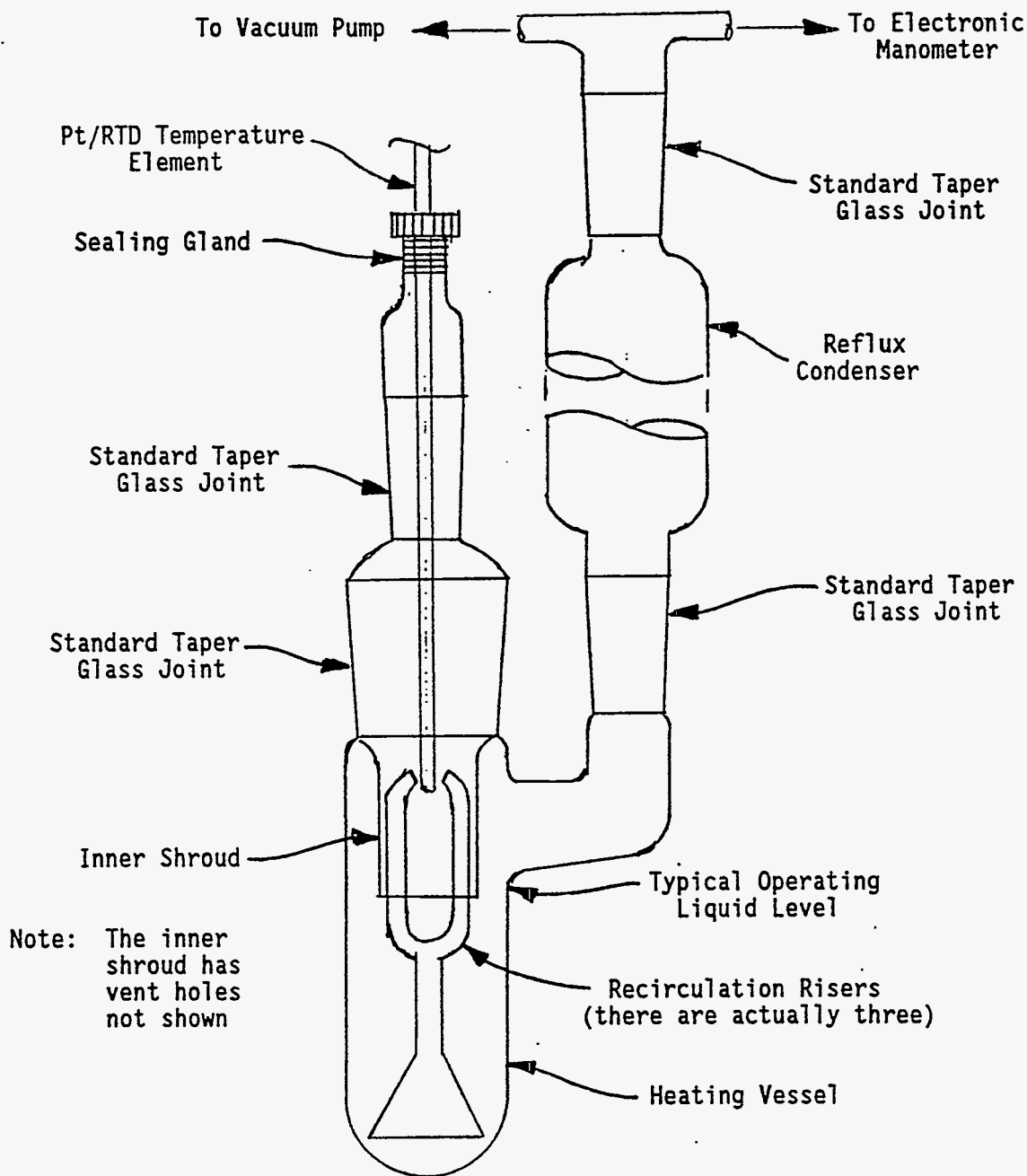


Figure 1. Cottrell Boiling Point Apparatus

\*\*\* TABLE 1. DI WATER VAPOR PRESSURE DATA WITH COTTRELL APPARATUS \*\*\*

ABSOLUTE PRESSURE mm Hg	- - - TEMPERATURE - °C - - -				
	Handbook	Oct 17	Oct 20	Oct 25	Nov 1,7
65	43.1	43.2	43.2	--	
80	47.1	47.2	47.1	47.2	
81	47.3				46.9
94	50.3				50.4
100	51.6	51.7	51.6	51.8	
120.5	55.4				55.6
150	60.1	60.2	60.1	60.3	
200	66.5	66.6	66.4	66.6	
202	66.7				66.8
231	69.7				69.8
250	71.6	71.6	71.7	71.9	
288.5	75.0				74.9
300	75.9	75.9	75.9	76.1	
400	83.0	83.1	82.9	83.3	
450	85.9				85.9
500	88.7	88.7	88.6	88.9	
600	93.5	93.6	93.3	93.6	
621	94.4				94.7
697	97.6	97.4	97.5	97.7	

Note: The DI water "Handbook" data is from the Handbook of Chemistry and Physics, Thirty-third Edition, Chemical Rubber Publishing Company, 1951.

\* \* \* TABLE 2. VAPOR PRESSURE DATA ON TEST SOLUTIONS IN COTTRELL APPARATUS \* \* \*

ABSOLUTE PRESSURE mm HG	- - - TEMPERATURE - °C - - -										
	--- DI WATER ---		30.5% NaOH		10M NaOH	TEST SOL'N 5		TEST SOL'N 6		CC:WASTE SURR	
	Handbook	Exp	Oct 17	Oct 18	Oct 19	Oct 24	Oct 24	Nov 11	Nov 11	Oct 26	Oct 26
65	43.1	43.2	58.3	58.0	58.2	59.5	58.6	57.2	57.2	54.6	54.6
80	47.1	47.2	62.4	62.1	62.5	63.8	63.4	62.2	62.2	58.8	58.8
100	51.6	51.7	66.9	66.8	67.0	68.5	68.3	66.8	66.8	63.2	63.4
150	60.1	60.2	75.9	75.8	75.9	77.3	77.3	75.7	75.4	72.5	72.5
200	66.5	66.5	82.6	82.3	82.5	83.9	84.1	82.4	82.2	79.1	79.1
250	71.6	71.7	87.8	87.8	87.9	89.3	89.2	87.6	87.6	84.3	84.3
300	75.9	76.0	92.3	92.2	92.4	93.8	93.8	92.2	92.1	88.8	88.9
400	83.0	83.0	99.7	99.6	99.7	101.1	101.2	99.4	99.4	96.1	96.2
500	88.7	88.7	105.7	105.6	105.7	107.2	106.7	105.3	105.2	101.9	102.0
600	93.5	93.5	110.7	110.3	110.6	112.1	111.7	110.3	110.3	107.1	107.1
697	97.6	97.5	114.6	114.5	114.5	116.1	115.1	114.1	114.1		

Note: The DI water experimental data ("Exp") are mean values of the test data shown in Table 1.

A-6

MHC-SD-W236A-ER-009  
Rev. 0

8A400-94-039  
ATTACHMENT  
Page 3 of 4



10  
 \* \* \* TABLE 3. VAPOR PRESSURE DATA ON REFERENCE SOLUTIONS \* \* \*

- - - TEMPERATURE - °C - - -

ABSOLUTE PRESSURE mm HG	-- DI WATER --		-- 20/100 NaOH-H <sub>2</sub> O --			-- 40/100 NaOH-H <sub>2</sub> O --			-- 70/100 NaOH-H <sub>2</sub> O --		
	Handbook	Nov 1,7	Ref	Oct 31	Oct 31	Ref	Nov 1	Nov 1	Ref	Nov 1	Nov 1
81	47.3	46.9				60	60.4	60.4			
94	50.3	50.4							80	78.8	78.7
120.5	55.4	55.6	60	60.6	60.7						
202	66.7	66.8				80	81.1	81.0			
231	69.7	69.8							100	99.4	99.6
288.5	75.0	74.9	80	80.8	80.7						
450	85.9	85.9				100	100.8	101.2			
515	89.5	89.8							120	119.8	120.1
621	94.4	94.7	100	100.4	100.6						

Notes: 20/100 NaOH-H<sub>2</sub>O means 20 gms NaOH dissolved in 100 gms H<sub>2</sub>O, etc.

20/100 = 16.7% NaOH  
 40/100 = 28.6% NaOH  
 70/100 = 41.2% NaOH

"Ref" is the temperature at which the specified NaOH solution has the corresponding vapor pressure shown in the ABSOLUTE PRESSURE column, per NaOH-H<sub>2</sub>O vapor pressure/temperature data from the Chemical Engineers' Handbook, Third Edition, McGraw-Hill Book Company, Inc., 1950.

A-7

WHC-SD-W236A-ER-009  
 Rev. 0

8A400-94-039  
 ATTACHMENT  
 Page 4 of 4

**Appendix B. Instrument List.**

B-1

Instrument/ Variable	Description/Location	Function	Manufacture/ Model	Accuracy	Calibration lab code #
TC1	Thermocouple teed into circulation heater output	Control input for circulation heater temperature controller	Type K thermocouple	$\pm 2$ °F	Used as Received
TC2	Thermocouple internal to circulation heater	Independent over temperature cutout for circulation heater controller	Type K thermocouple	$\pm 2$ °F	Used as Received
TC3	Thermocouple in solution at center of tank	Solution temp, data	Type K thermocouple	$\pm 2$ °F	Used as Received
TC4	Thermocouple in solution at center of tank	Solution temp, data	Type K thermocouple	$\pm 2$ °F	Used as Received
TC5	Thermocouple in tank solution at radius of vent outlet and displaced -90 °	Solution temp, data	Type K thermocouple	$\pm 2$ °F	Used as Received
TC6	Thermocouple in tank solution at radius of vent outlet and displaced +90 °	Solution temp, data	Type K thermocouple	$\pm 2$ °F	Used as Received
TC7	Thermocouple on top of tank under insulating rubber	Dome/head temperature, data	Type K thermocouple	$\pm 2$ °F	Used as Received
TC8	Thermocouple on sloped part of tank head under insulating rubber	Dome/head temperature, data	Type K thermocouple	$\pm 2$ °F	Used as Received
P1	Inlet air static pressure	Ambient absolute air pressure, data	MKS Baratron 222 BHS 1000 Torr	$\pm .5$ % Reading	679-80-02-024
DP1	Inlet air differential pressure	Differential pressure from the inlet Venturi flow meter, data	MKS Baratron 223 B $\pm 0-5$ in/H <sub>2</sub> O	$\pm .5$ % Full Scale	679-80-02-022

MHC-SD-M236A-ER-009  
Rev. 0

Instrument/ Variable	Description/Location	Function	Manufacture/ Model	Accuracy	Calibration lab code #
FLOWIN	Inlet air flow venturi meter	Mass flow rate of the inlet air derived from: DP1, RTD1, RH1. computed value	Flow-Dyne Engineering VP0150979-PVC .979" Dia. throat	N/A	Used as Received
DP2	Outlet air differential pressure	Differential pressure from the pitot/static section at the outlet	MKS Baratron 223BD ± 0-1 torr	± .5% Full Scale	679-80-02-025
FLOWOUT	Outlet air flow Pitot/static section	Mass flow rate of the outlet air derived from: DP2, RTD4, RH4. computed value	Air Monitor Corp LO-FLO 0-50 SCFM	N/A	Used as Received
RTD1/Tempin	Inlet air temperature in plywood box surrounding inlet flowmeter	Inlet air dry bulb temp, data	Vaisala HMD 20YB	± .2 °C	679-32-03-006
RTD2/Temp2	Tank Vapor space air temperature ~ 12" above liquid surface, center of tank	Vapor space air dry bulb temperature, data	Vaisala HMP 135Y	± .2 °C	679-32-07-003
RTD3/Temp3	Tank Vapor space air temperature ~ 6" above liquid surface, center of tank	Vapor space air dry bulb temperature, data	Vaisala HMP 135Y	± .2 °C	679-32-07-002
RTD4/Tempout	Tank Outlet dry bulb air temperature, teed into air outlet line directly above tank	Outlet air dry bulb temperature, data	Vaisala HMP 135Y	± .2 °C	679-32-01-004
RH1/Epsin	Inlet air relative humidity. Probe in plywood box surrounding inlet flowmeter.	Relative humidity post processed with Tempin to give inlet moisture ratio. data, computed value	Vaisala HMD 20YB	± 2% R.H.	679-32-03-006

B-2

MHC-SD-M236A-ER-009  
Rev. 0

Instrument/ Variable	Description/Location	Function	Manufacture/ Model	Accuracy	Calibration lab code #
RH2/Eps2	Tank Vapor space air relative humidity ~ 12" above liquid surface, center of tank	Relative humidity post-processed with Temp2 to give moisture ratio. data, computed value	Vaisala HMP 135Y	± 2% R.H. 0 - 90% ± 3% R.H. 90 - 100%	679-32-01-003
RH3/Eps3	Tank Vapor space air relative humidity ~ 6" above liquid surface, center of tank	Relative humidity post-processed with Temp3 to give moisture ratio. data, computed value	Vaisala HMP 135Y	± 2% R.H. 0 - 90% ± 3% R.H. 90 - 100%	679-32-01-002
RH4/EPSOUT	Tank outlet relative humidity. Probe is teed into air outlet line directly above tank	Relative humidity post-processed with Tempout to give moisture ratio. data, computed value	Vaisala HMP 135Y	± 2% R.H. 0 - 90% ± 3% R.H. 90 - 100%	679-32-01-004
EPSOURC	Moisture ratio at simulant surface, based on simulant temp and vapor pressure reduction to 55% of water	Provide a measure of the driving potential available for evaporation	derived value	N/A	N/A

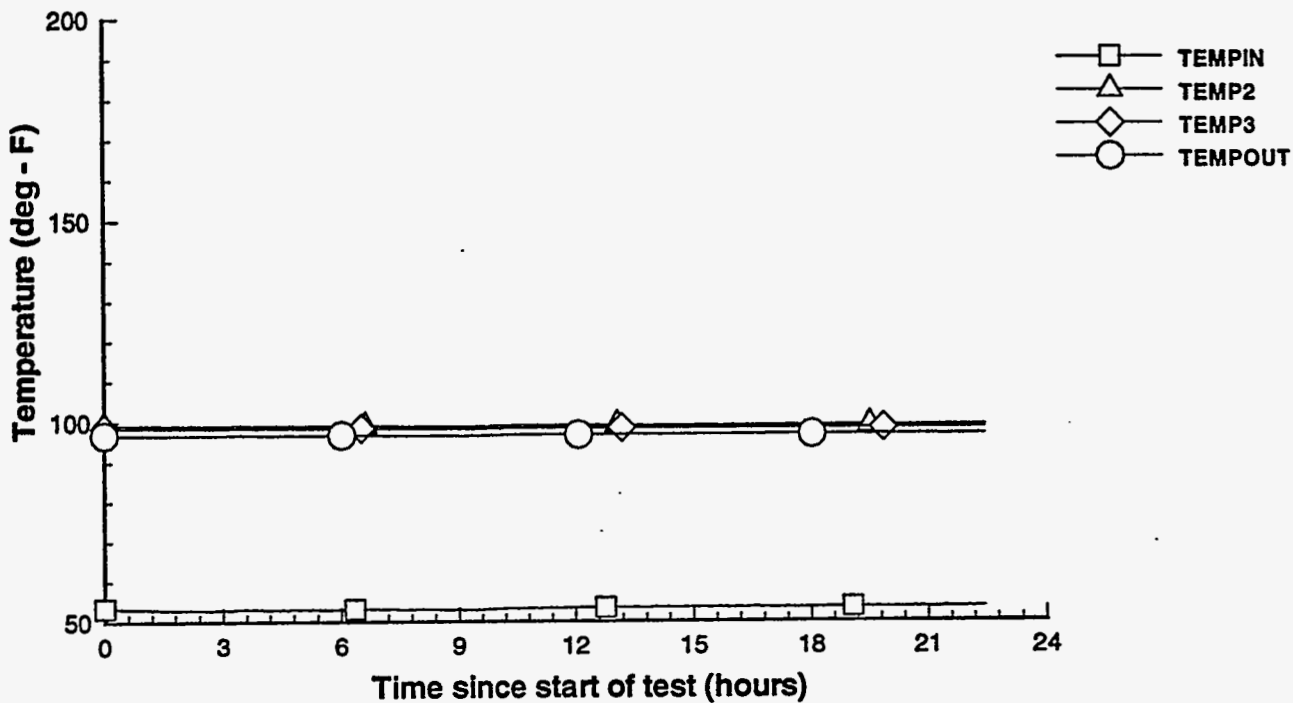
B-3

MHC-SD-W236A-ER-009  
Rev. 0

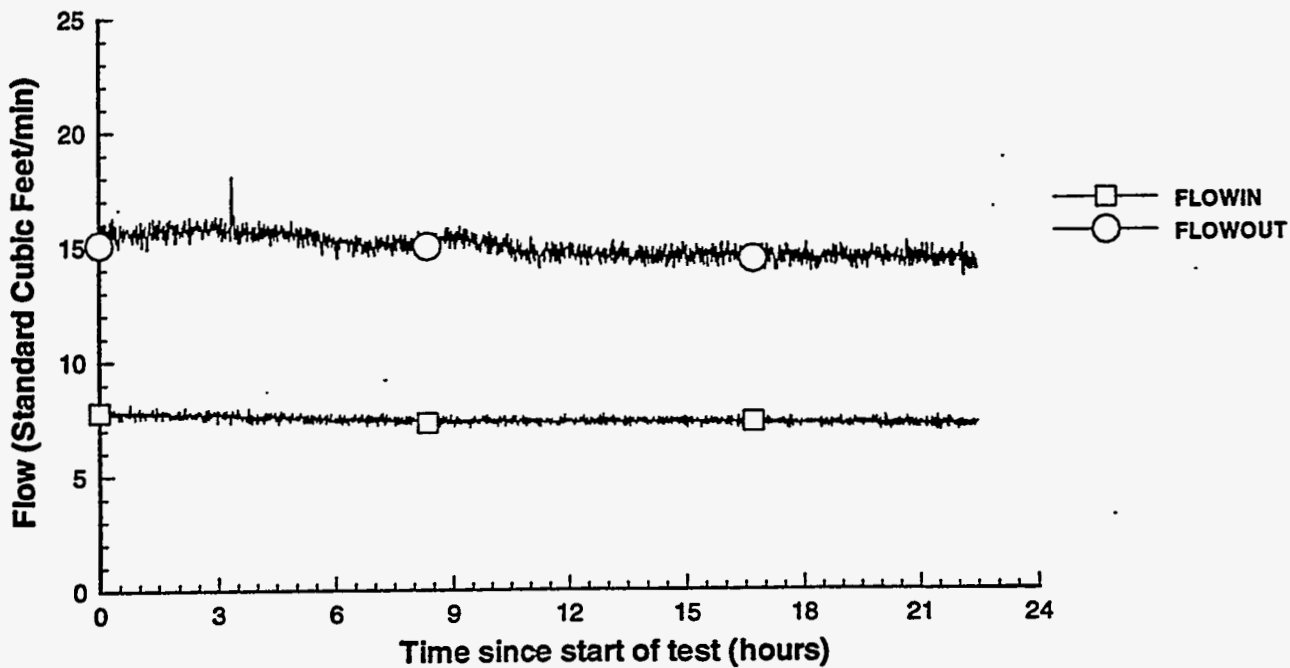
**Appendix C. Test Data.**

(2D) || Print || 17 Jun 1994 || test1.plt || TEST\_1\_DATA

### RTD Temperatures (test 1)

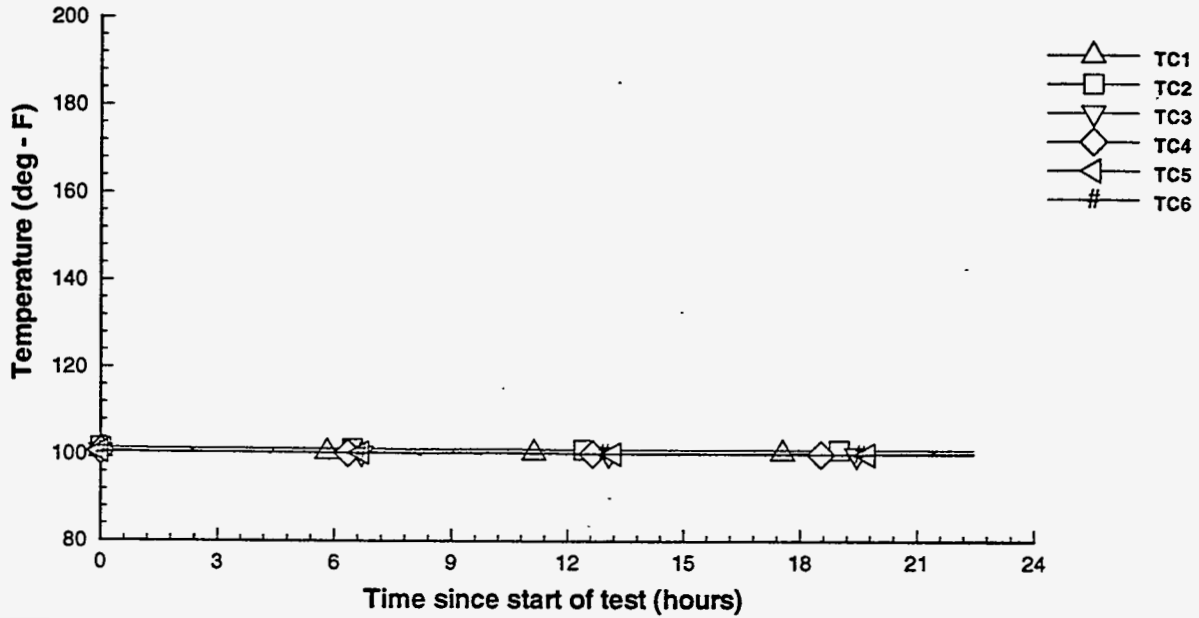


### Vapor Space Air Flow (test 1)

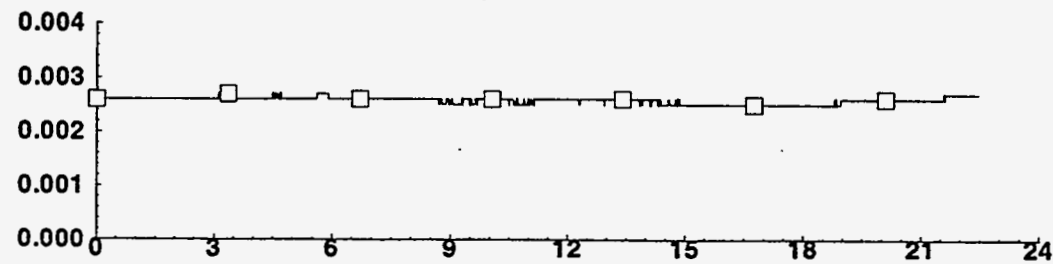
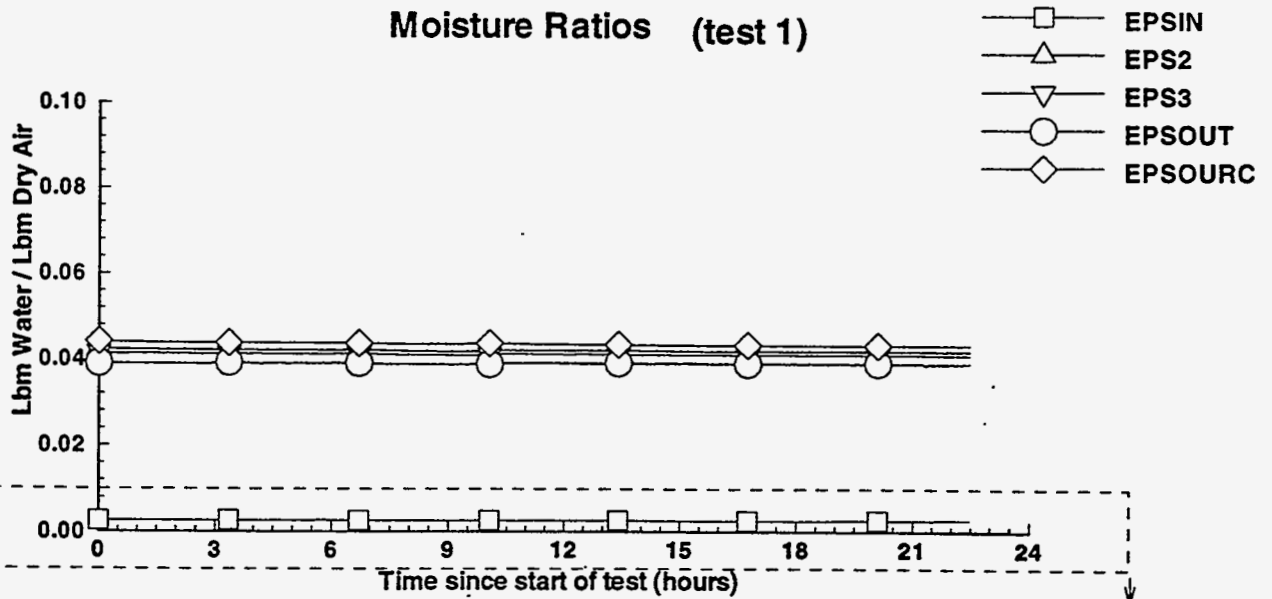


(2D) II Print II 22 Aug 1994 II test1.plt II TEST\_1\_DATA

### Thermocouple Temperatures (test 1)



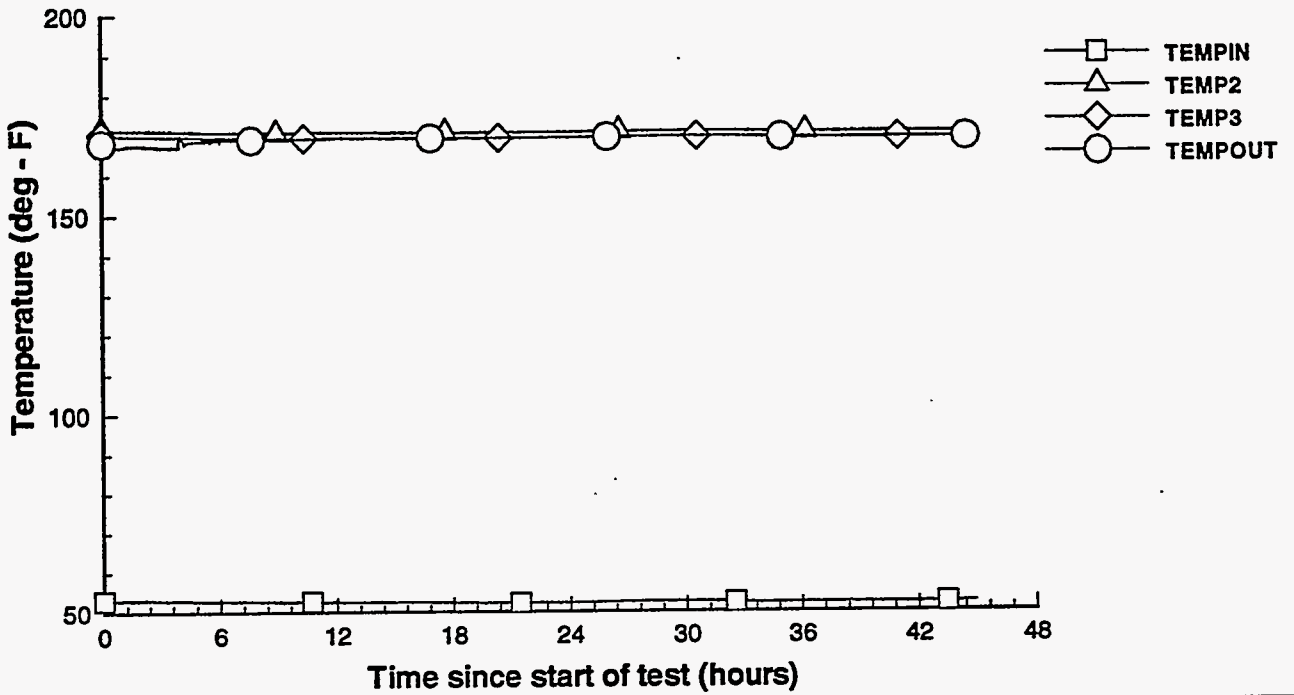
### Moisture Ratios (test 1)



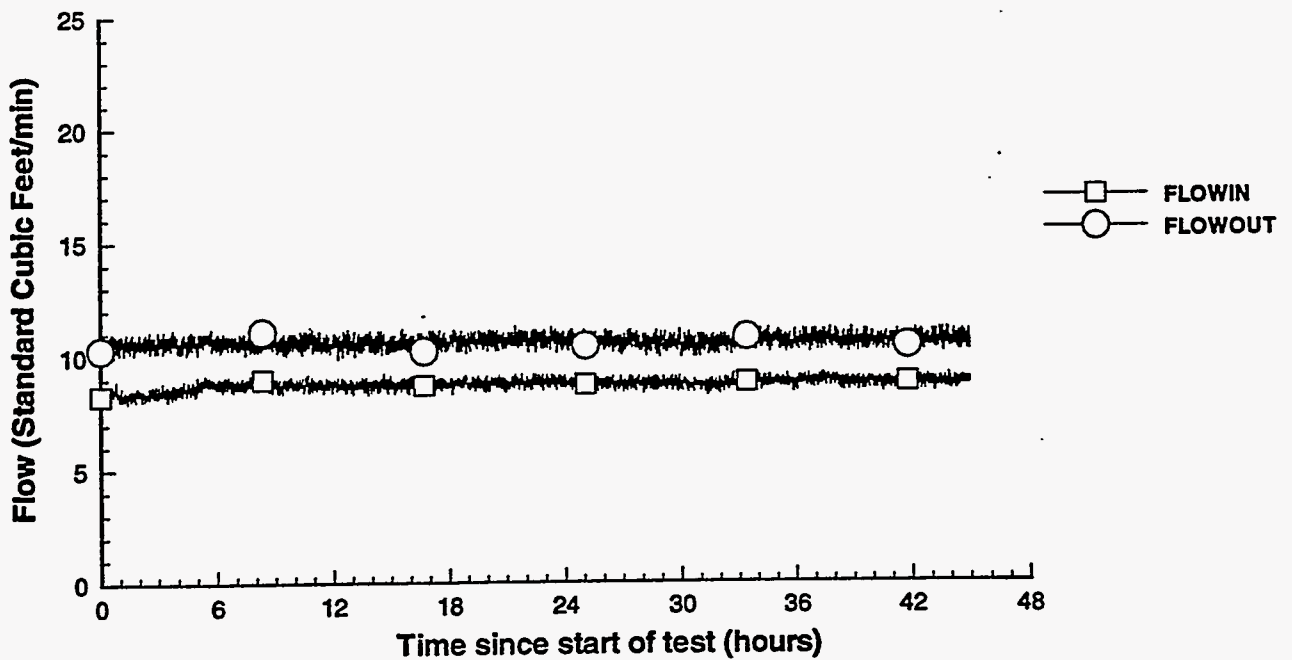


(2D) II Print II 17 Jun 1994 II test2.plt II TEST\_2\_DATA

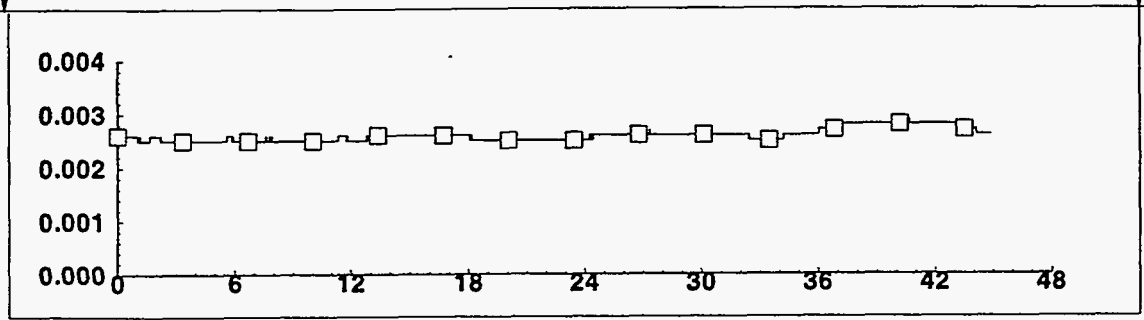
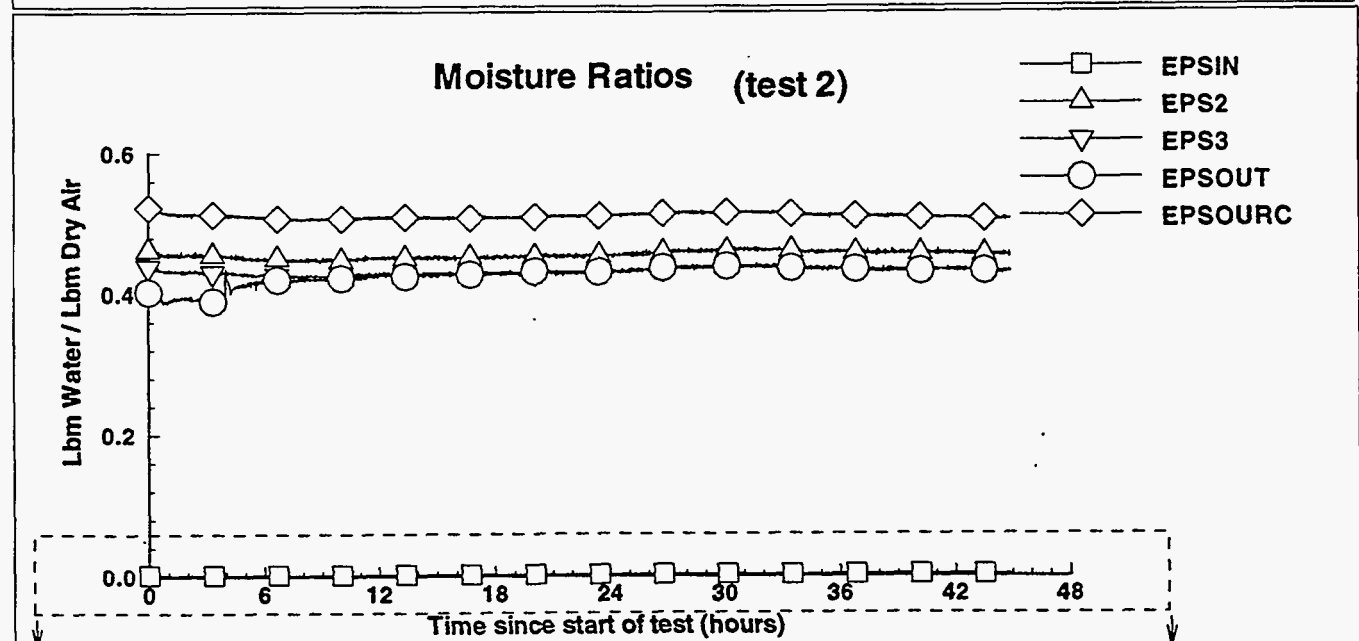
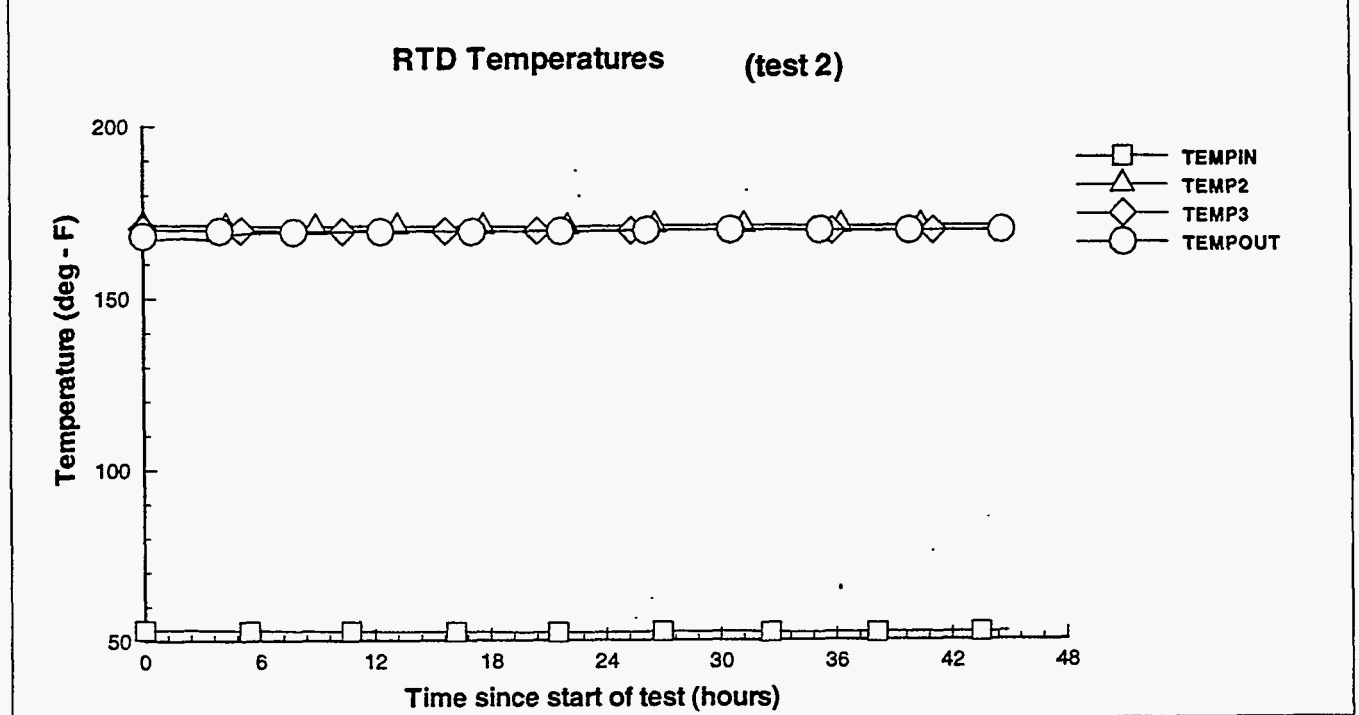
### RTD Temperatures (test 2)



### Vapor Space Air Flow (test 2)

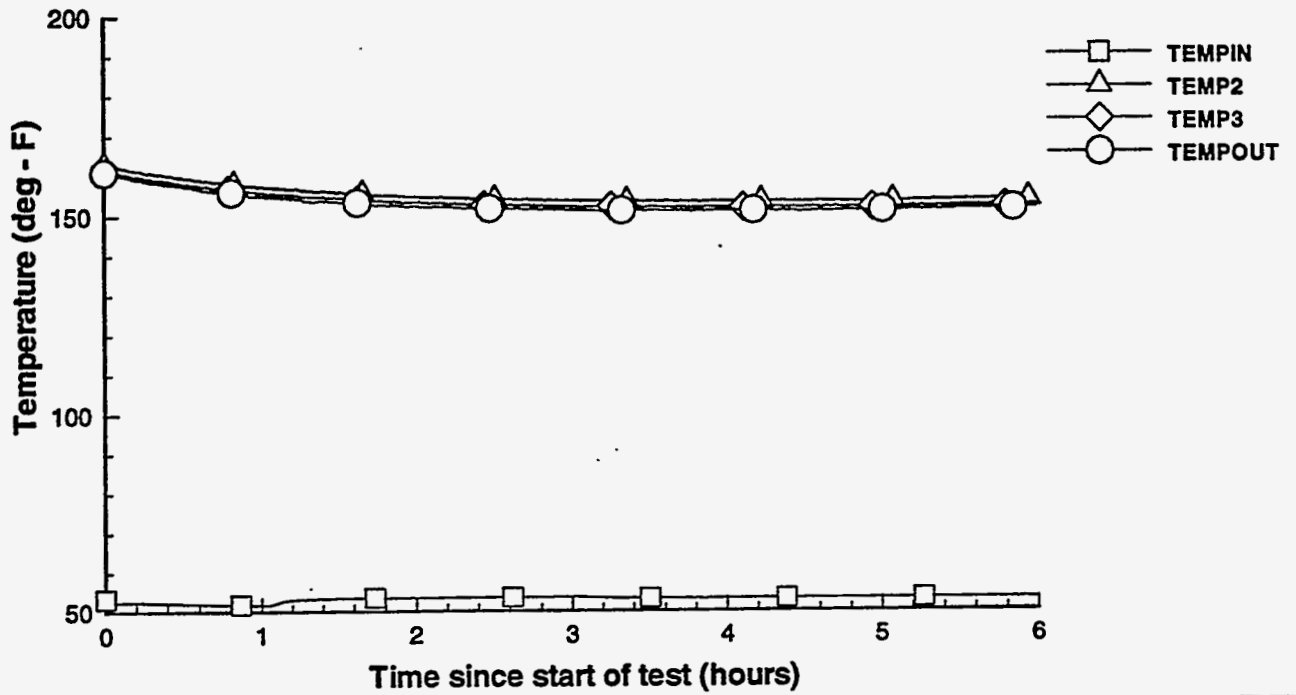


(2D) II Print II 19 Aug 1994 II test2.pt II TEST\_2\_DATA

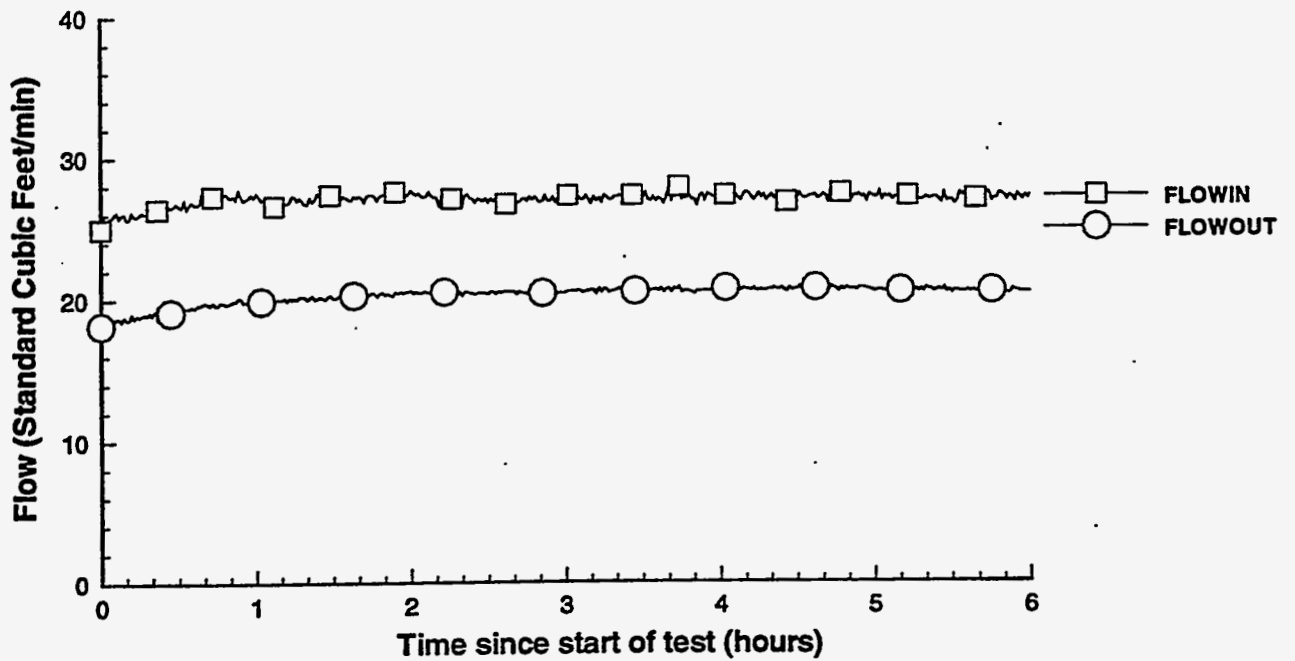


(2D) II Print II 3 Jun 1994 II test3.plt II TEST\_3\_DATA

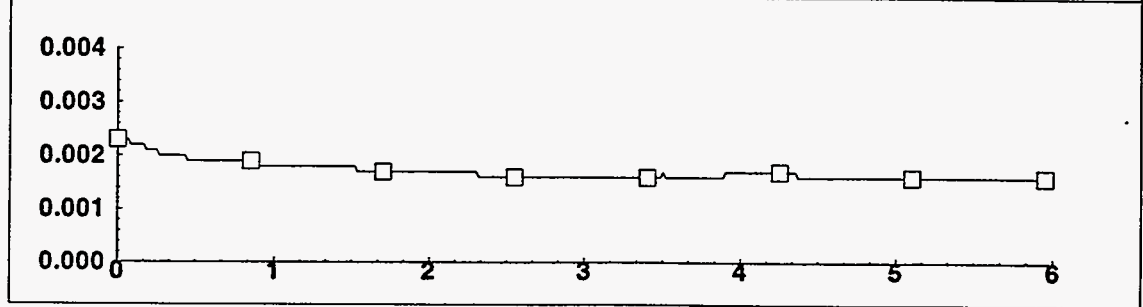
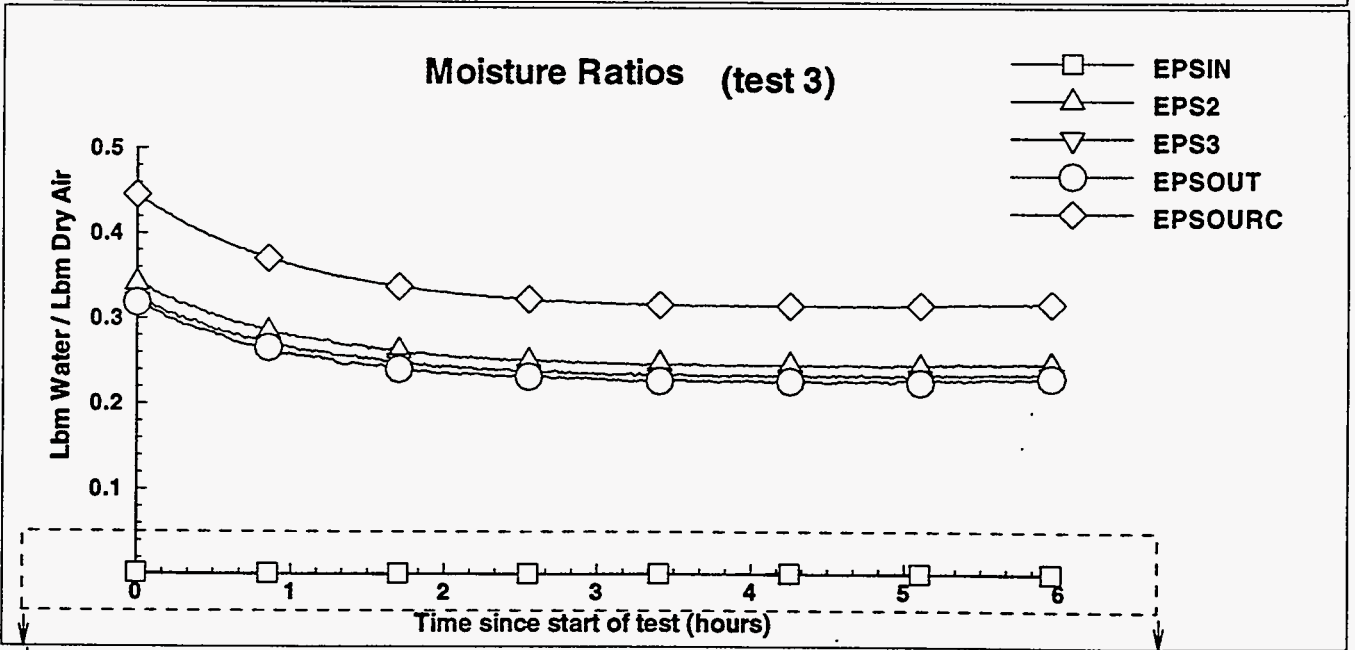
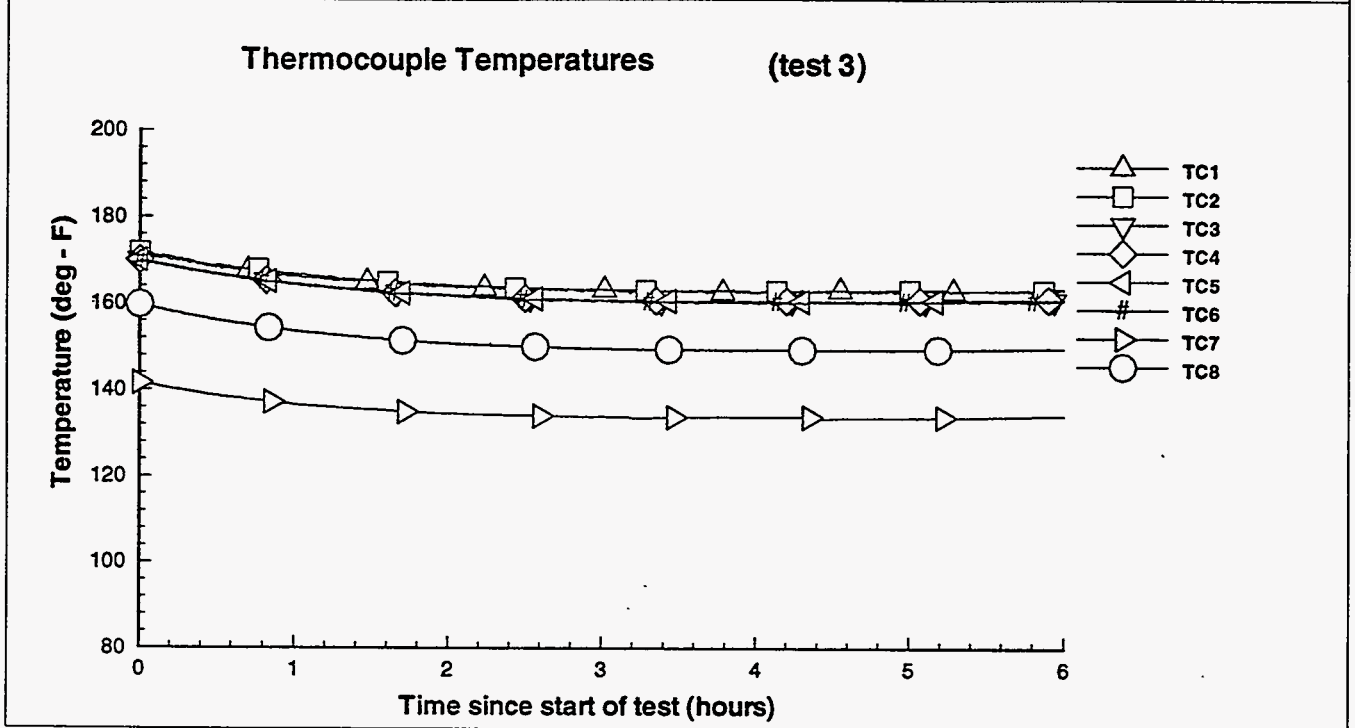
### RTD Temperatures (test 3)



### Vapor Space Air Flow (test 3)

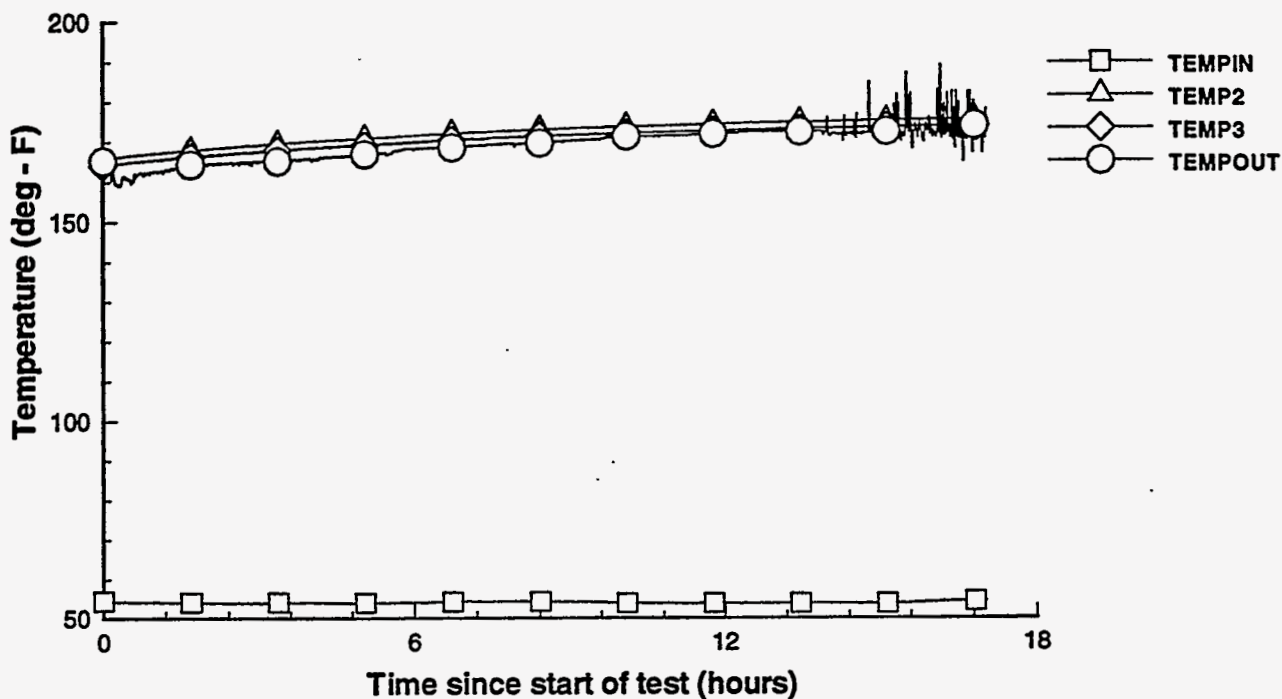


(2D) II Print II 19 Aug 1994 II test3.pt II TEST\_3\_DATA

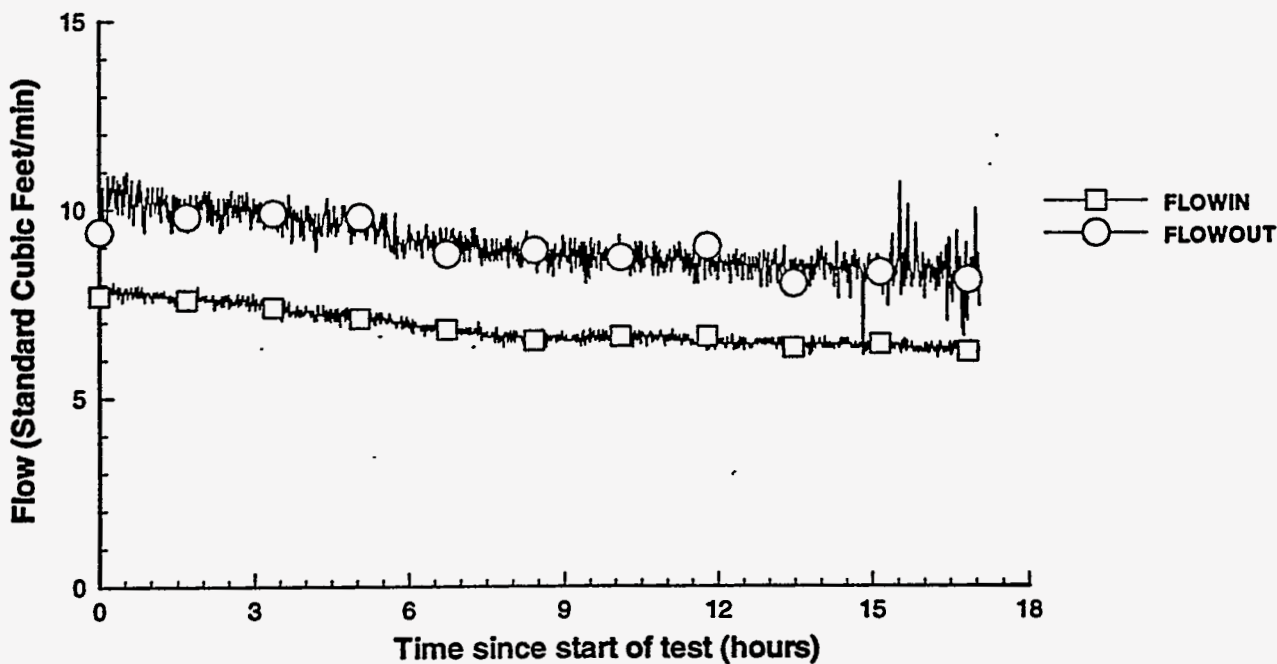


(2D) II Print II 3 Jun 1994 II test4.plt II TEST\_4\_DATA

### RTD Temperatures (test 4)

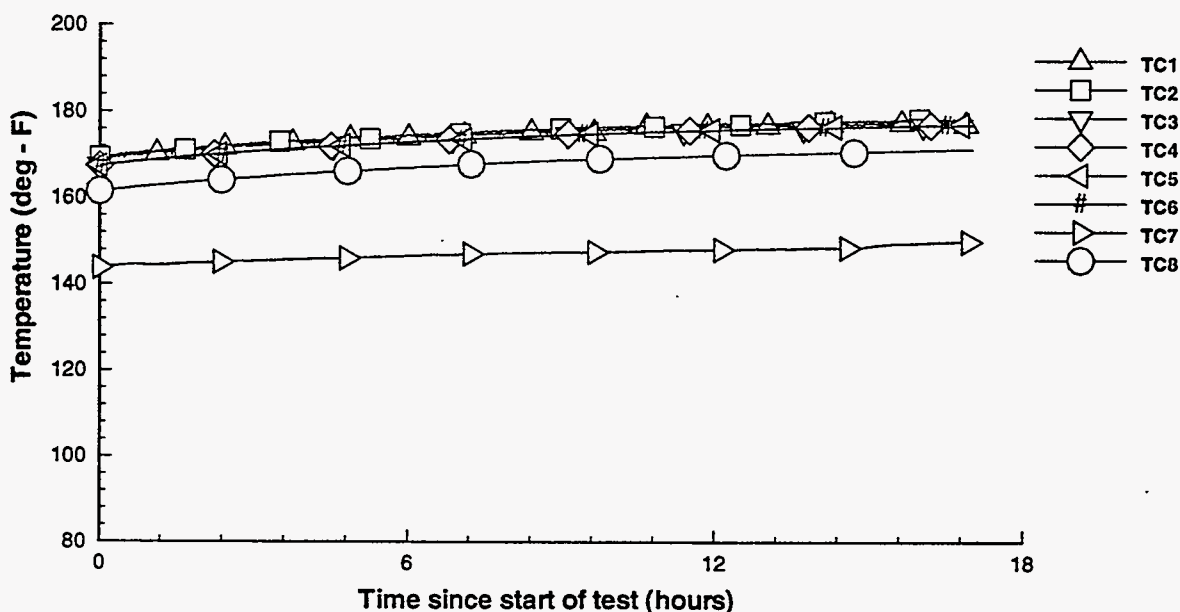


### Vapor Space Air Flow (test 4)

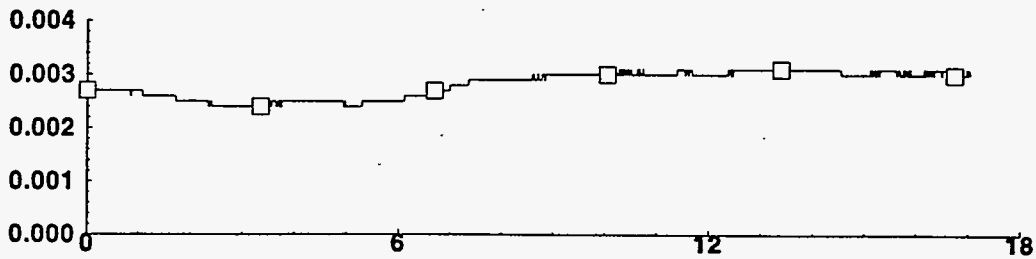
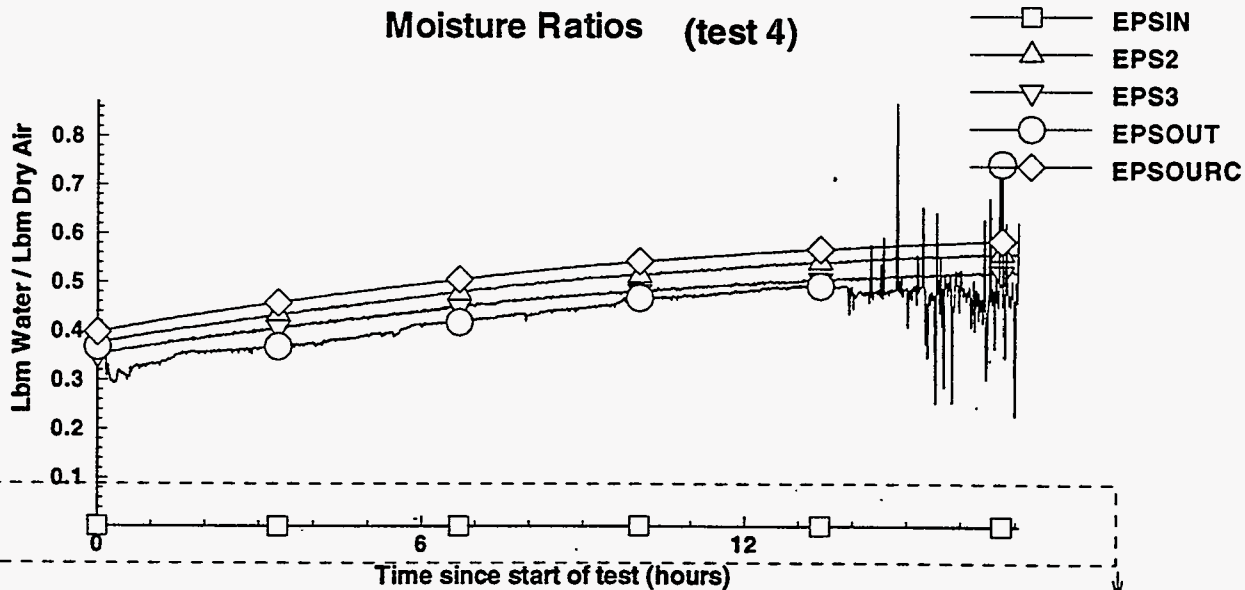


(2D) II Print II 19 Aug 1994 II test4.plt II TEST\_4\_DATA

### Thermocouple Temperatures (test 4)

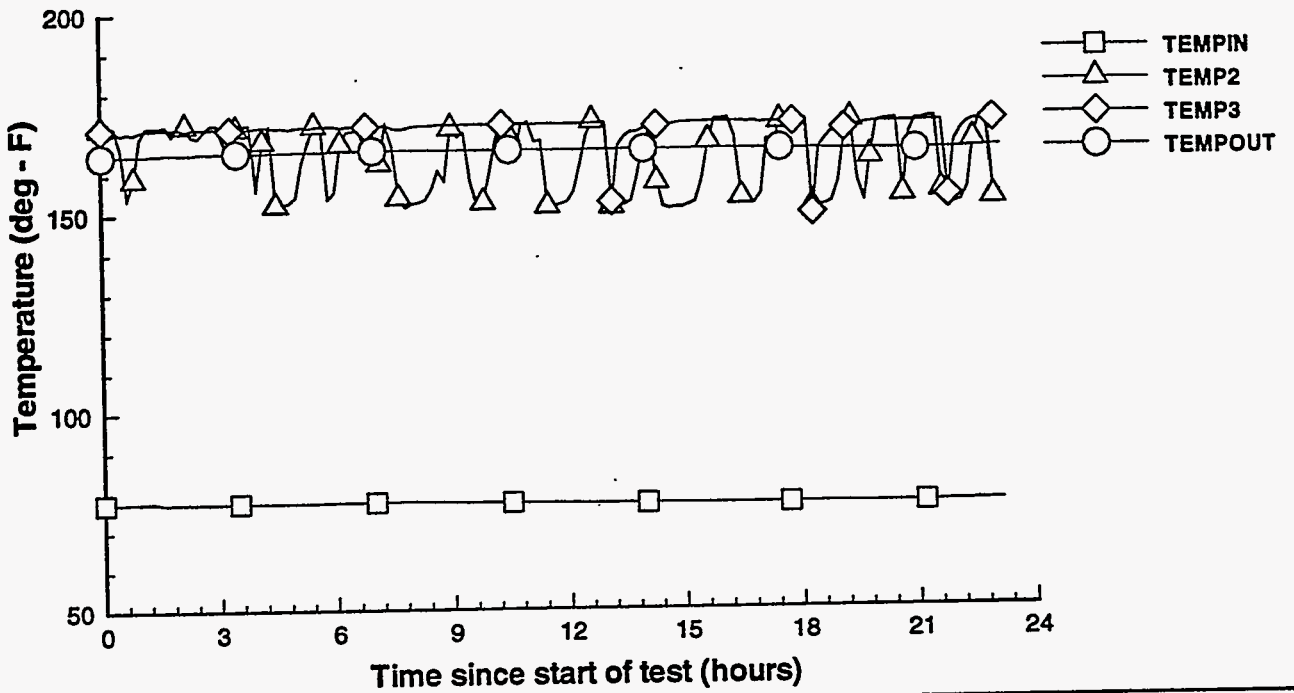


### Moisture Ratios (test 4)

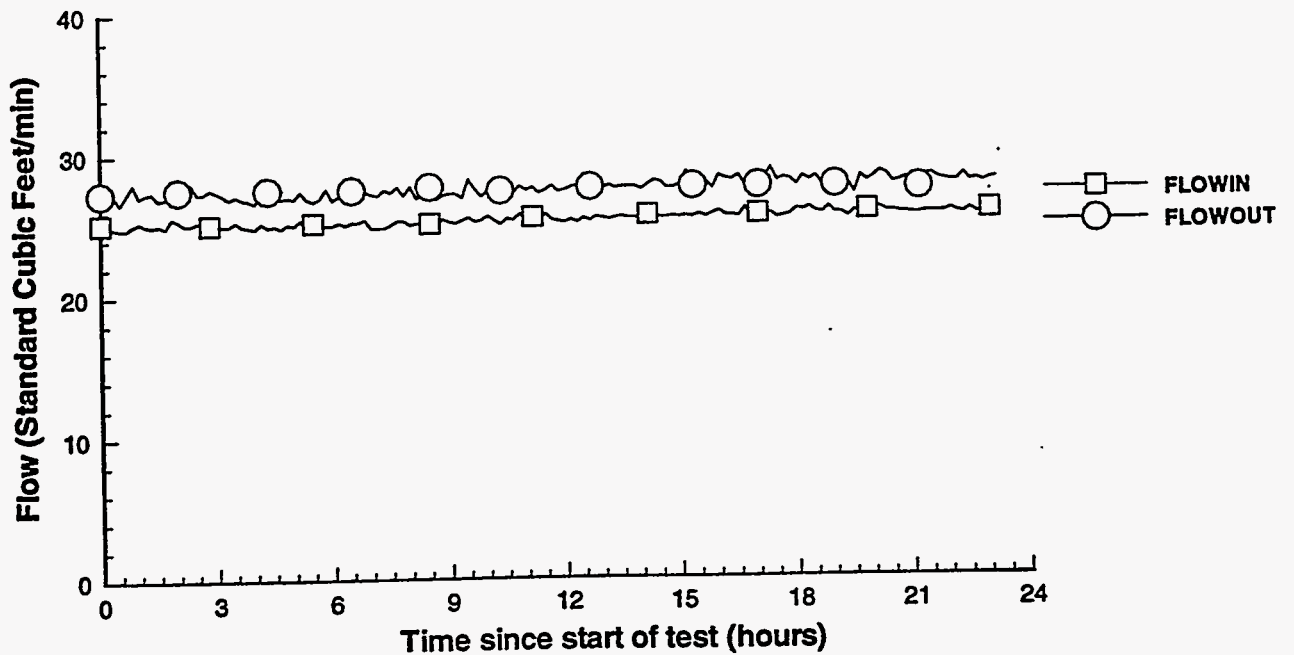


(2D) II Print II 3 Jun 1994 II test5.plt II TEST\_5\_DATA

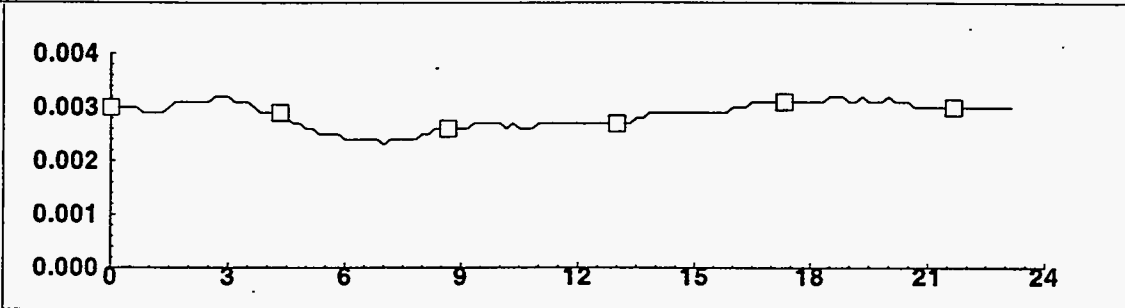
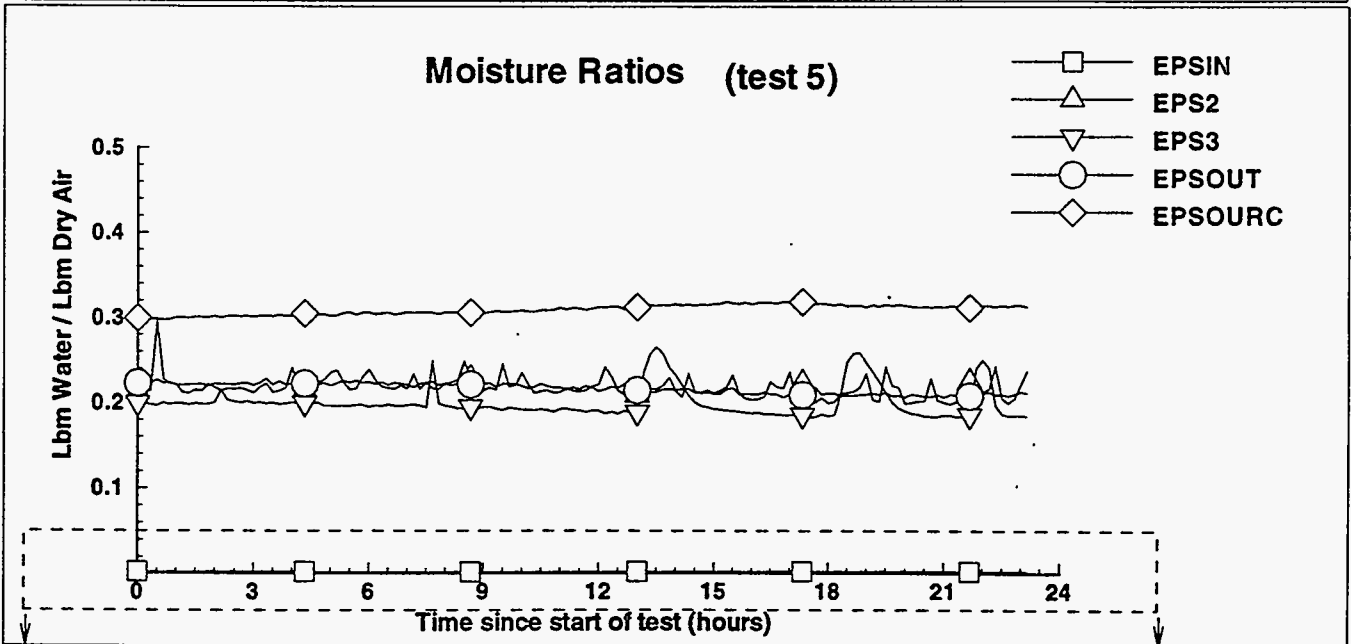
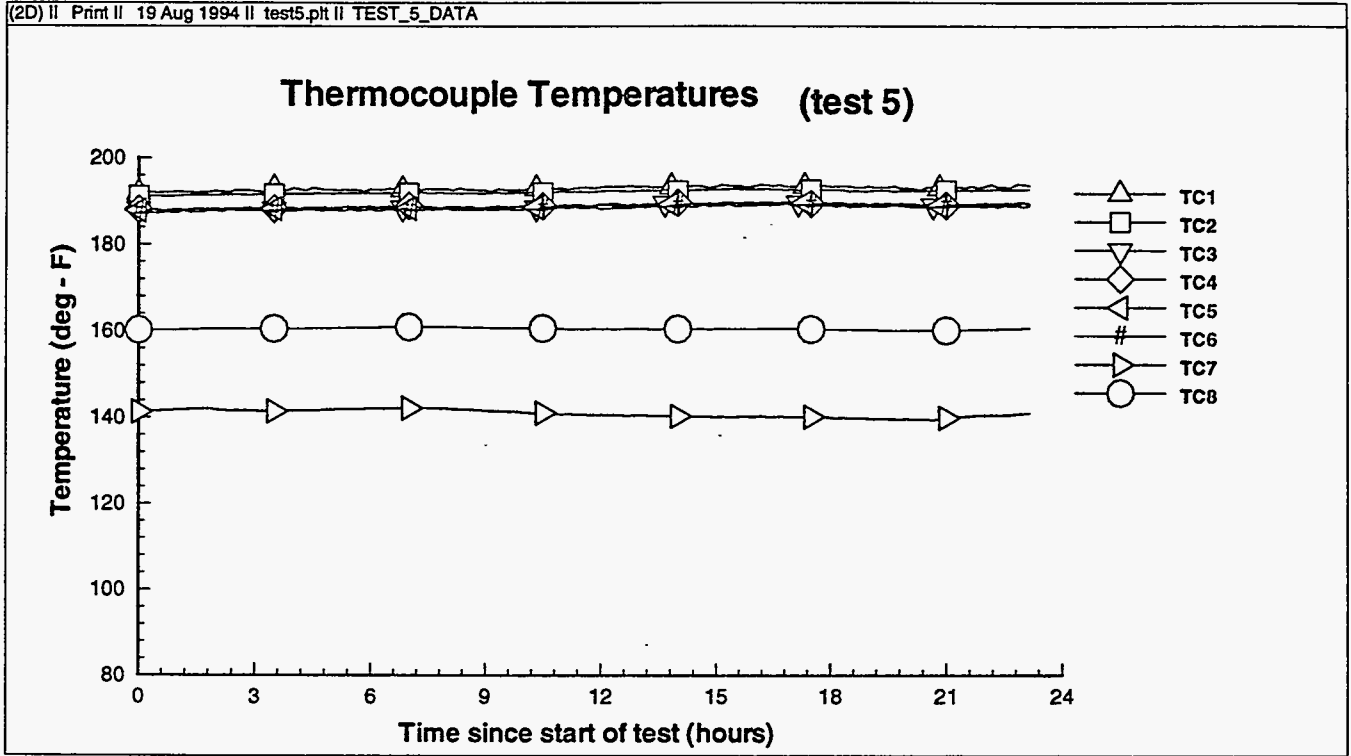
### RTD Temperatures (test 5)



### Vapor Space Air Flow (test 5)



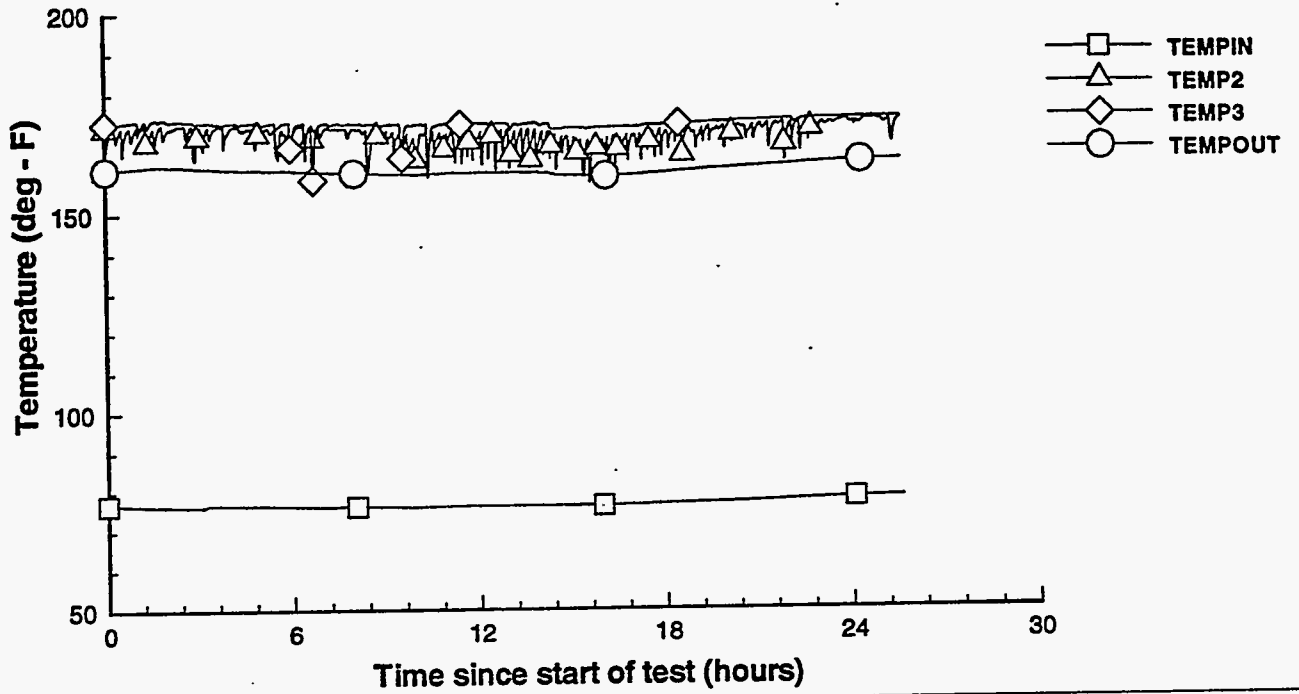
(2D) II Print II 19 Aug 1994 II test5.plt II TEST\_5\_DATA



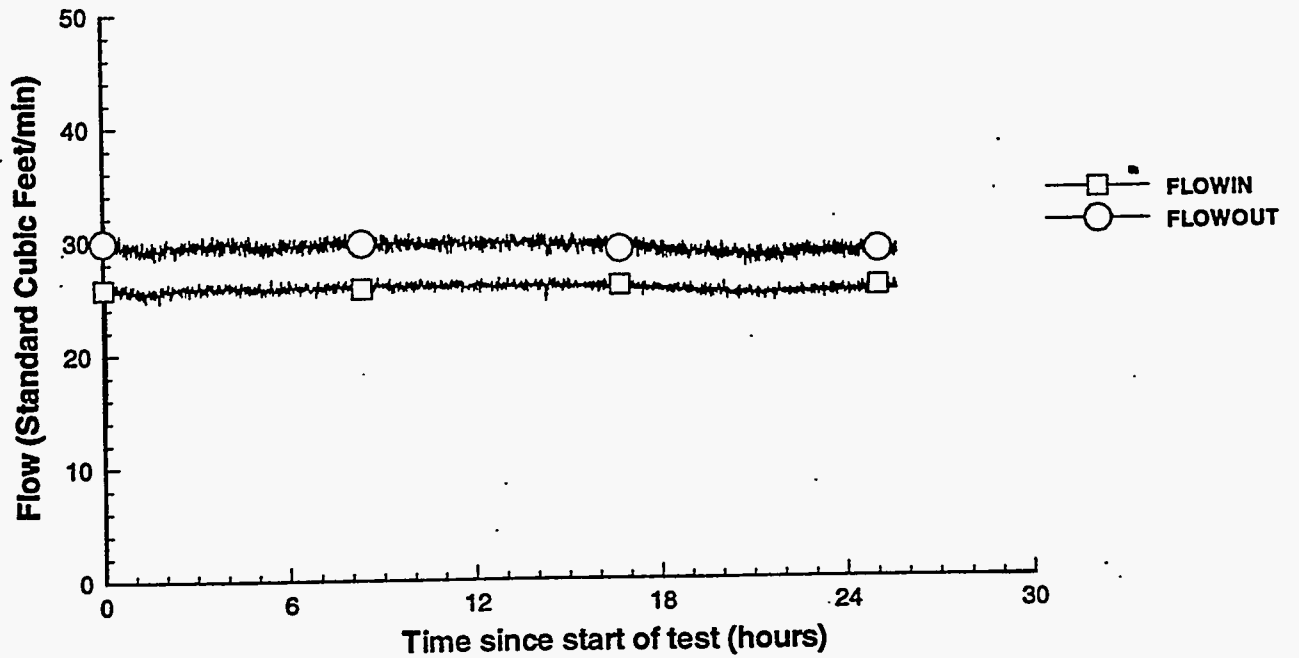


(2D) II Print II 22 Jun 1994 II test5.r.plt II TEST\_5R\_DATA

### RTD Temperatures (test 5R)

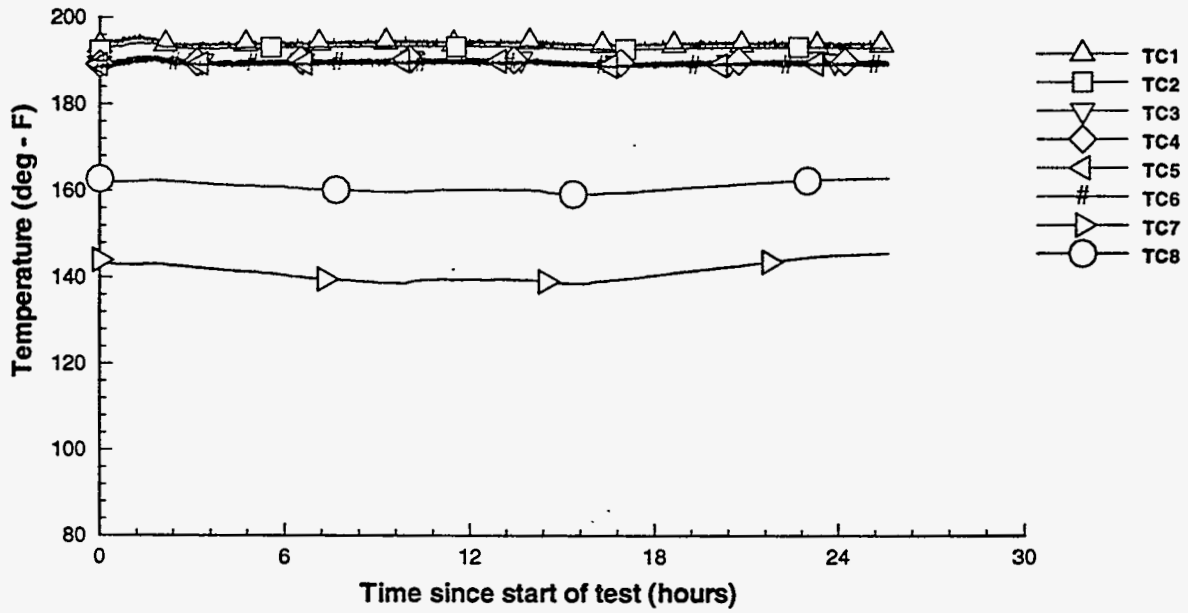


### Vapor Space Air Flow (test 5R)

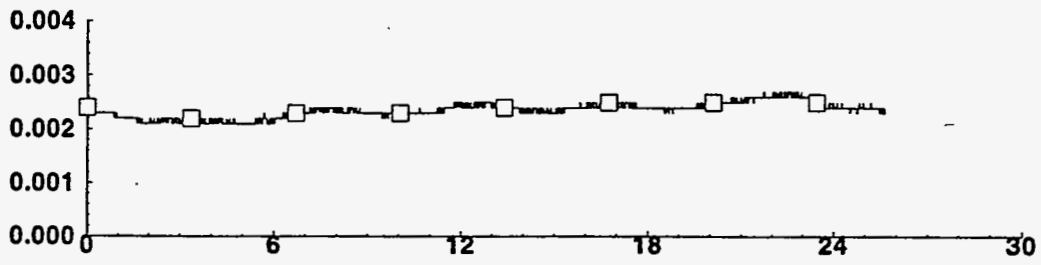
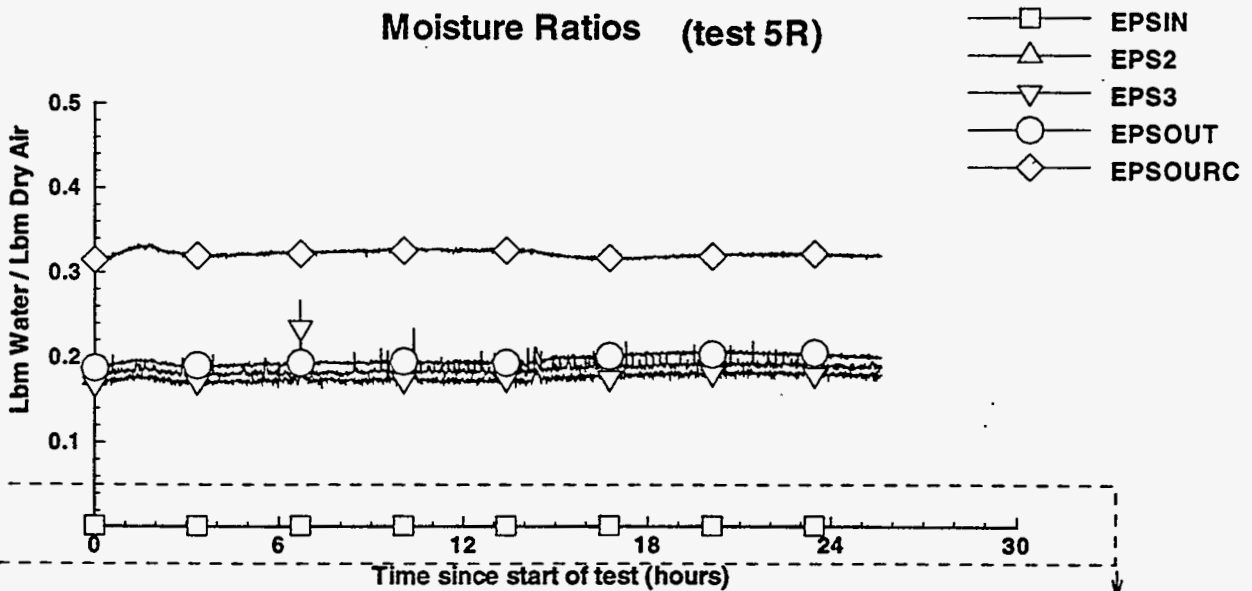


(2D) II Print II 19 Aug 1994 II test5.r.plt II TEST\_5R\_DATA

### Thermocouple Temperatures (test 5R)

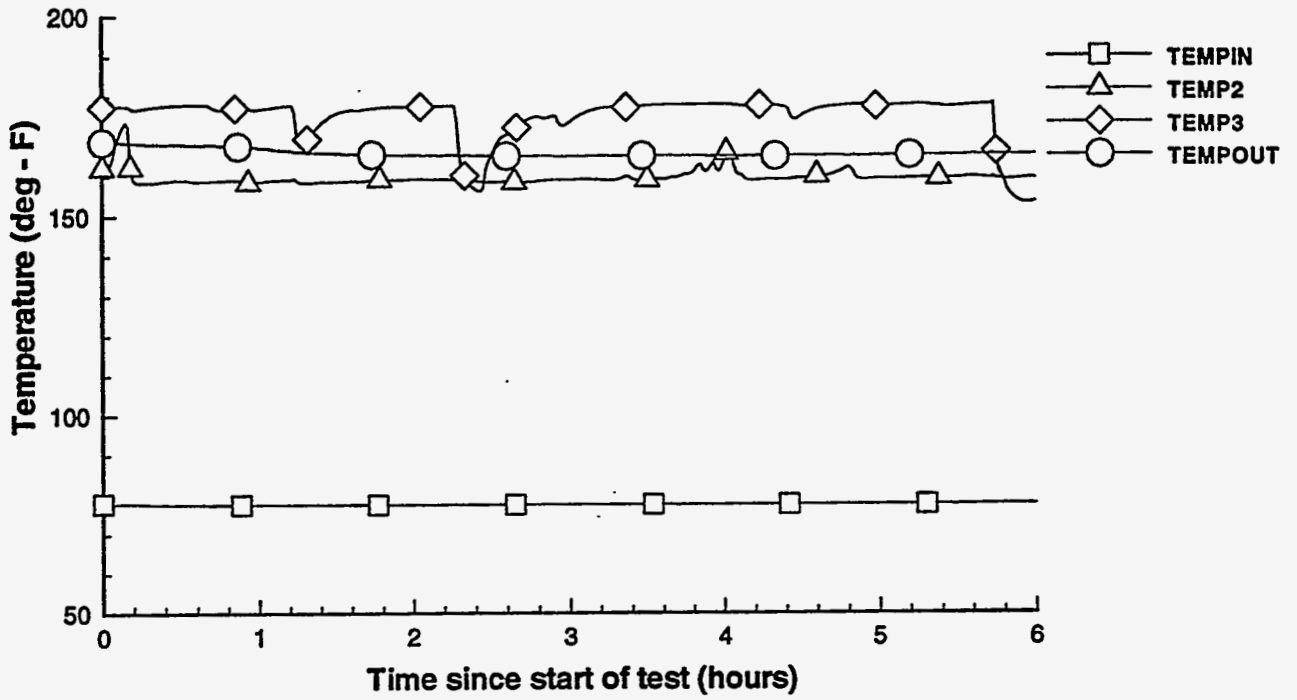


### Moisture Ratios (test 5R)

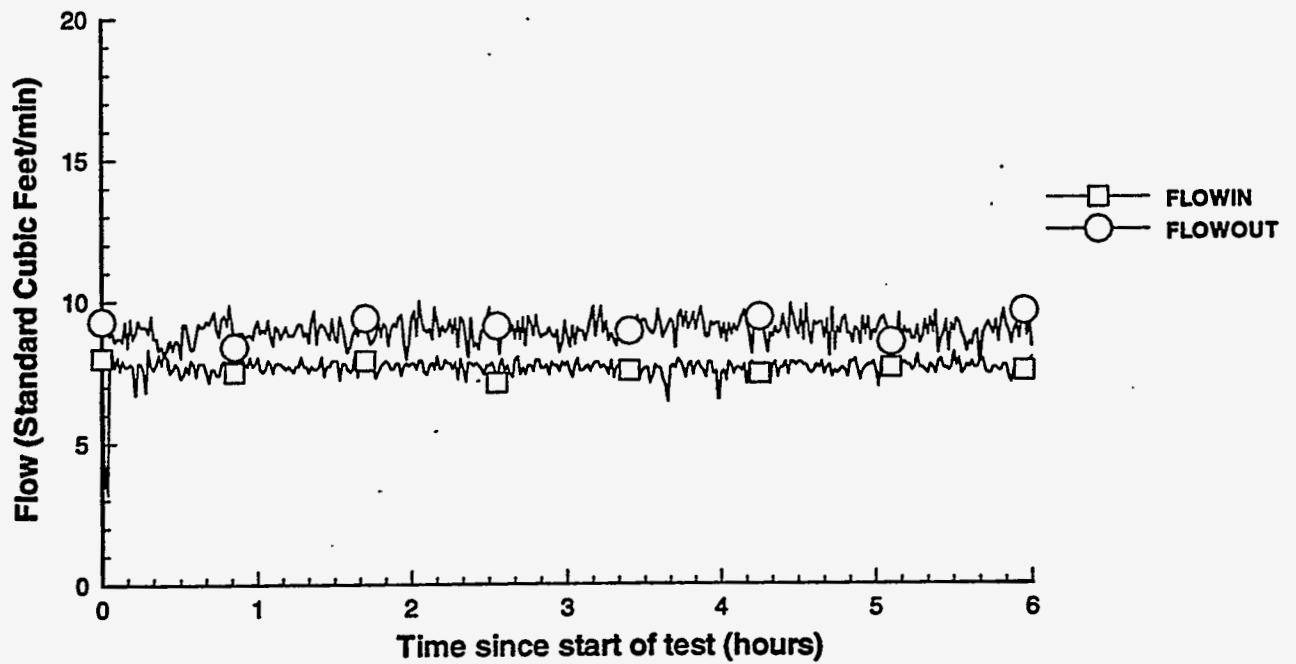


(2D) II Print II 3 Jun 1994 II test6.plt II TEST\_6\_DATA

### RTD Temperatures (test 6)

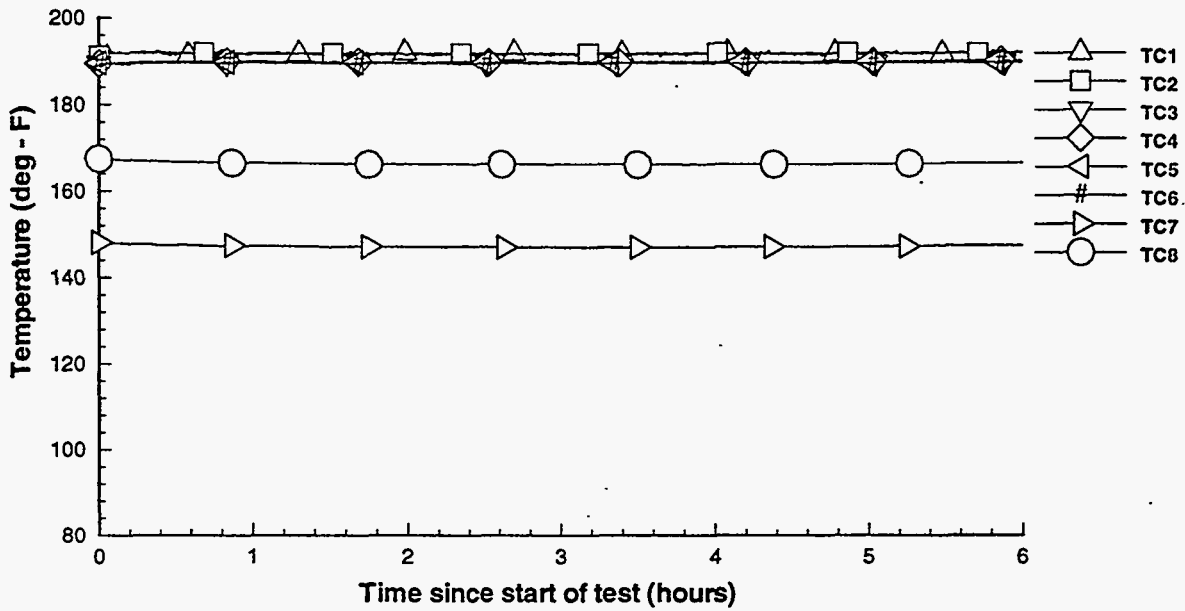


### Vapor Space Air Flow (test 6)

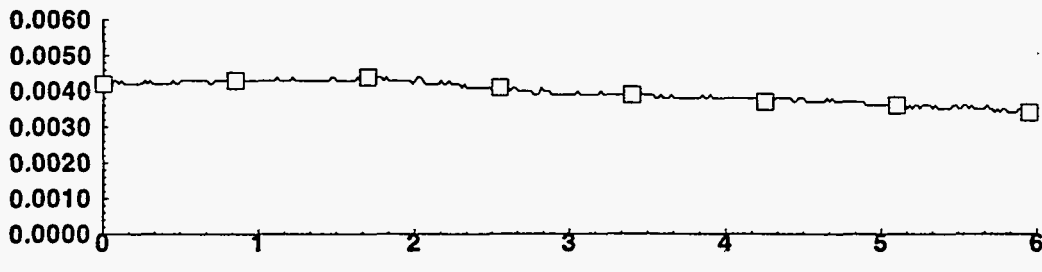
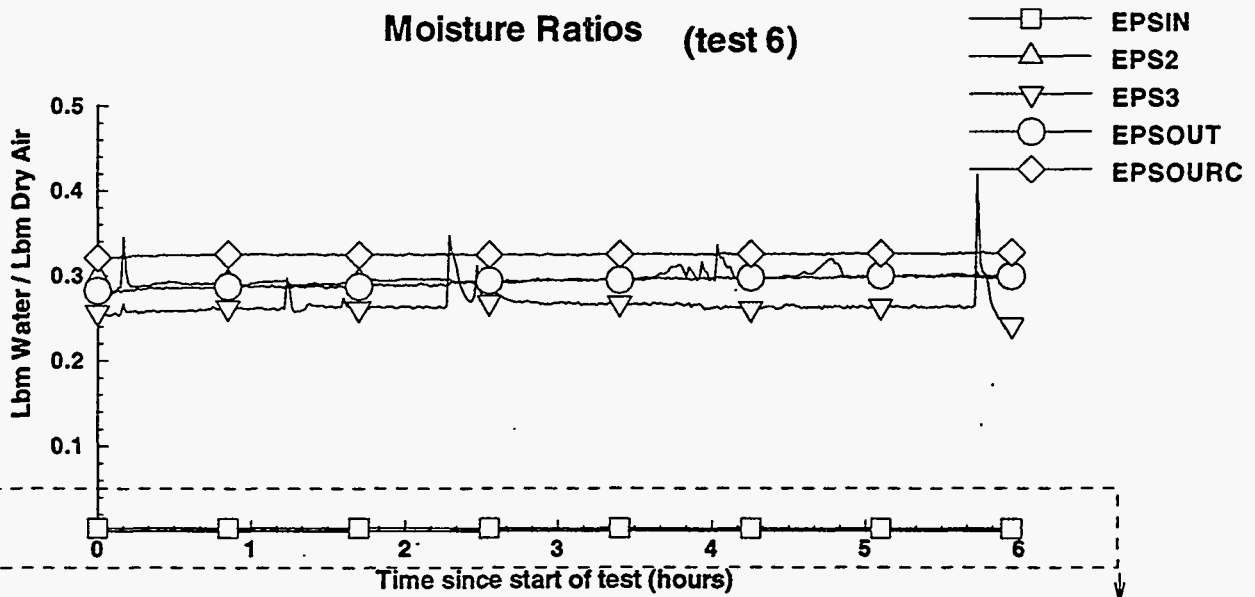


(2D) II Print II 19 Aug 1994 II test6.plt II TEST\_6\_DATA

### Thermocouple Temperatures (test 6)

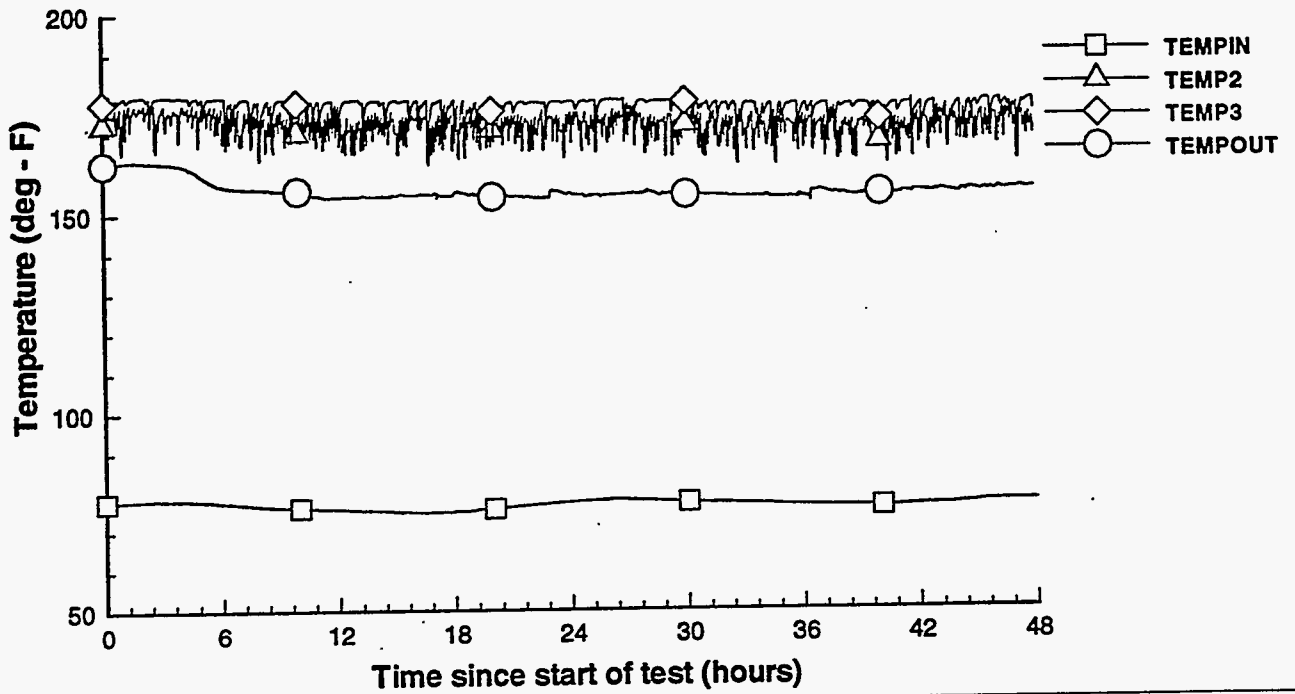


### Moisture Ratios (test 6)

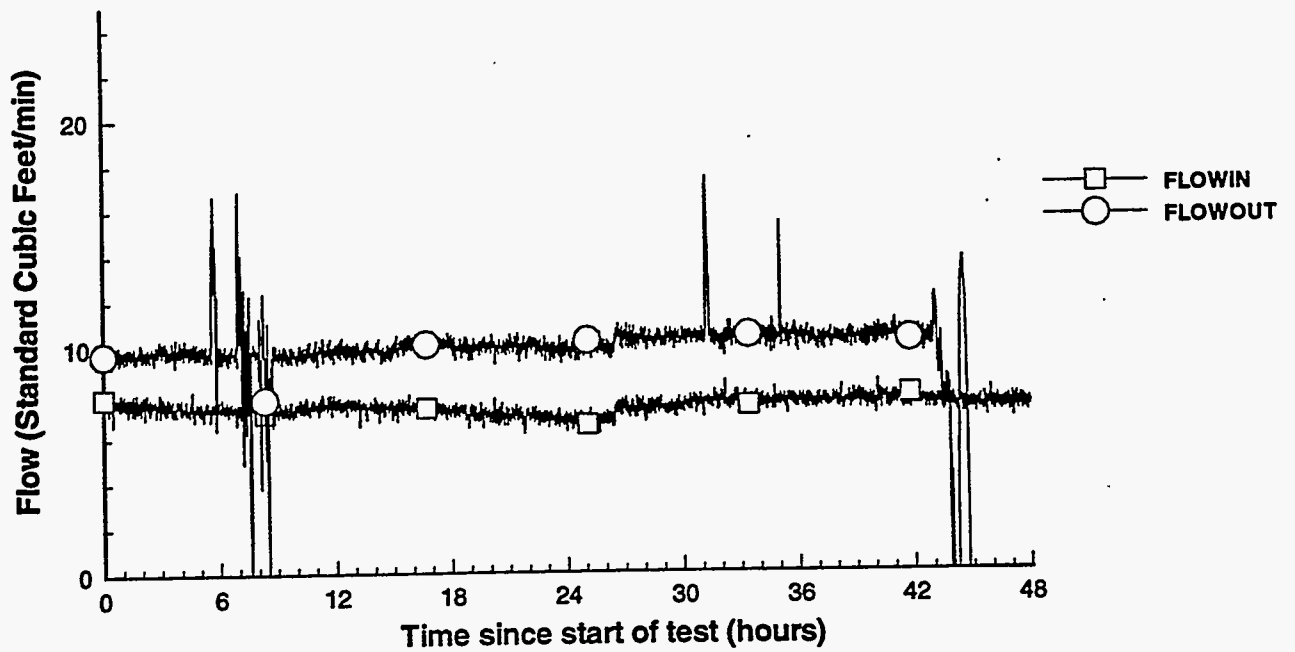


(2D) II Print II 22 Jun 1994 II test6.r.plt II TEST\_6R\_DATA

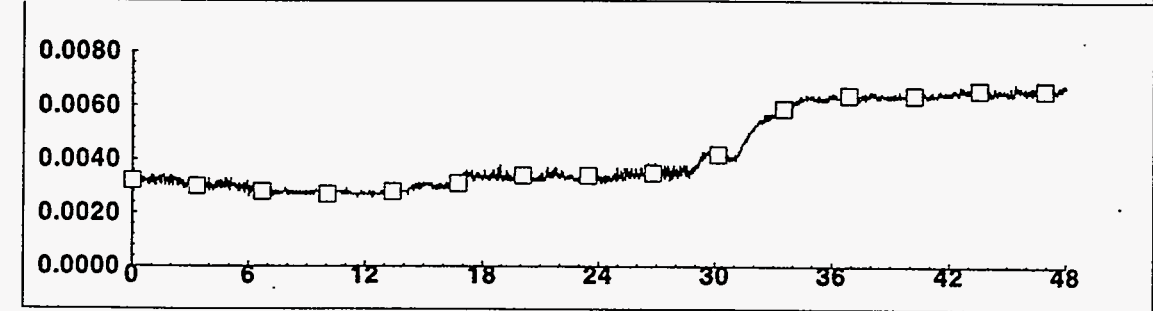
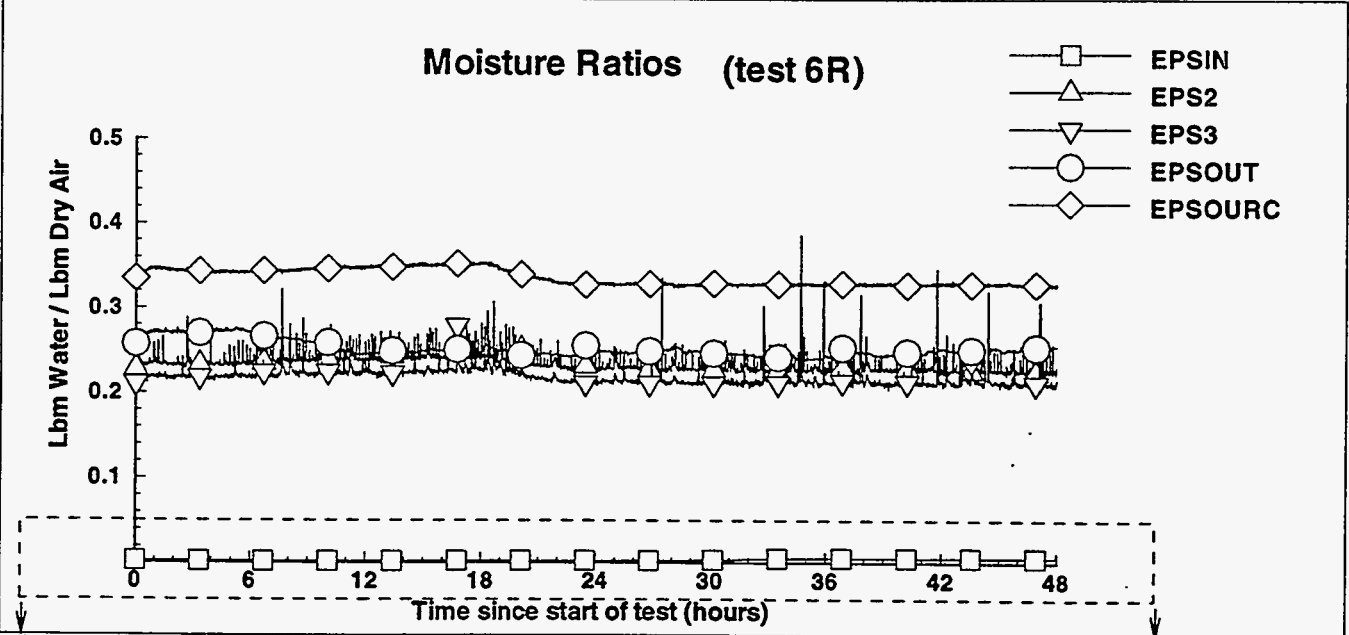
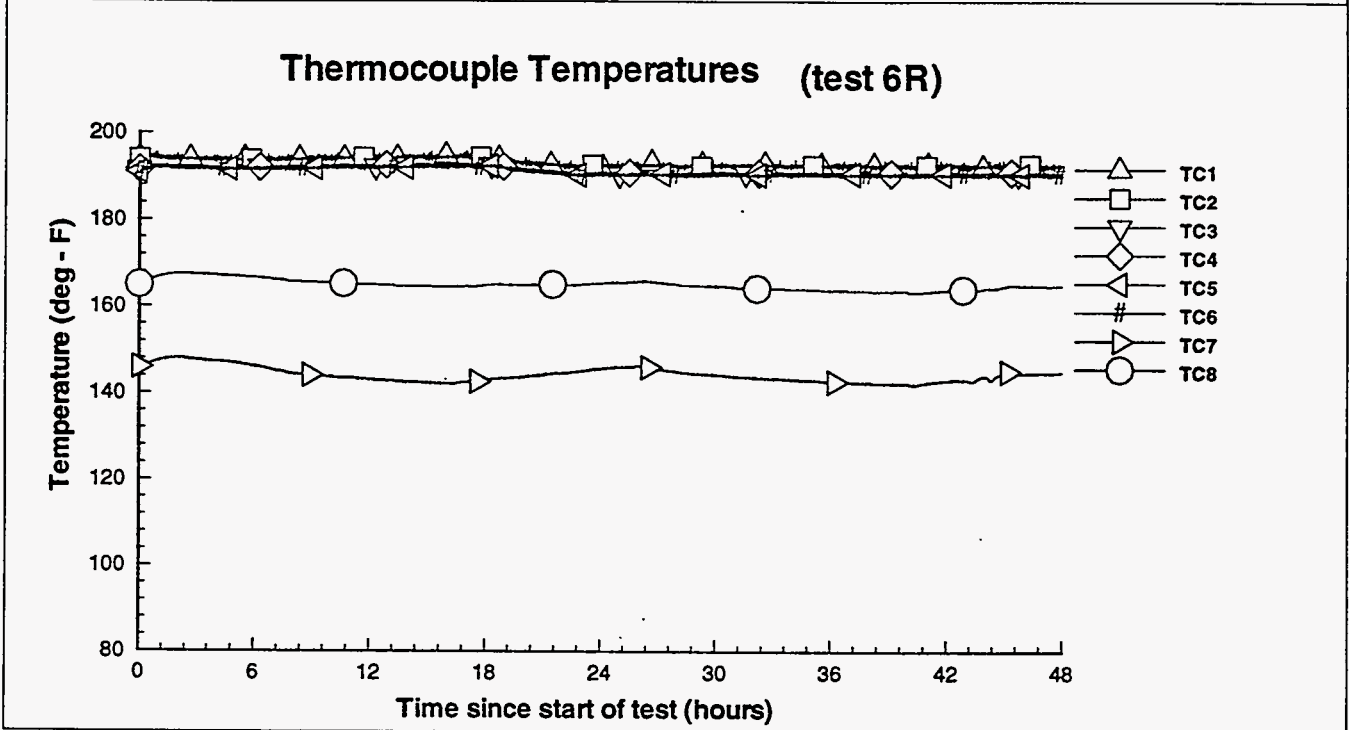
### RTD Temperatures (test 6R)



### Vapor Space Air Flow (test 6R)

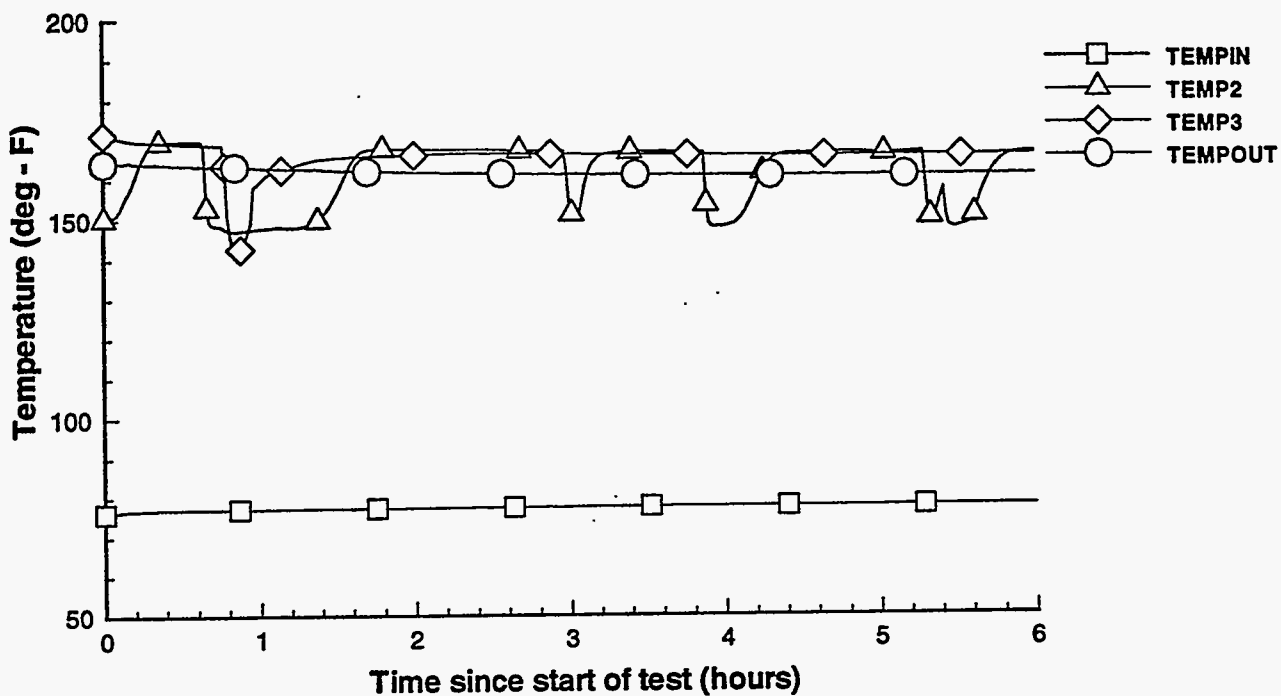


(2D) II Print II 19 Aug 1994 II test6.r.plt II TEST\_6R\_DATA

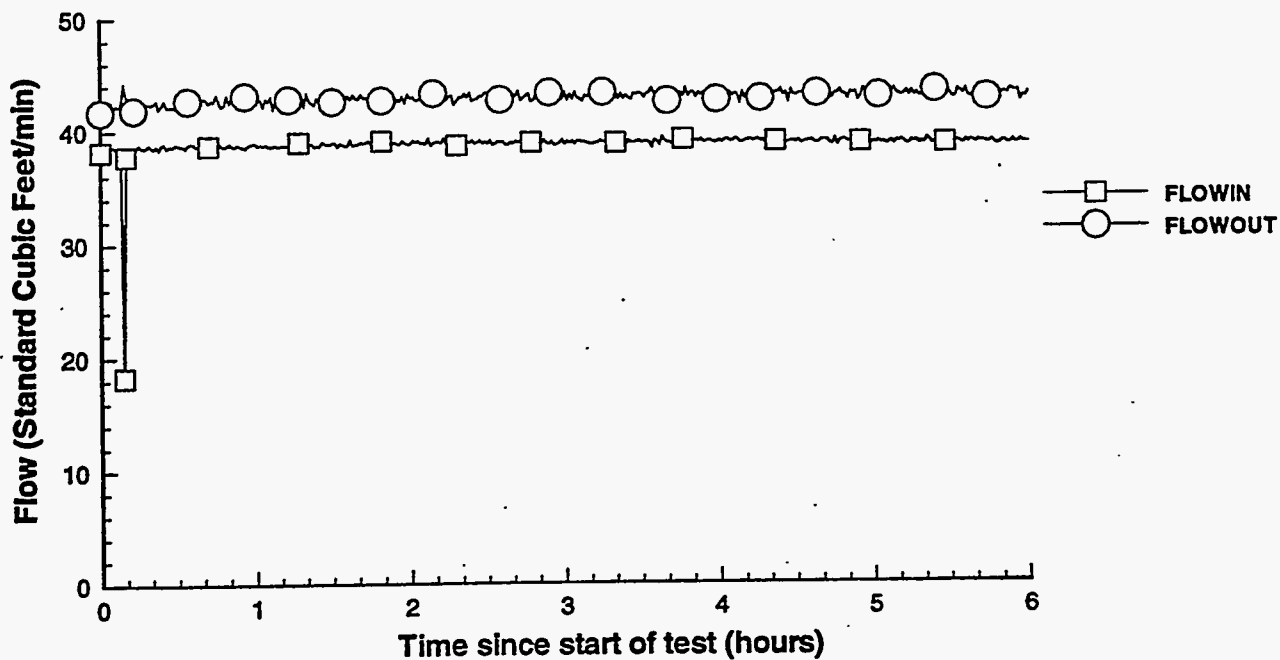


(2D) II Print II 8 Jun 1994 II test7.plt II TEST\_7\_DATA

### RTD Temperatures (test 7)

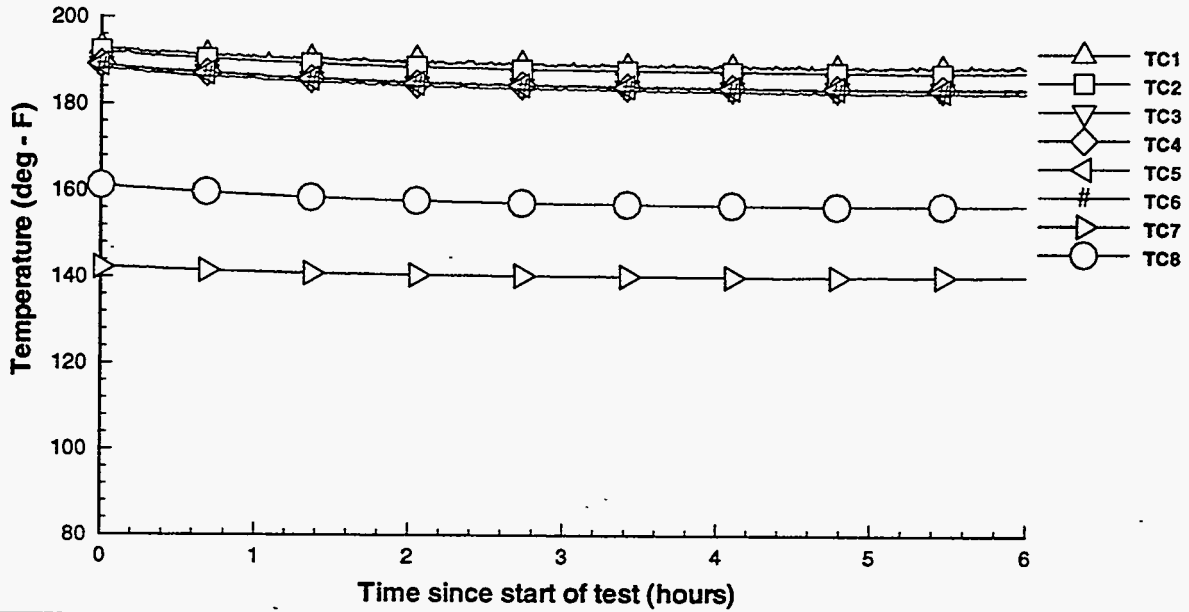


### Vapor Space Air Flow (test 7)

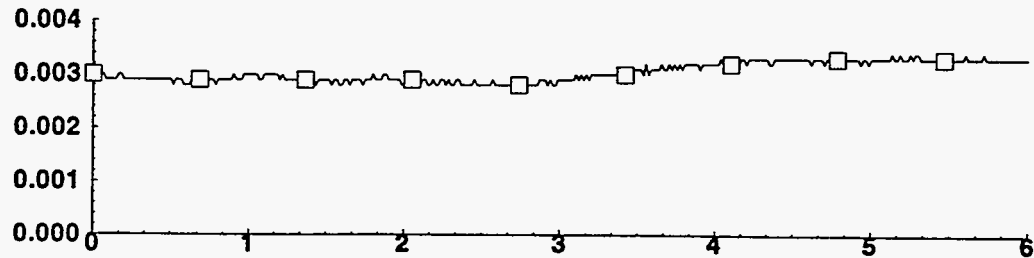
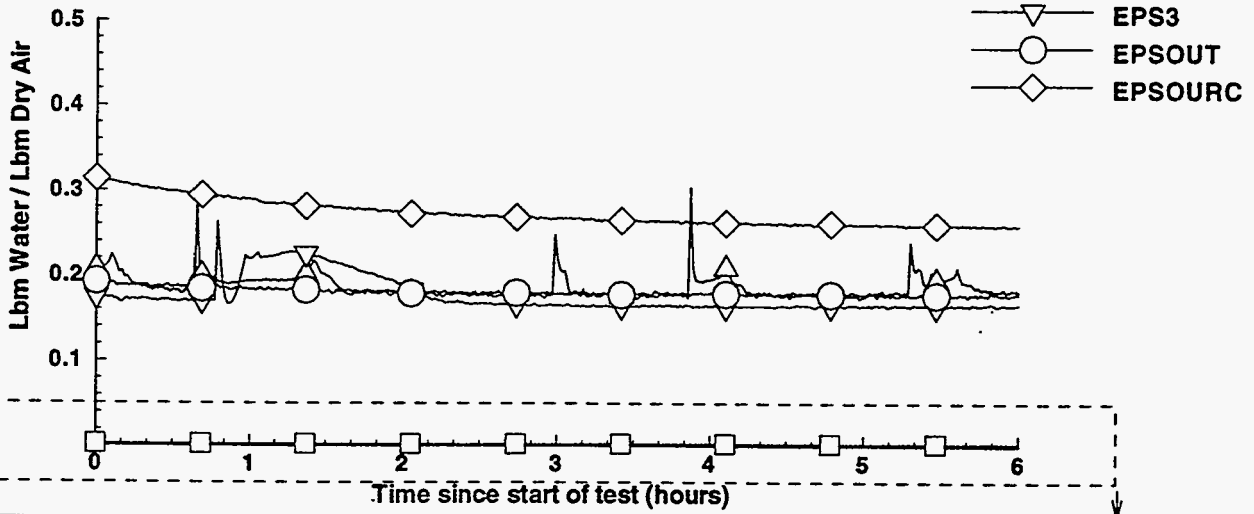


(2D) II Print II 19 Aug 1994 II test7.plt II TEST\_7\_DATA

### Thermocouple Temperatures (test 7)



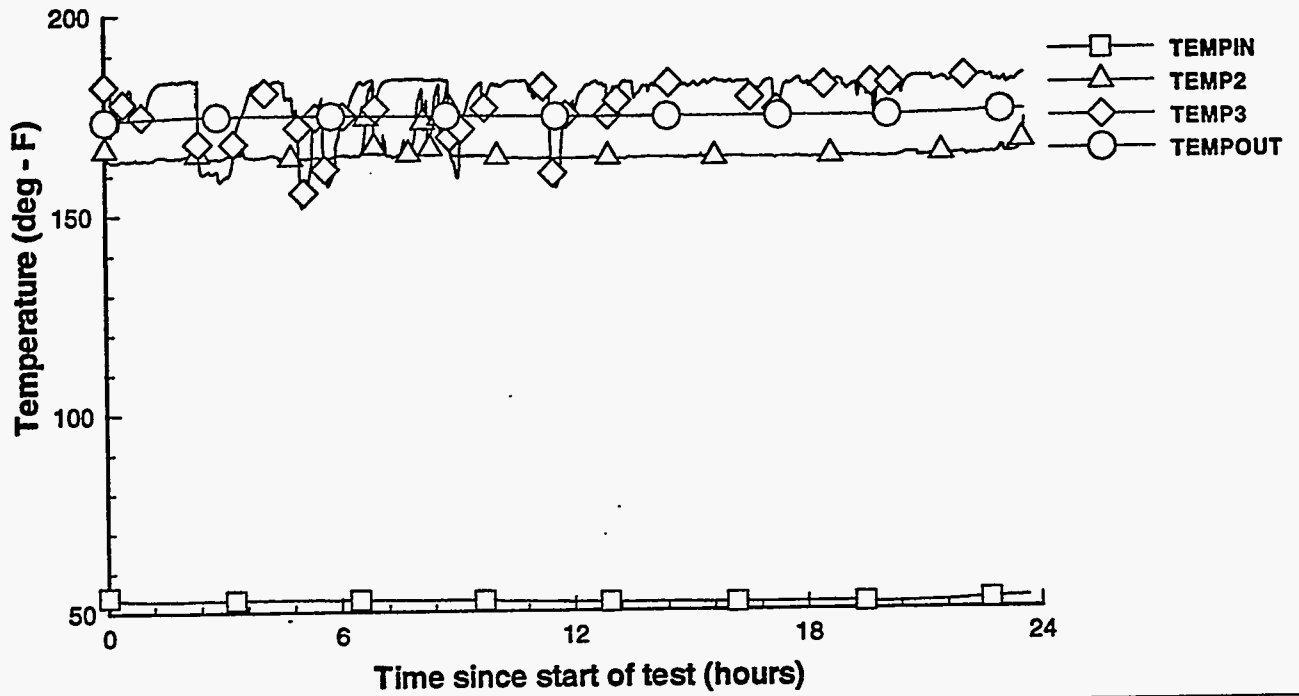
### Moisture Ratios (test 7)



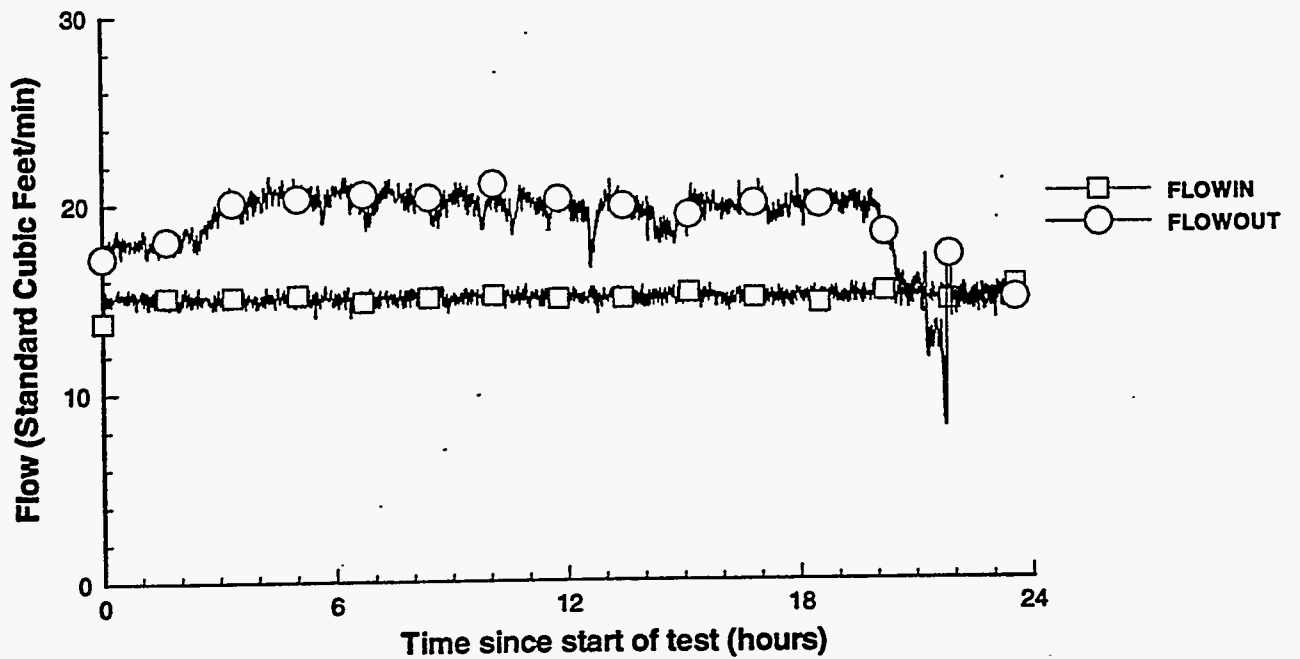


(2D) II Print II 8 Jun 1994 II test8.plt II TEST\_8\_DATA

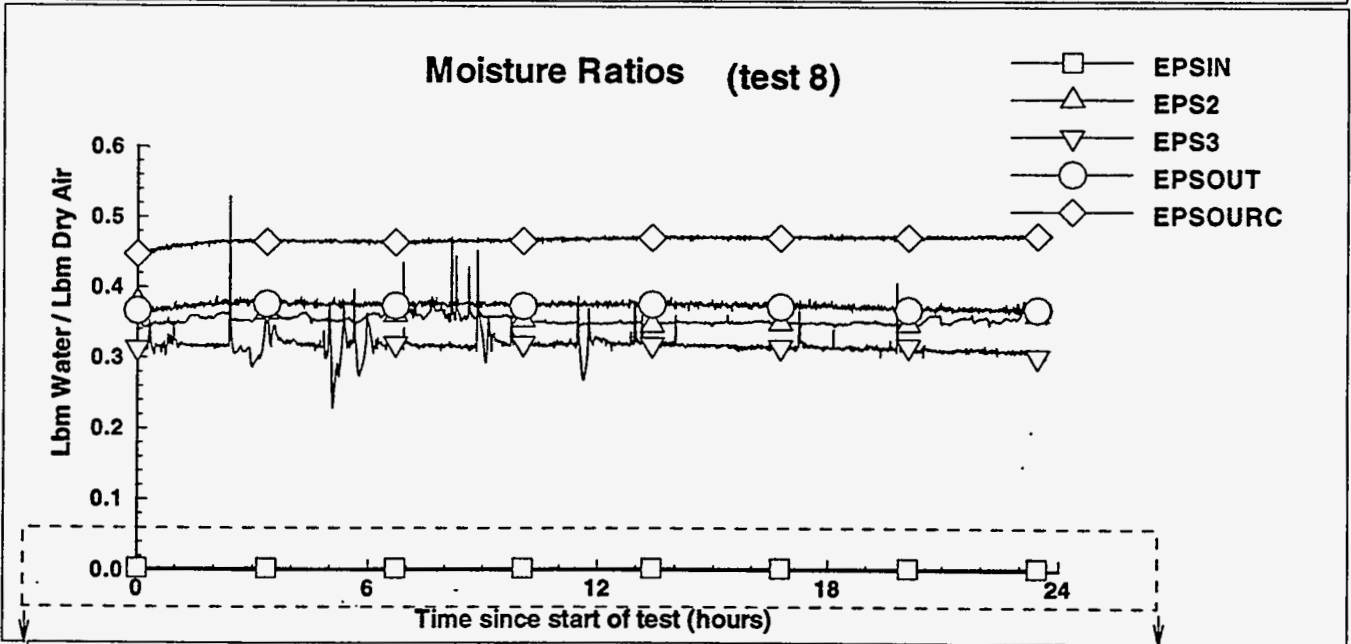
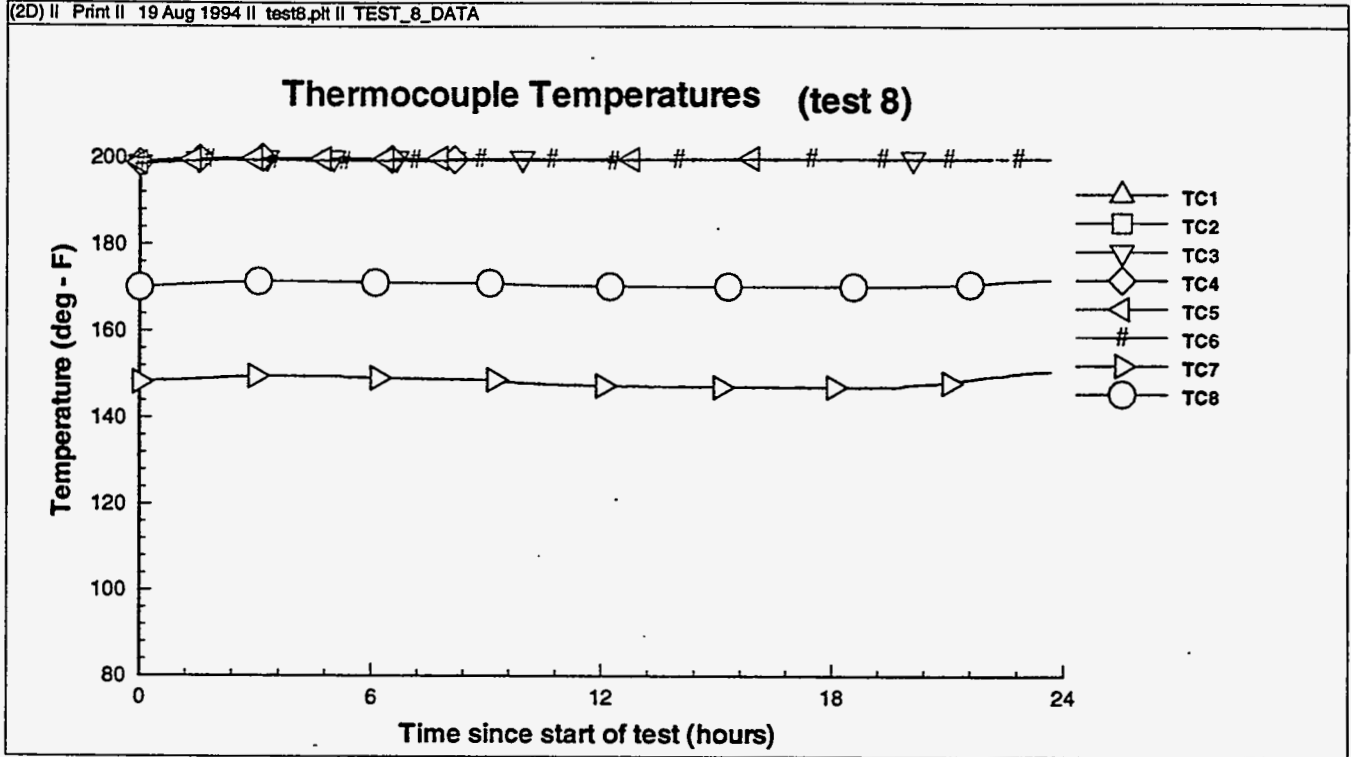
### RTD Temperatures (test 8)



### Vapor Space Air Flow (test 8)

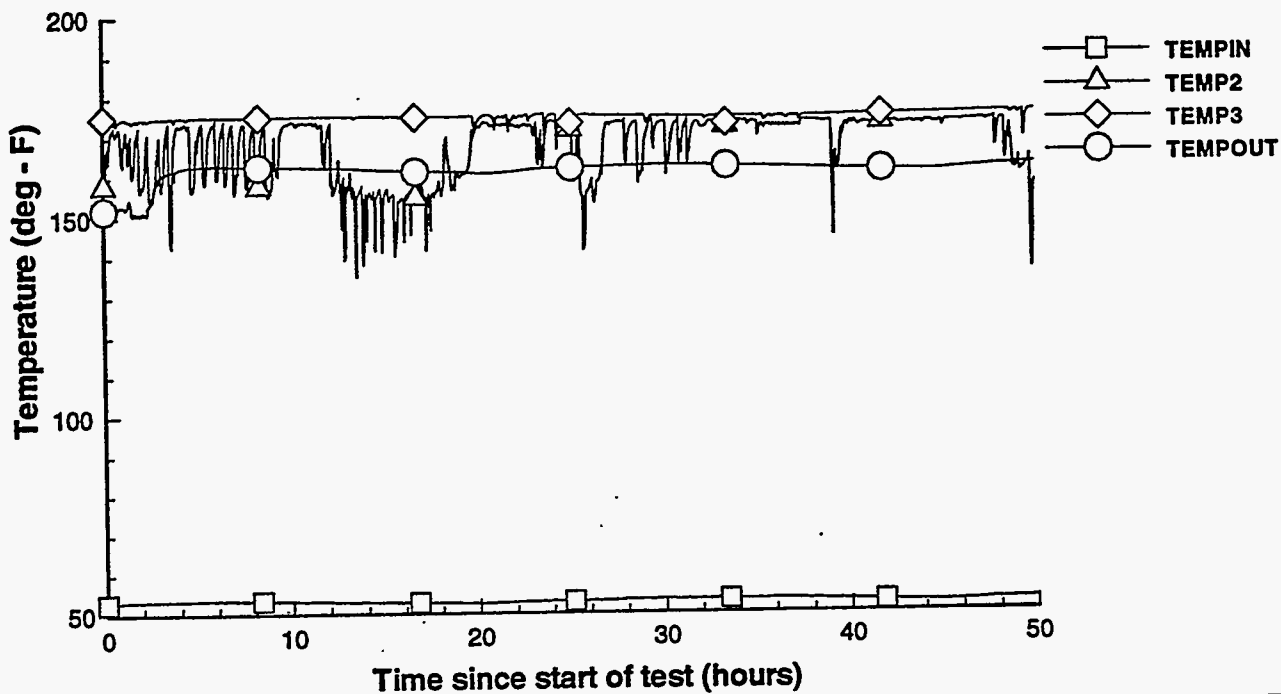


(2D) II Print II 19 Aug 1994 II test8.plt II TEST\_8\_DATA

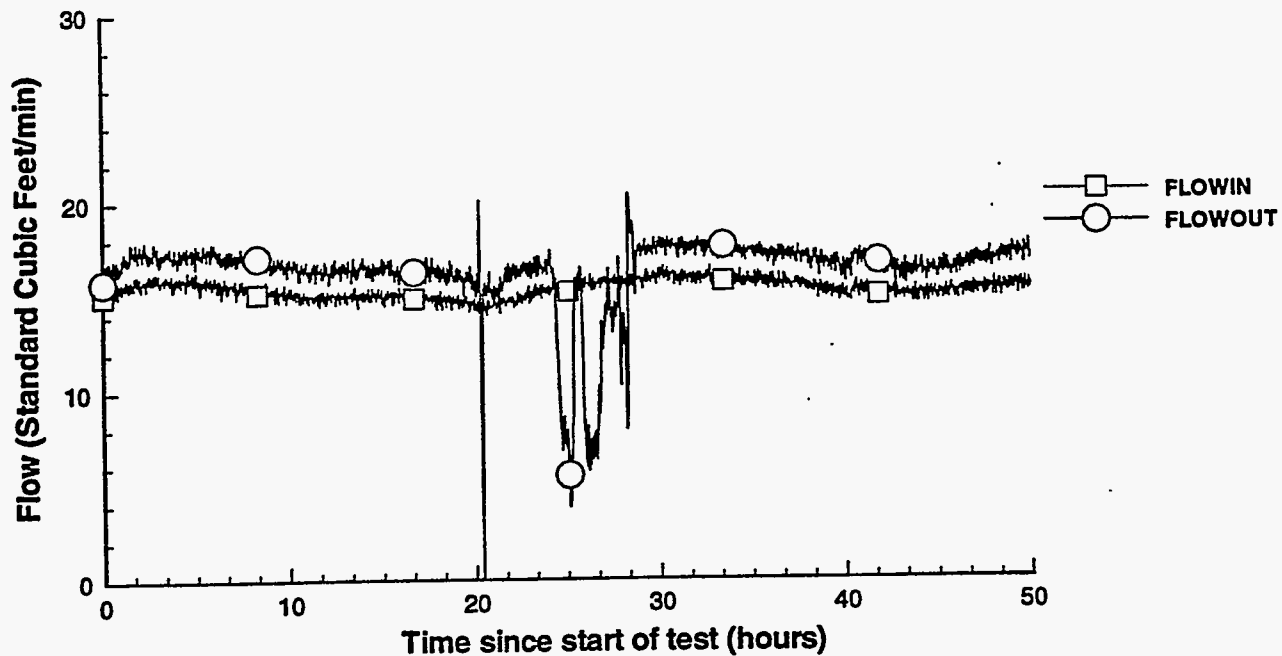


(2D) II Print II 8 Jun 1994 II test9.plt II TEST\_9\_DATA

### RTD Temperatures (test 9)

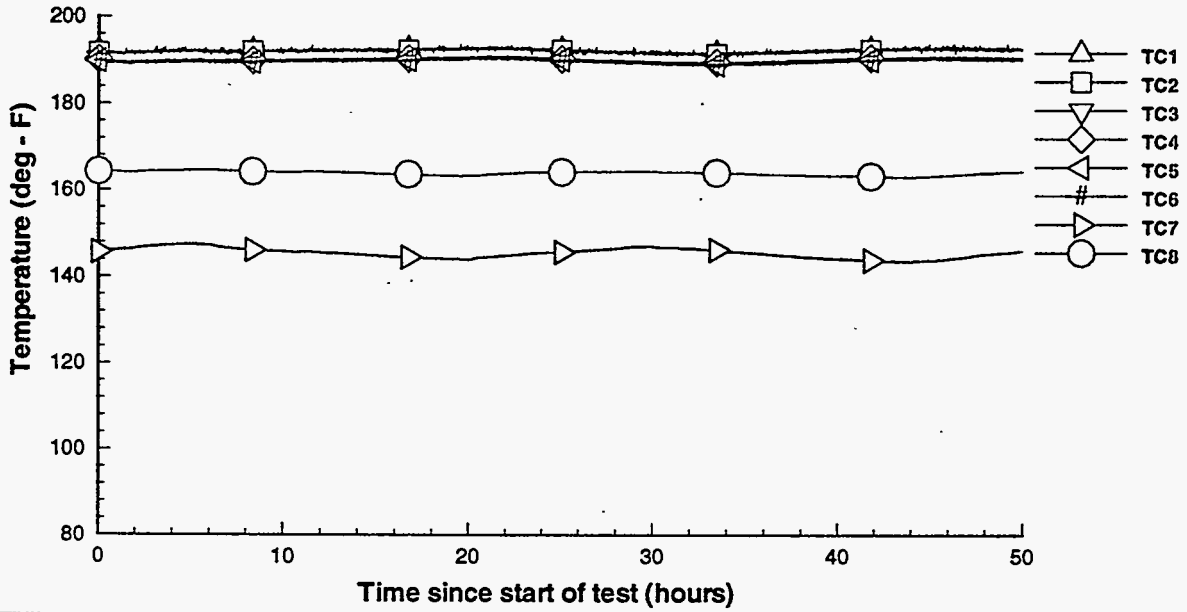


### Vapor Space Air Flow (test 9)

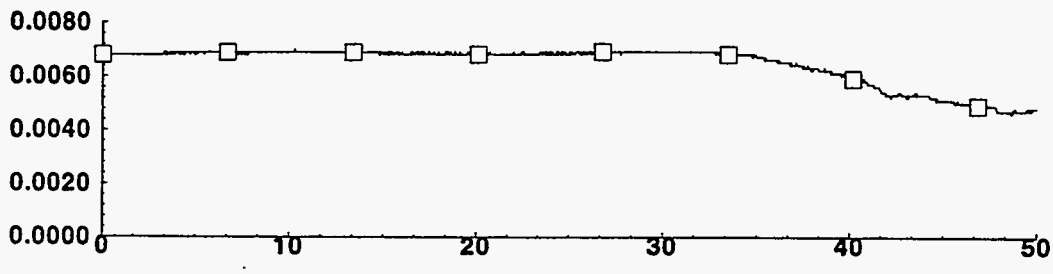
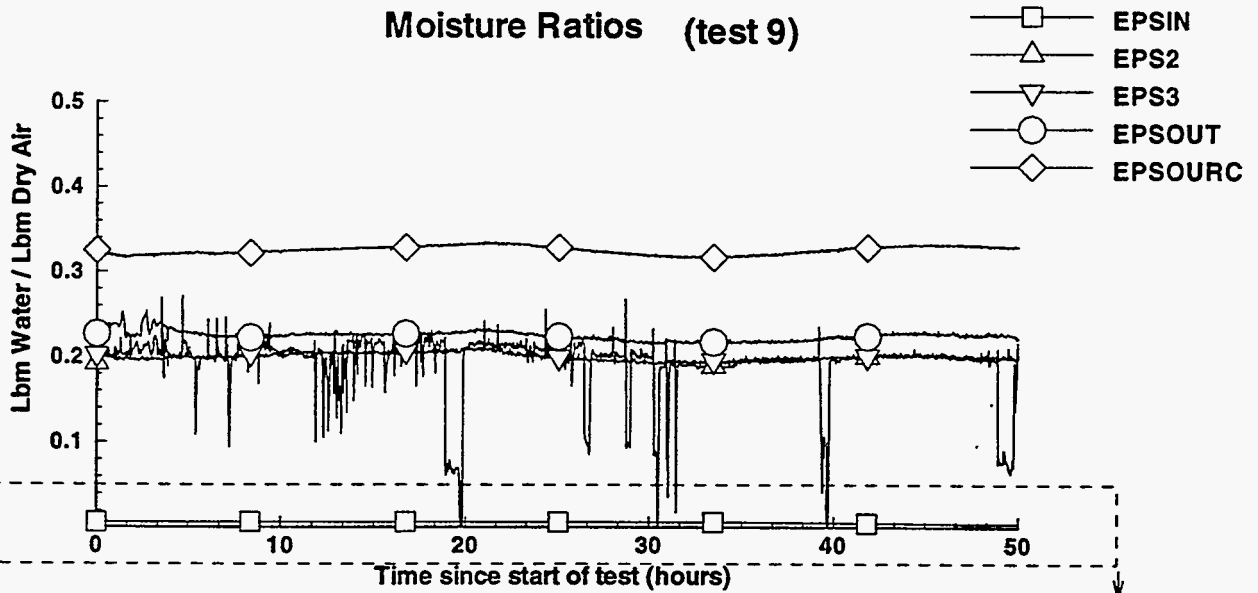


(2D) II Print II 19 Aug 1994 II test9.ph II TEST\_9\_DATA

### Thermocouple Temperatures (test 9)

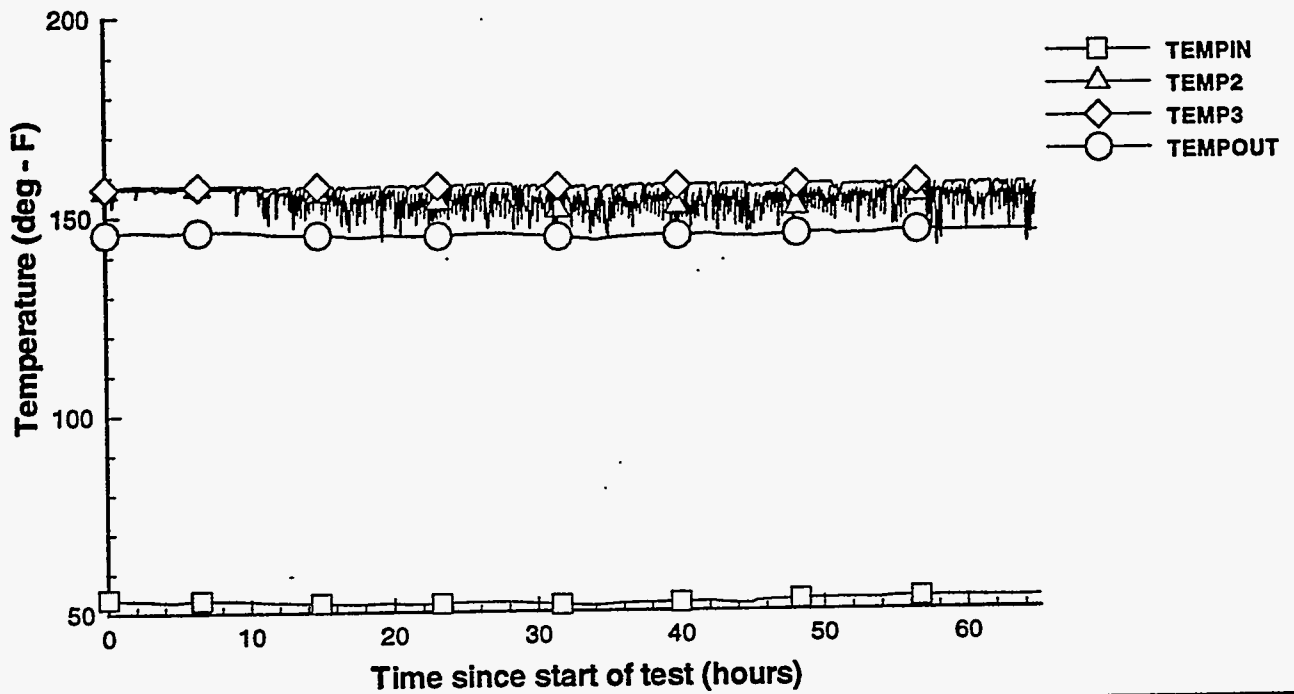


### Moisture Ratios (test 9)

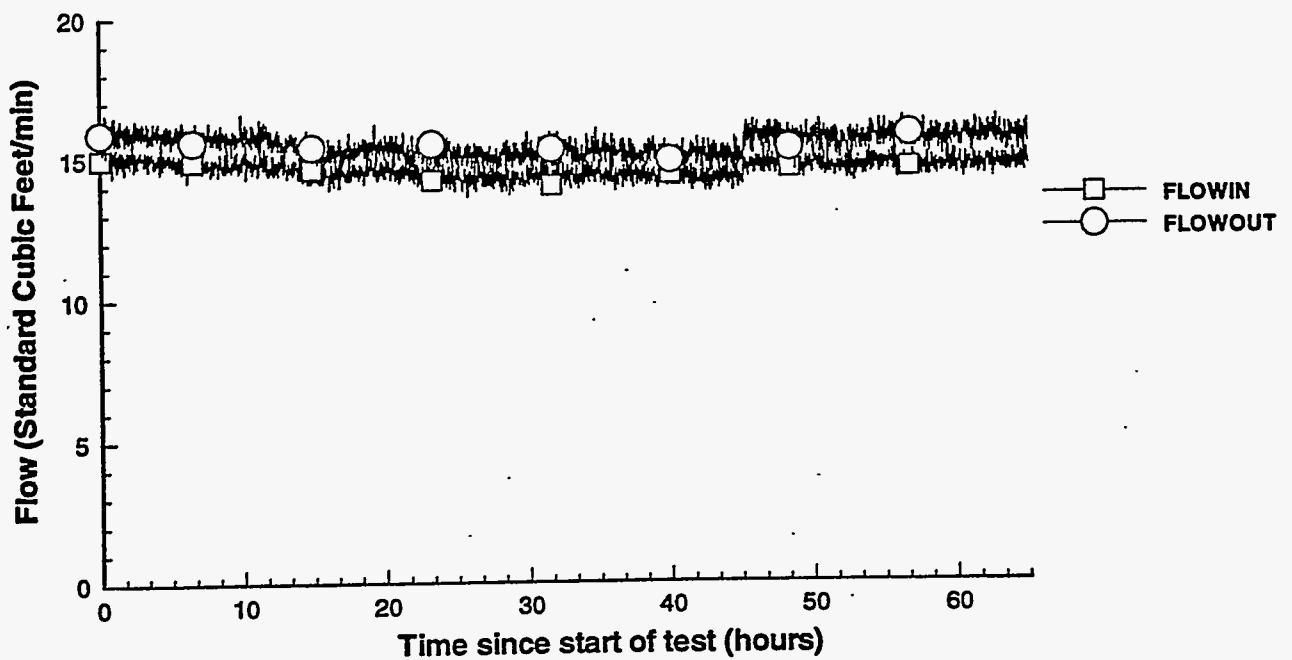


(2D) II Print II 1 Jul 1994 II test10.pt II TEST\_10\_DATA

### RTD Temperatures (test 10-10R)

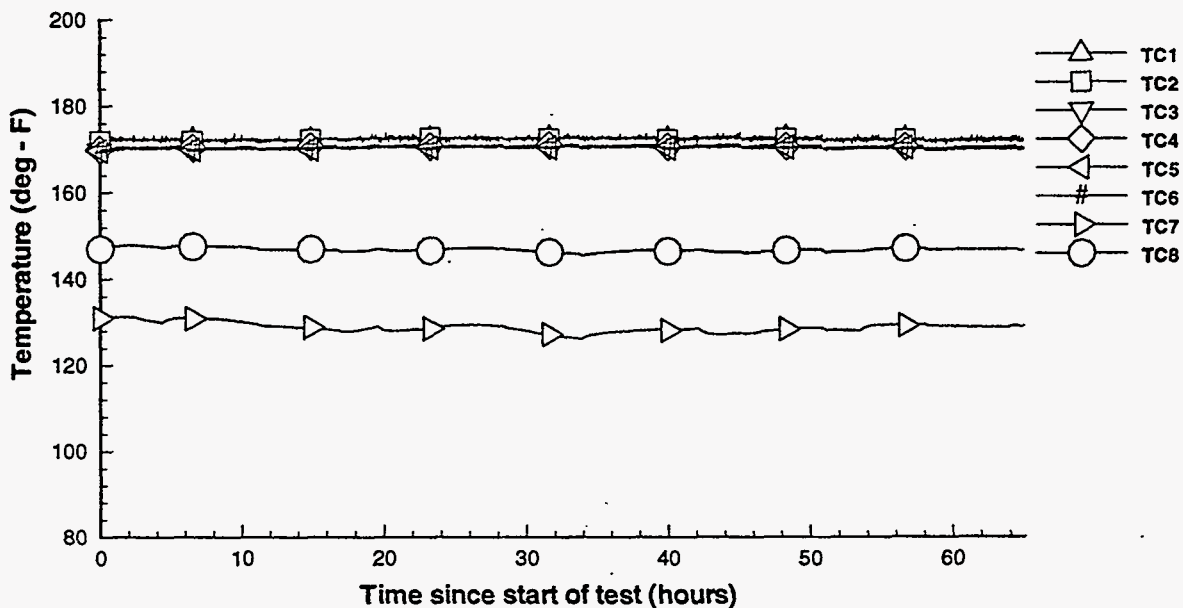


### Vapor Space Air Flow (test 10-10R)

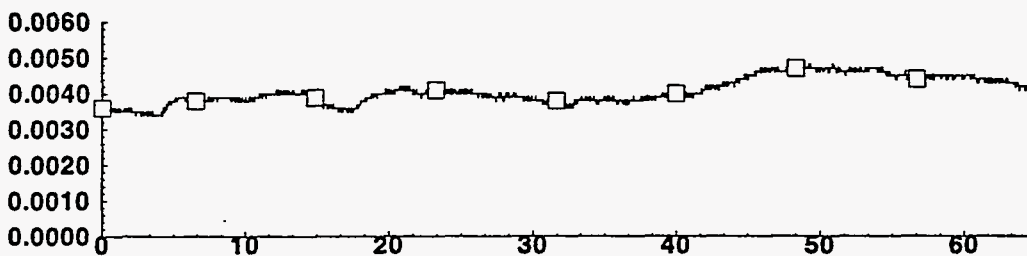
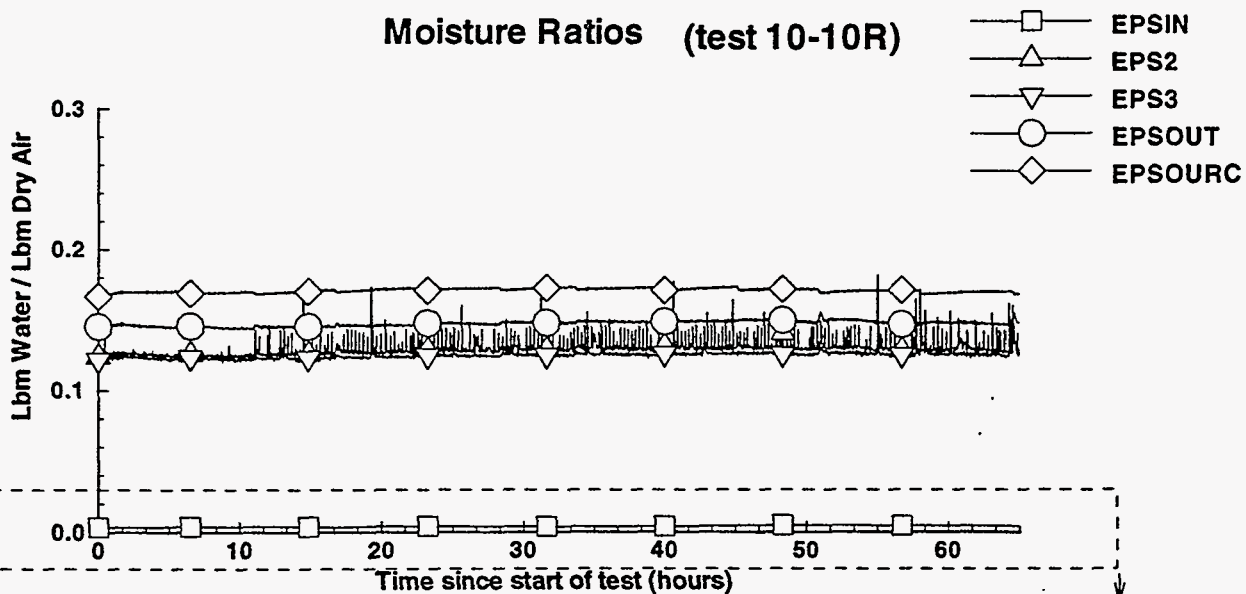


(2D) II Print II 19 Aug 1994 II test10.plt II TEST\_10\_DATA

### Thermocouple Temperatures (test 10-10R)

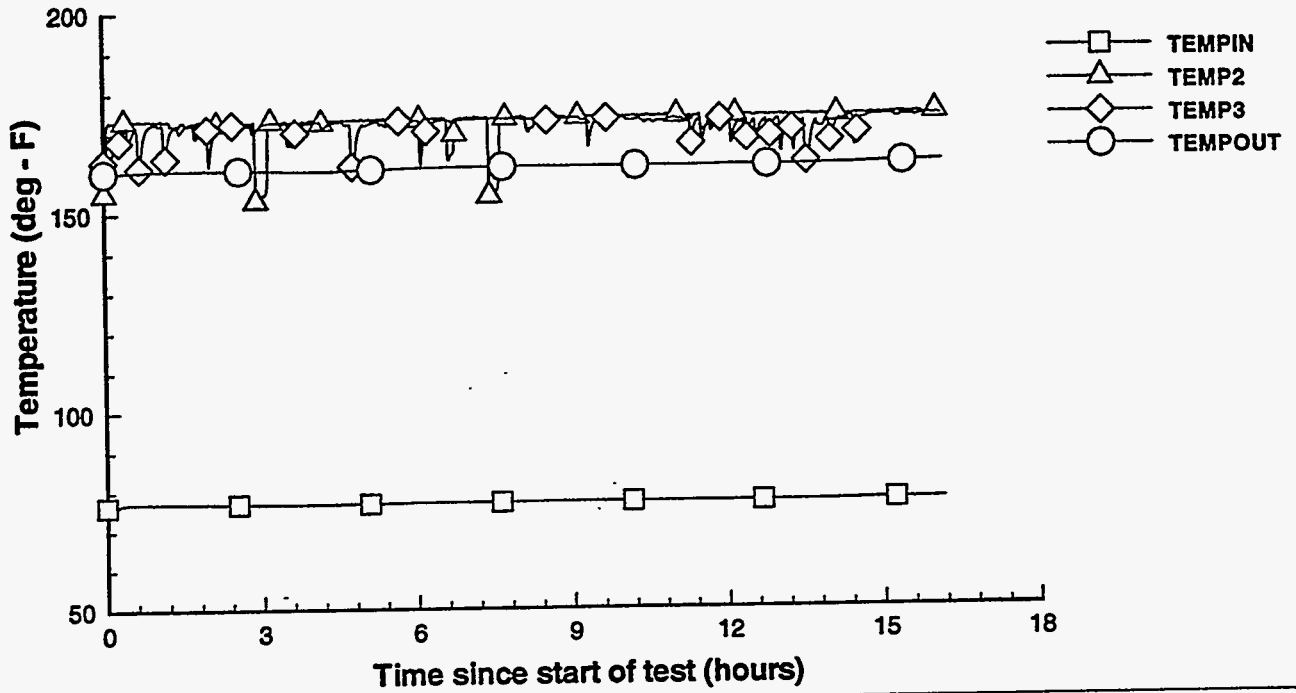


### Moisture Ratios (test 10-10R)

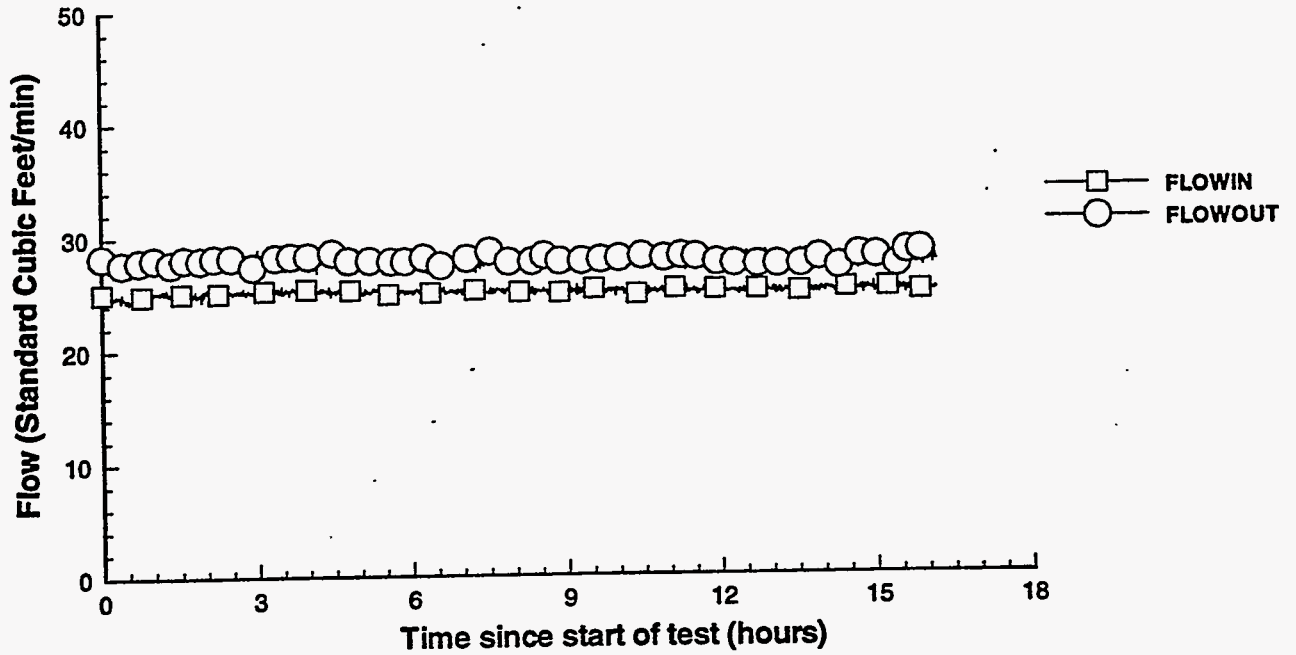


(2D) II Print II 16 Jun 1994 II test11.plt II TEST\_11\_DATA

### RTD Temperatures (test 11)

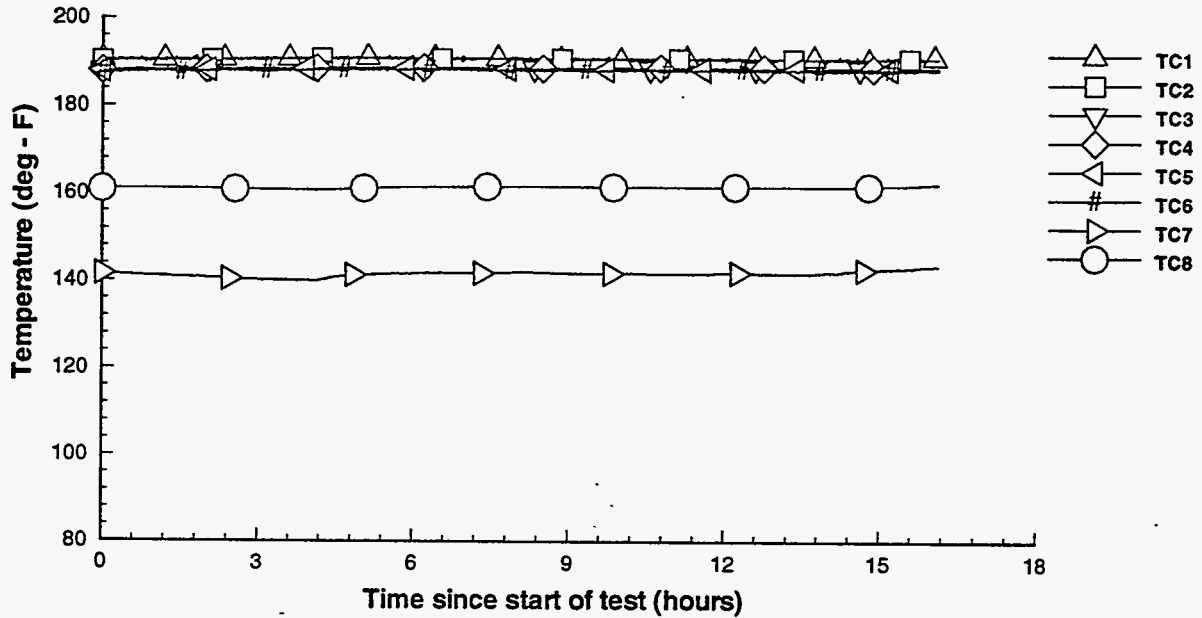


### Vapor Space Air Flow (test 11)

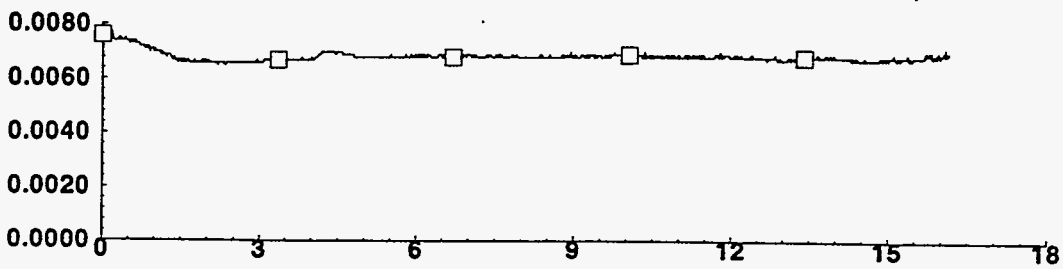
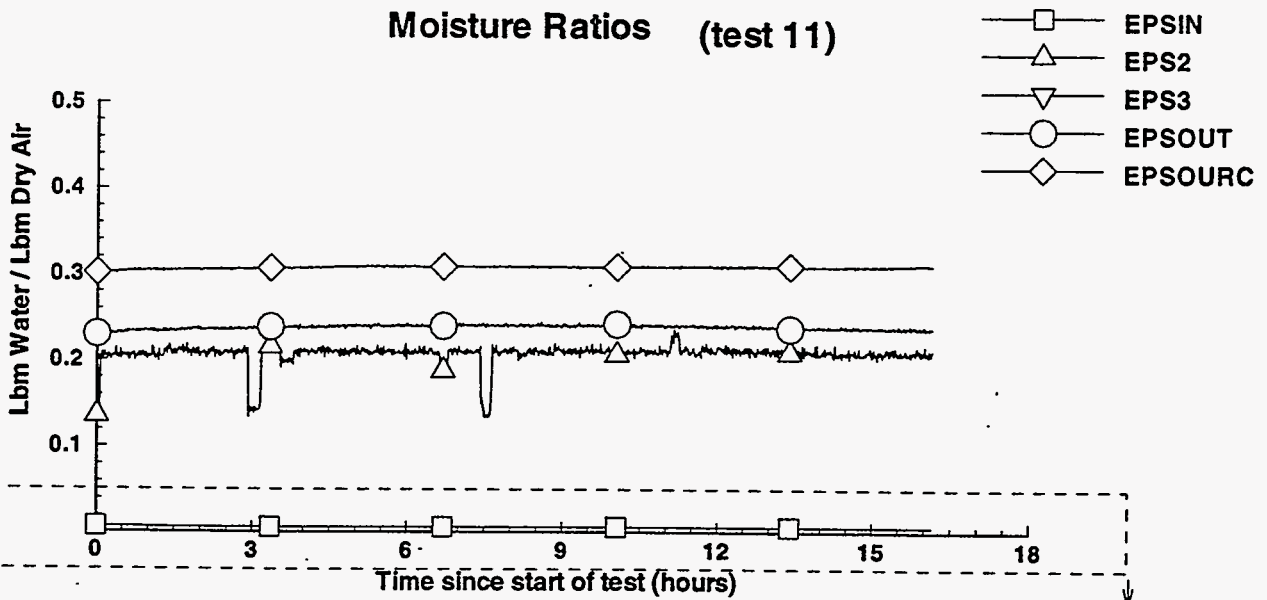


(2D) II Print II 19 Aug 1994 II test11.pt II TEST\_11\_DATA

### Thermocouple Temperatures (test 11)



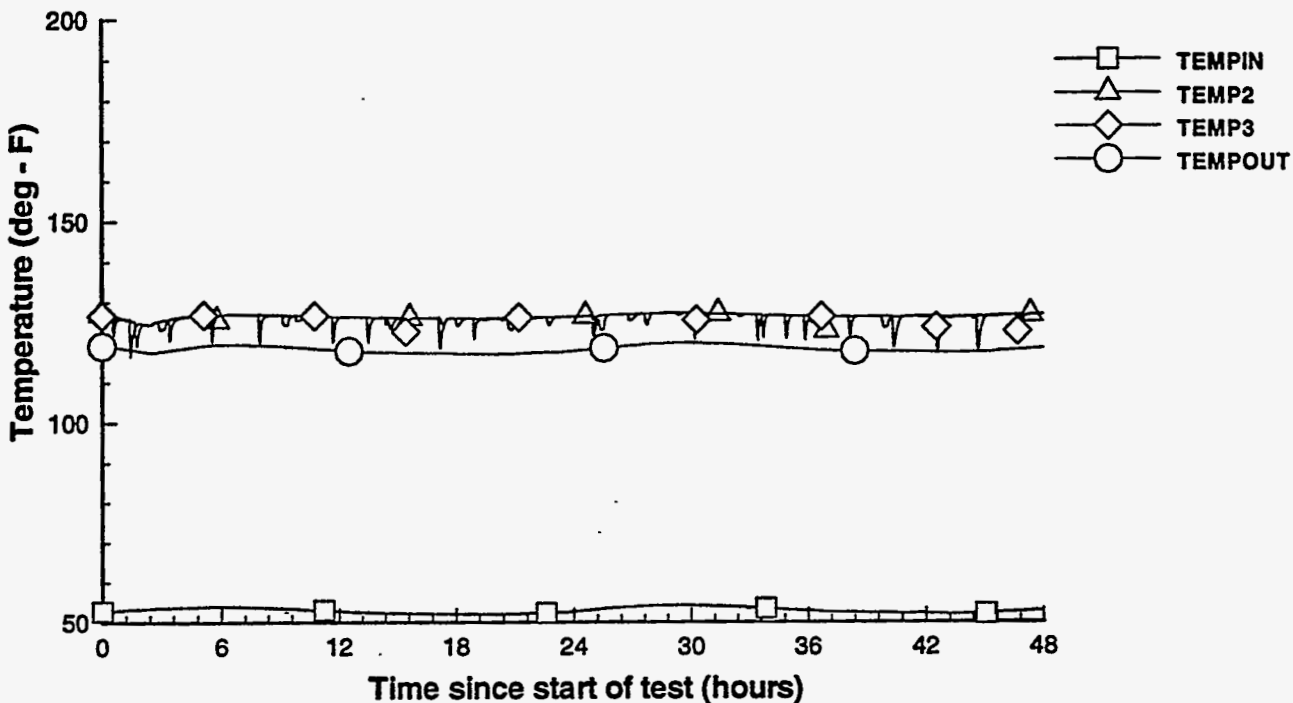
### Moisture Ratios (test 11)



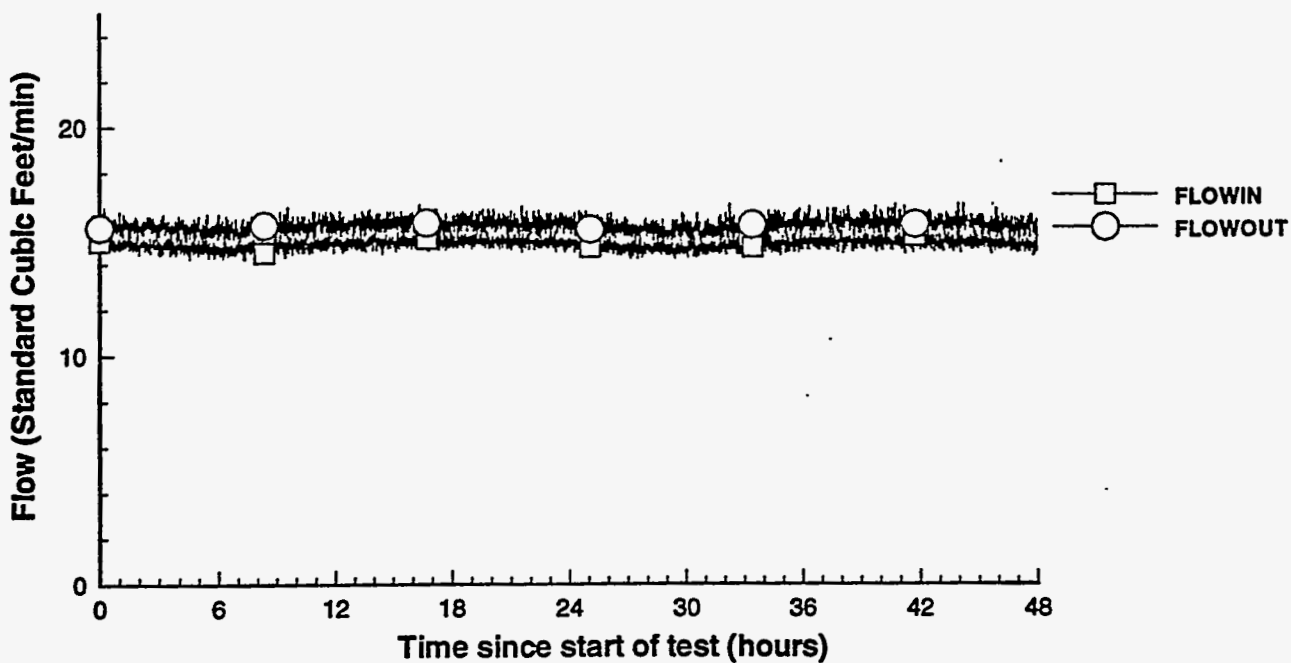


(2D) II Print II 16 Jun 1994 II test12.plt II TEST\_12\_DATA

### RTD Temperatures (test 12)

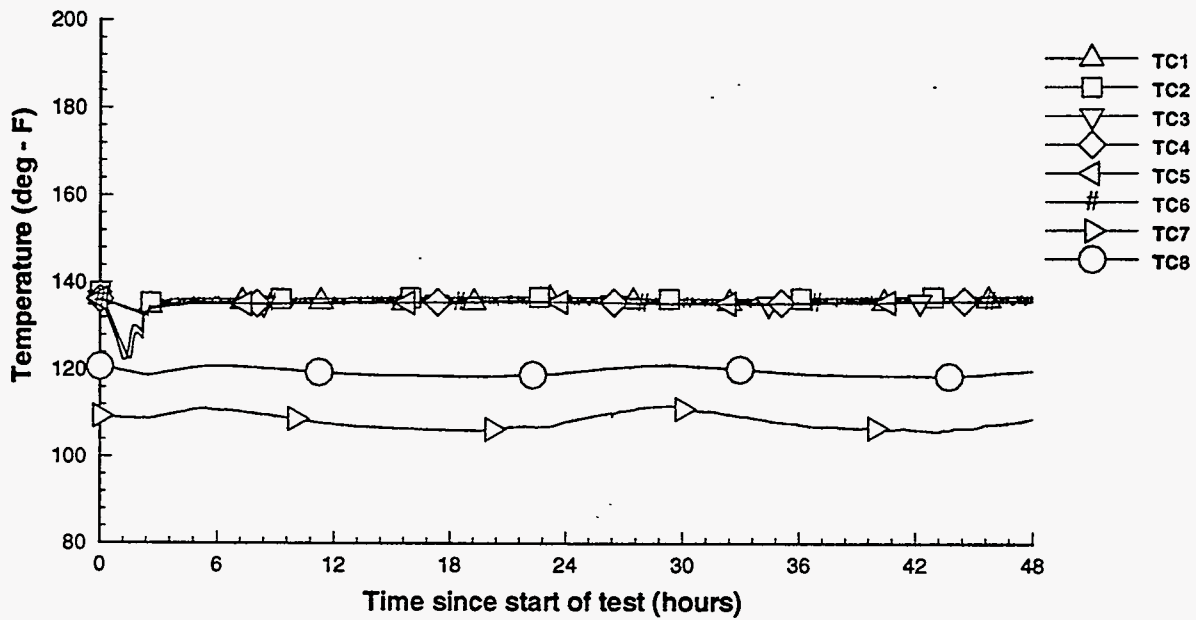


### Vapor Space Air Flow (test 12)

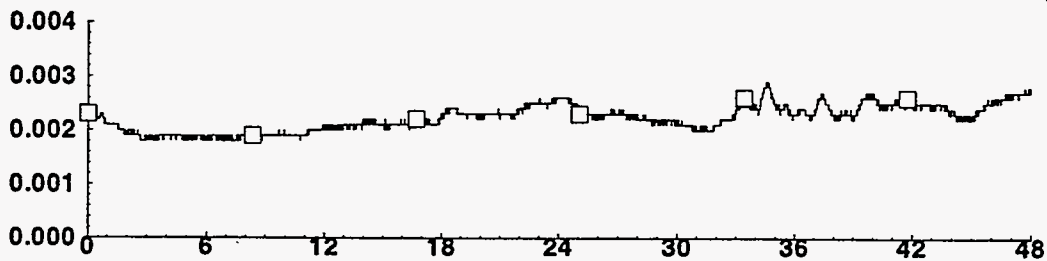
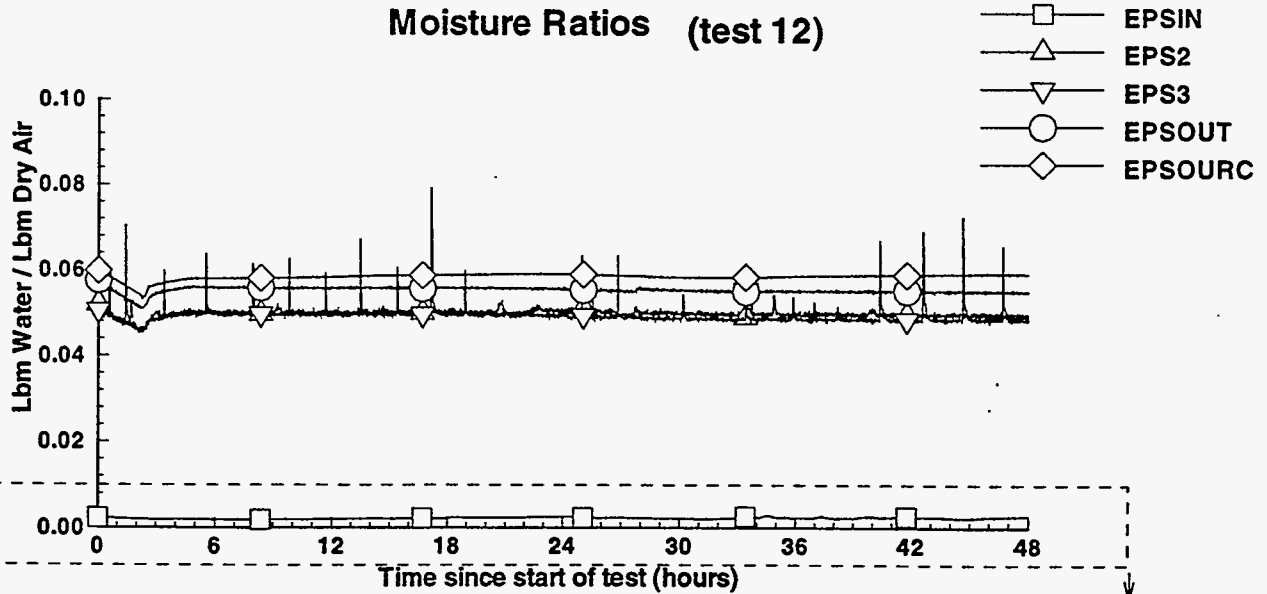


(2D) II Print II 19 Aug 1994 II test12.plt II TEST\_12\_DATA

### Thermocouple Temperatures (test 12)

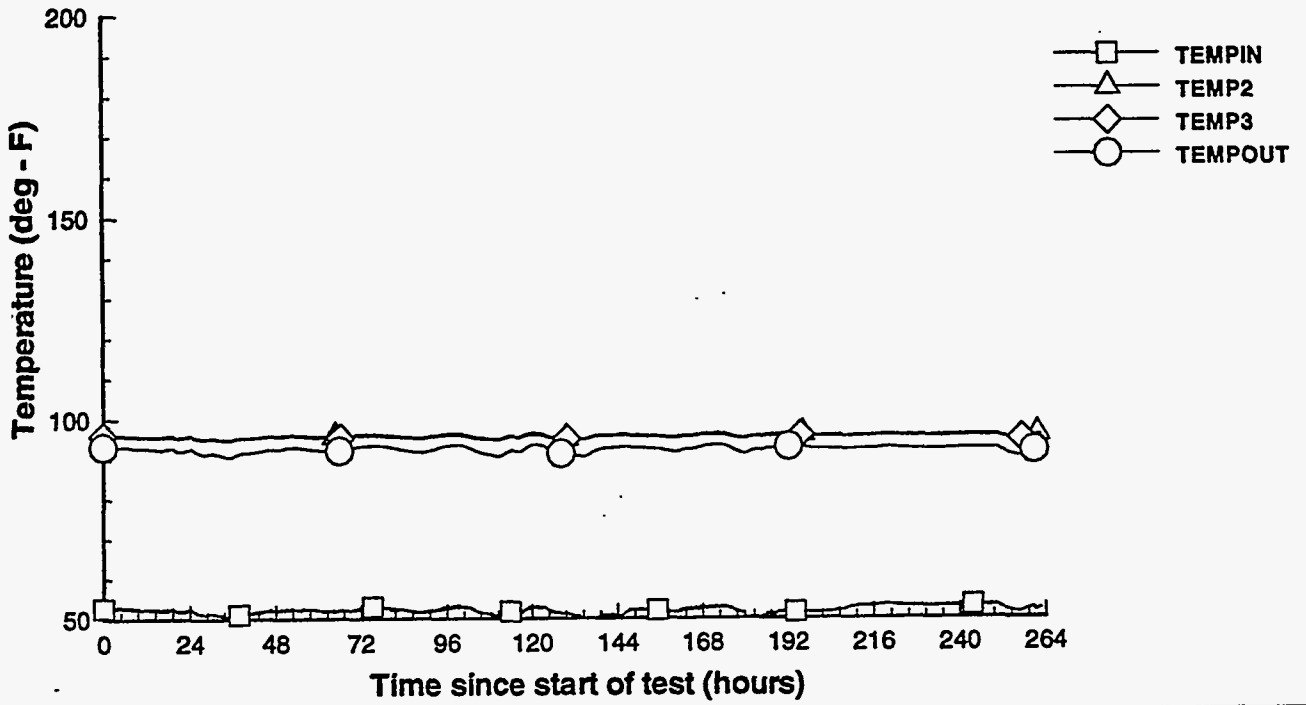


### Moisture Ratios (test 12)

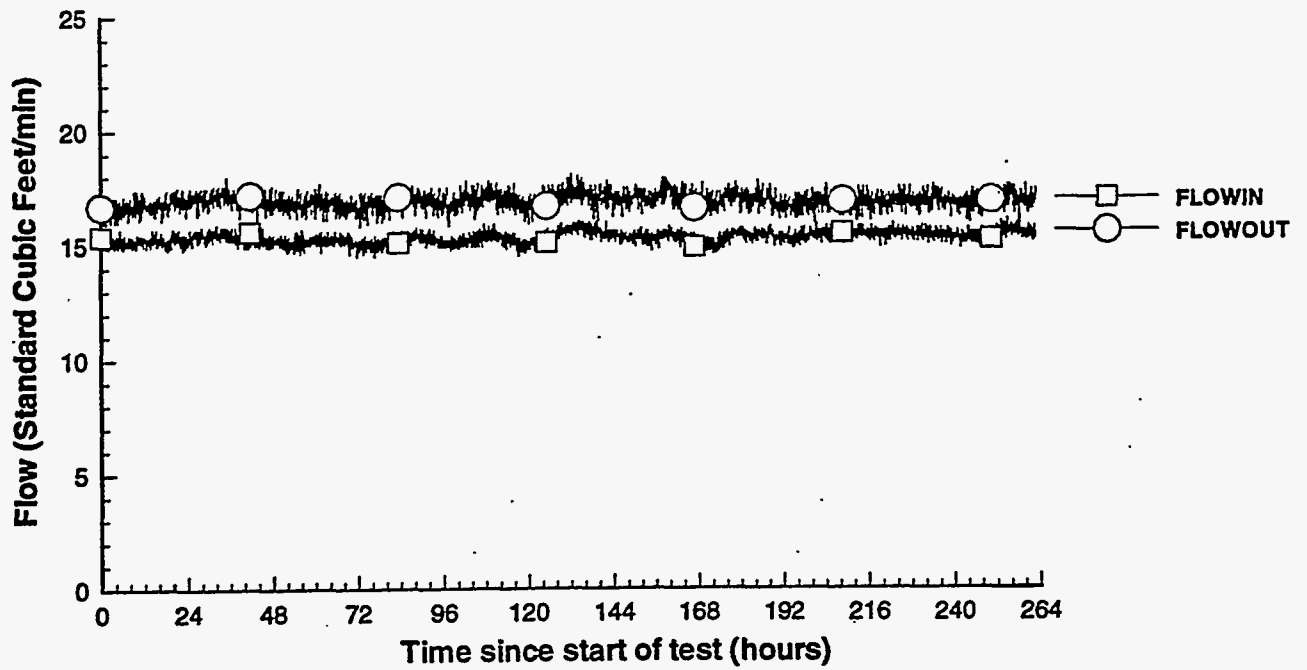


(2D) II Print II 16 Jun 1994 II test13.plt II TEST\_13\_DATA

### RTD Temperatures (test 13)

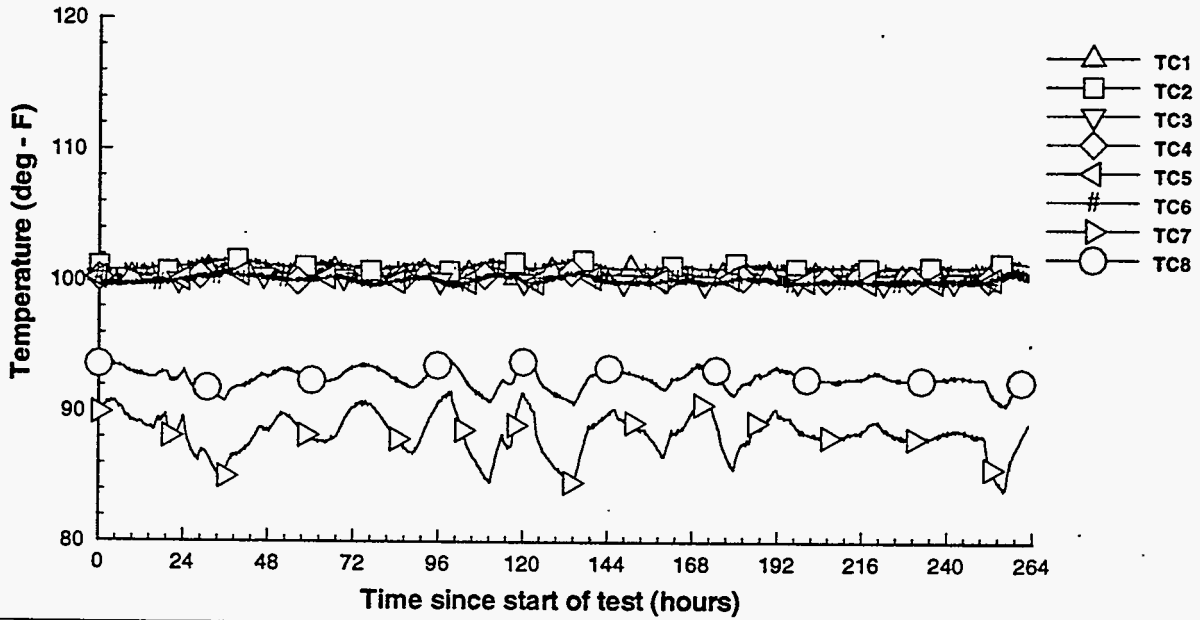


### Vapor Space Air Flow (test 13)

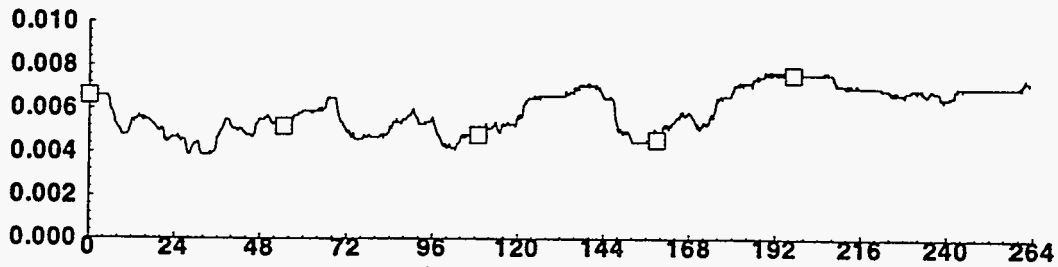
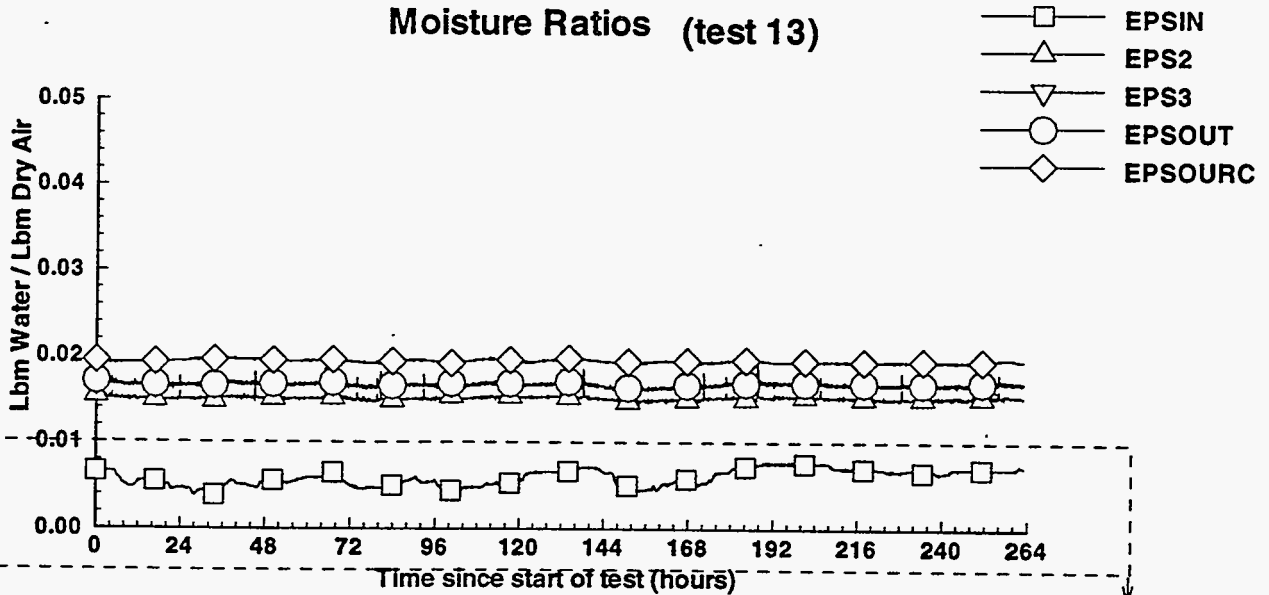


(2D) II Print II 19 Aug 1994 II test13.pt II TEST\_13\_DATA

### Thermocouple Temperatures (test 13)

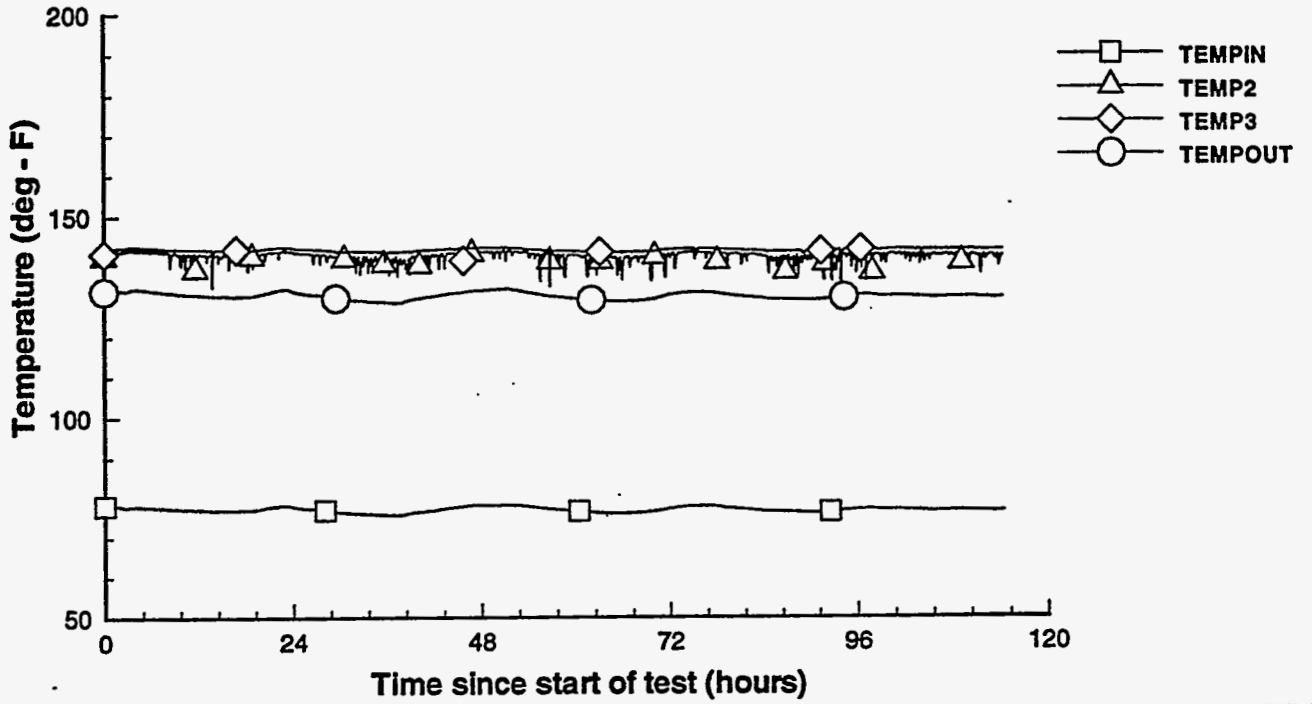


### Moisture Ratios (test 13)

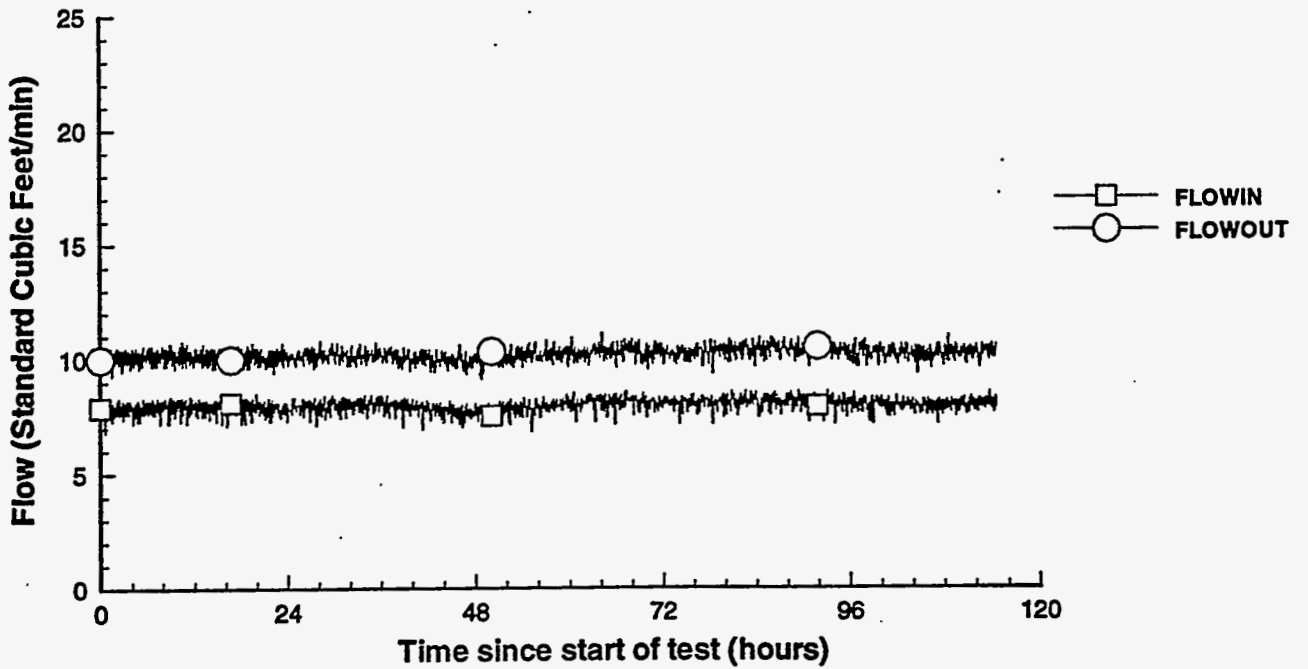


(2D) II Print II 16 Jun 1994 II test17.plt II TEST\_17\_DATA

### RTD Temperatures (test 17)

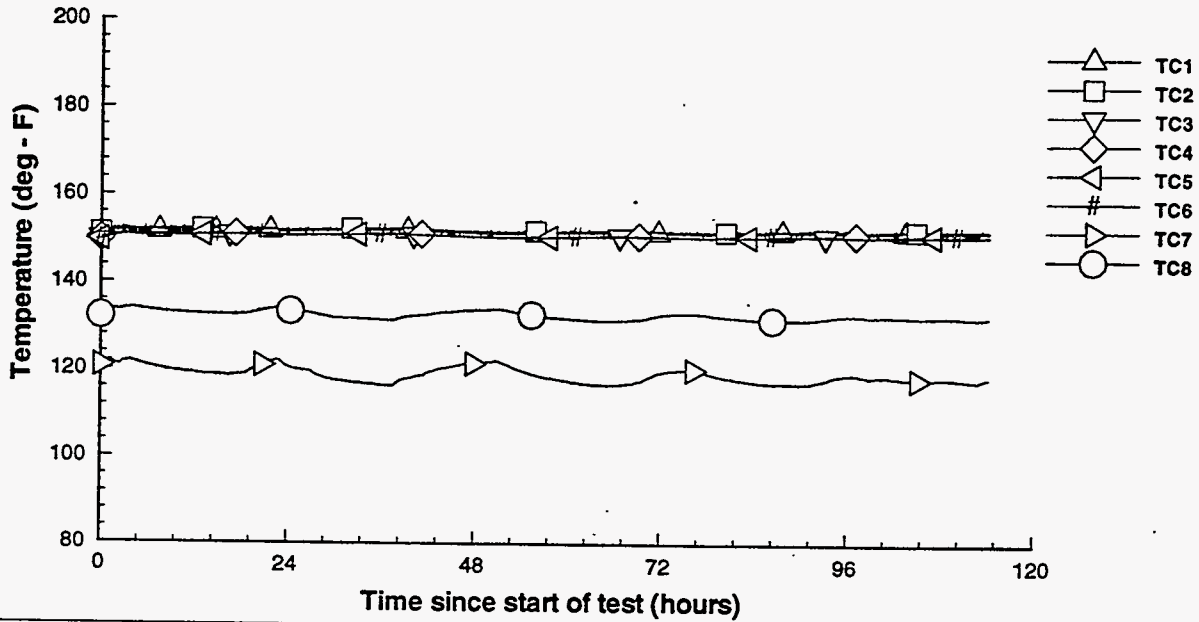


### Vapor Space Air Flow (test 17)

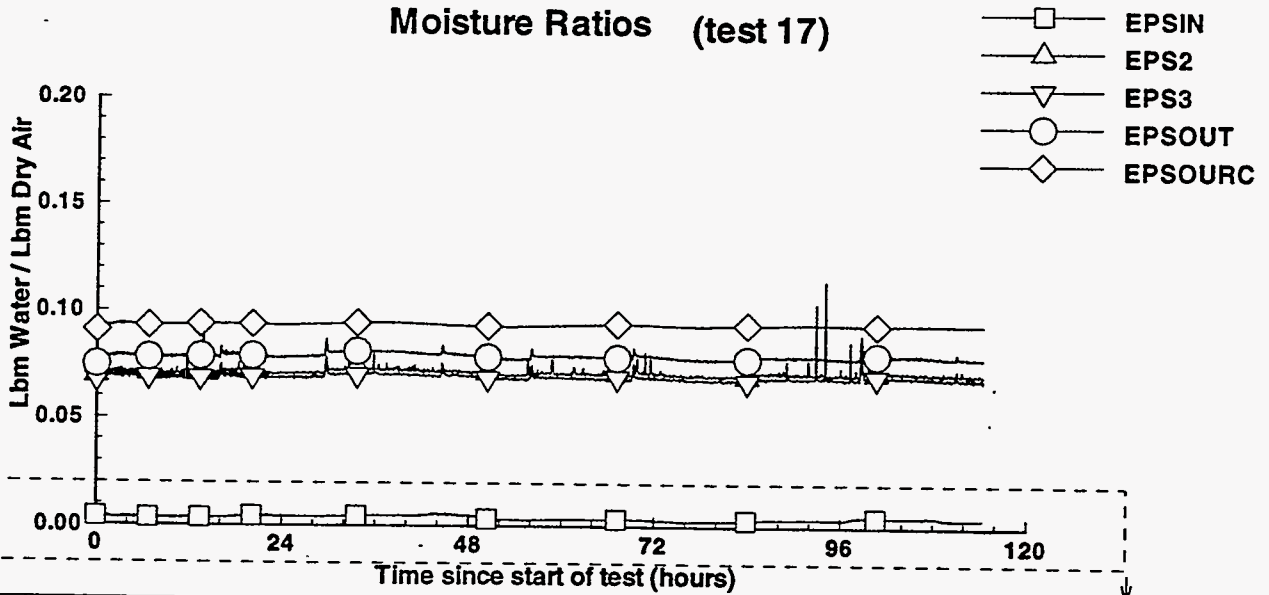


(2D) II Print II 19 Aug 1994 II test17.pit II TEST\_17\_DATA

### Thermocouple Temperatures (test 17)

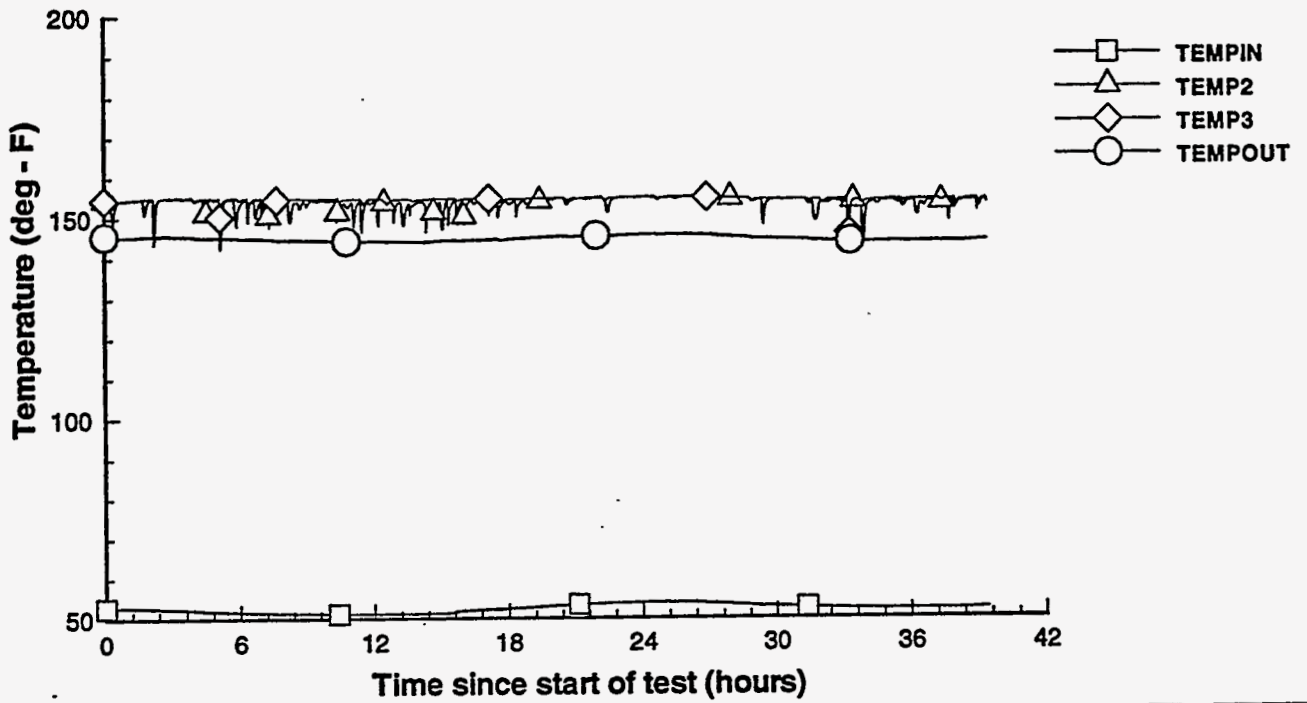


### Moisture Ratios (test 17)

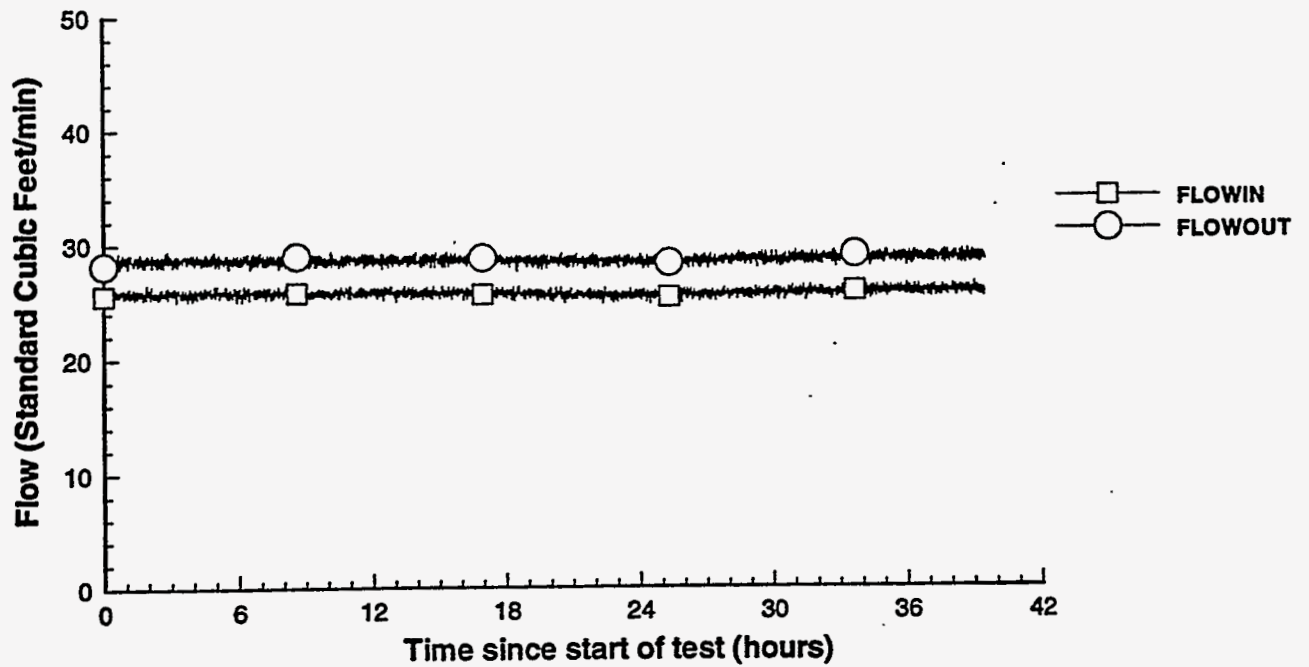


(2D) || Print || 16 Jun 1994 || test20.pit || TEST\_20\_DATA

### RTD Temperatures (test 20)

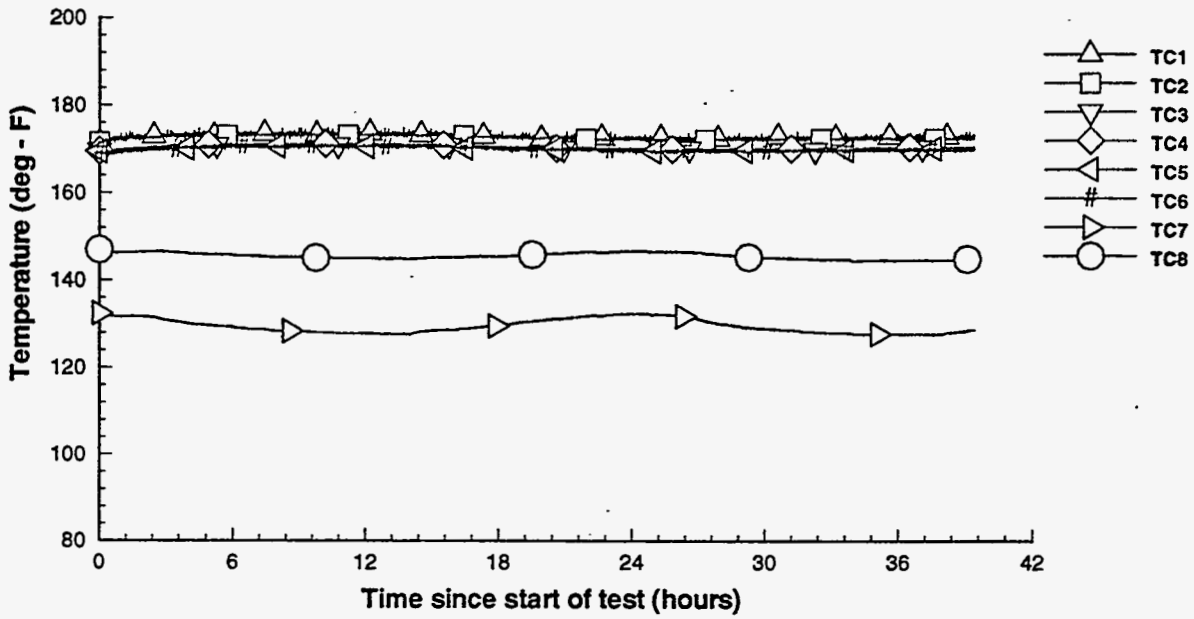


### Vapor Space Air Flow (test 20)

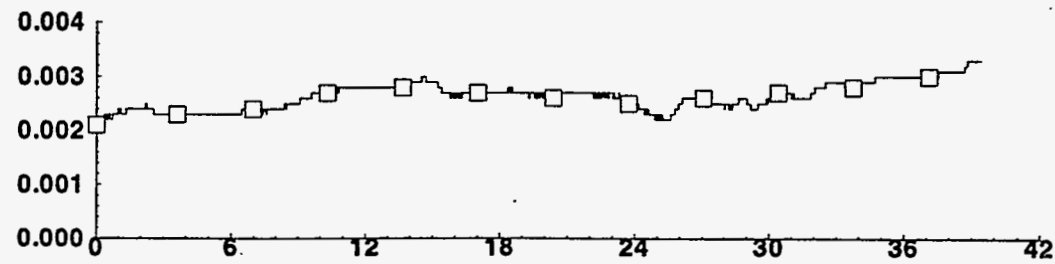
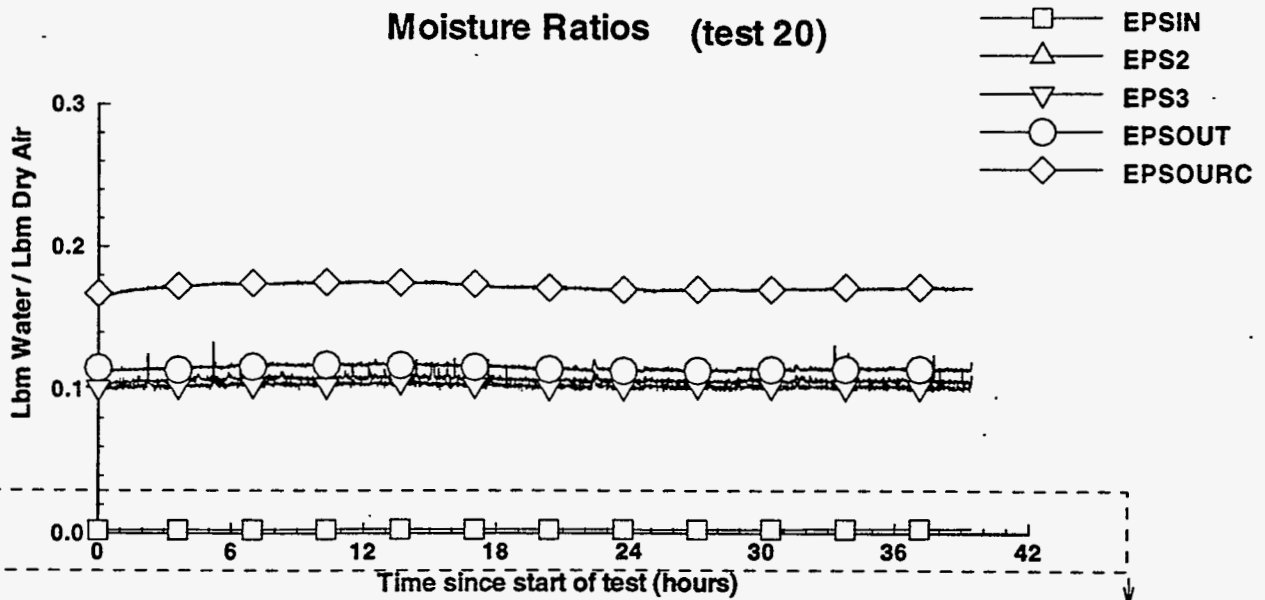


(2D) II Print II 19 Aug 1994 II test20.plt II TEST\_20\_DATA

### Thermocouple Temperatures (test 20)



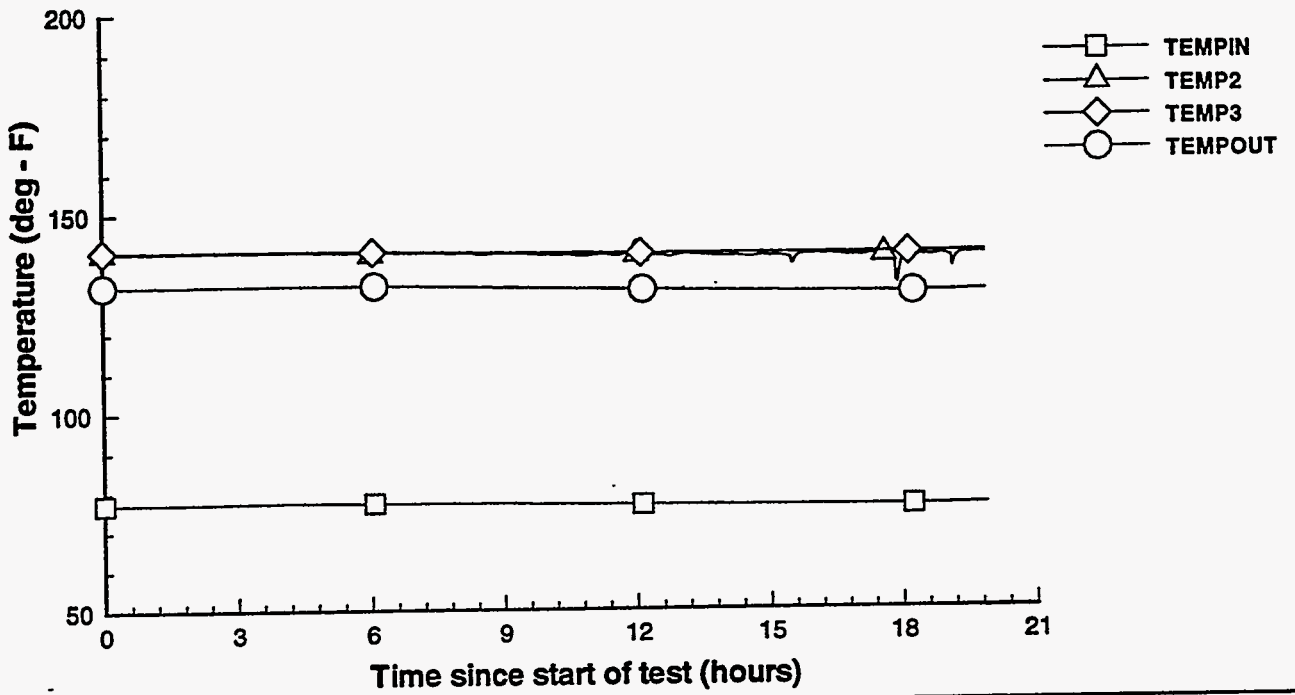
### Moisture Ratios (test 20)



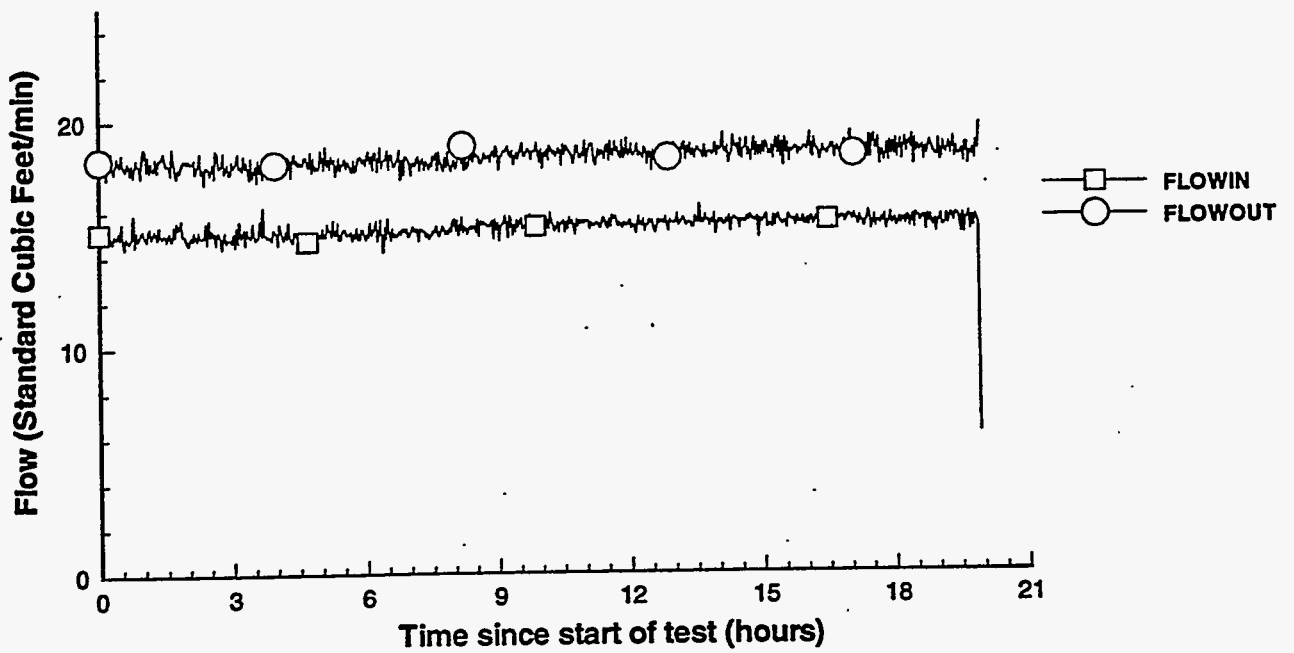


(2D) II Print II 17 Jun 1994 II test21.plt II TEST\_21\_DATA

### RTD Temperatures (test 21)

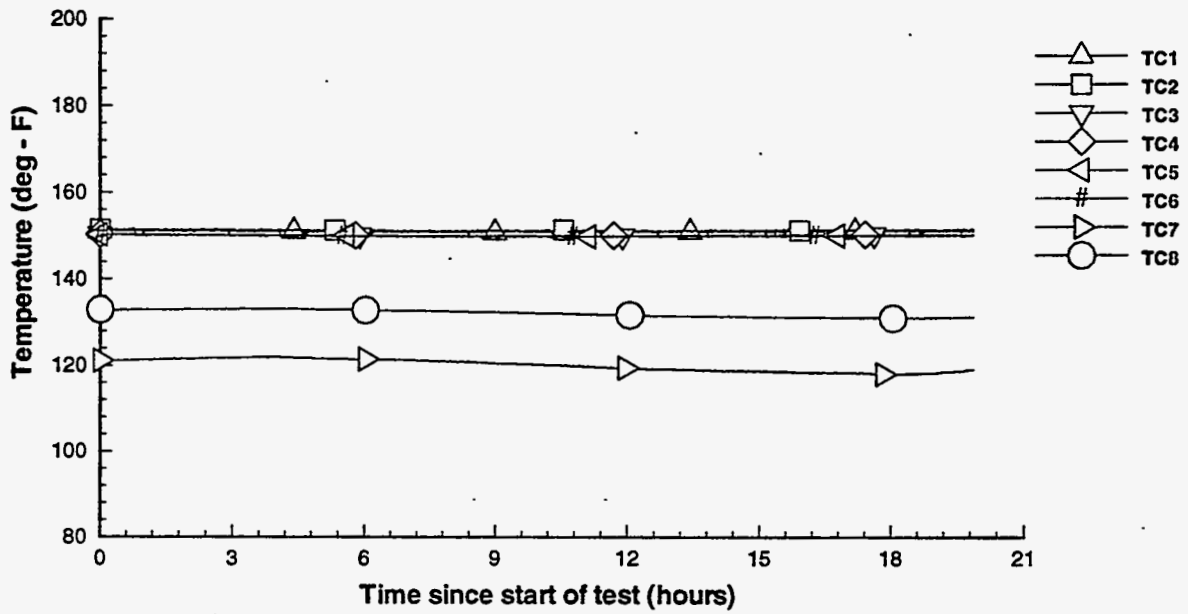


### Vapor Space Air Flow (test 21)

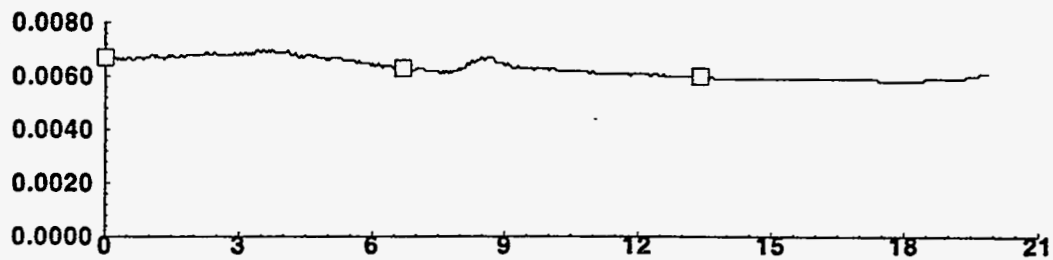
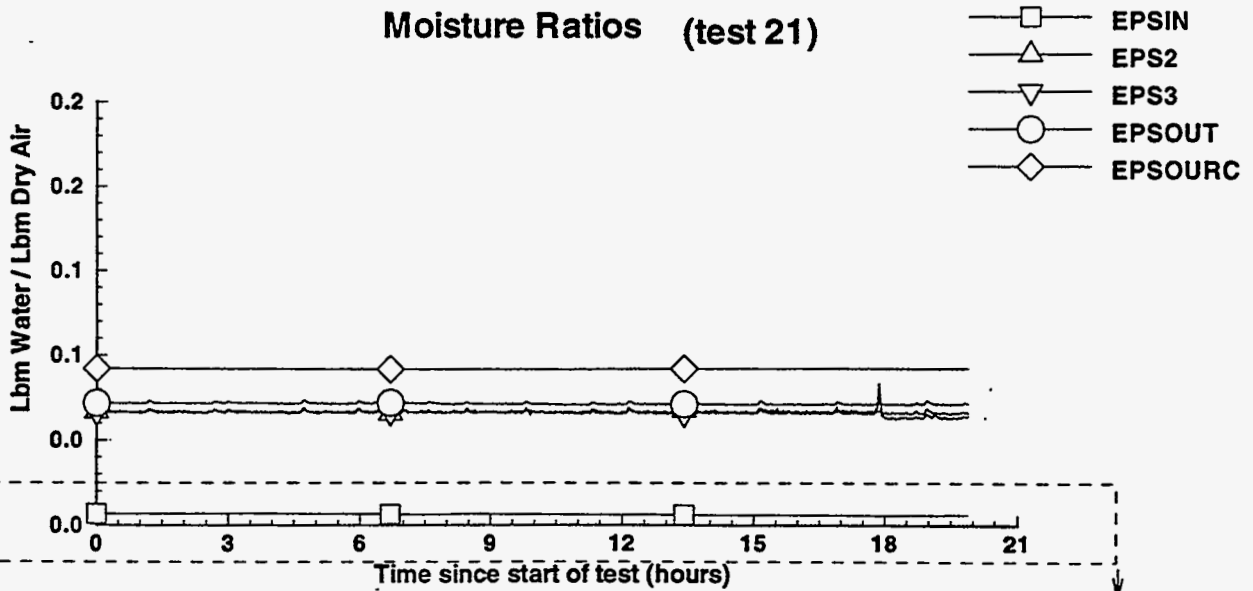


(2D) II Print II 19 Aug 1994 II test21.plt II TEST\_21\_DATA

### Thermocouple Temperatures (test 21)

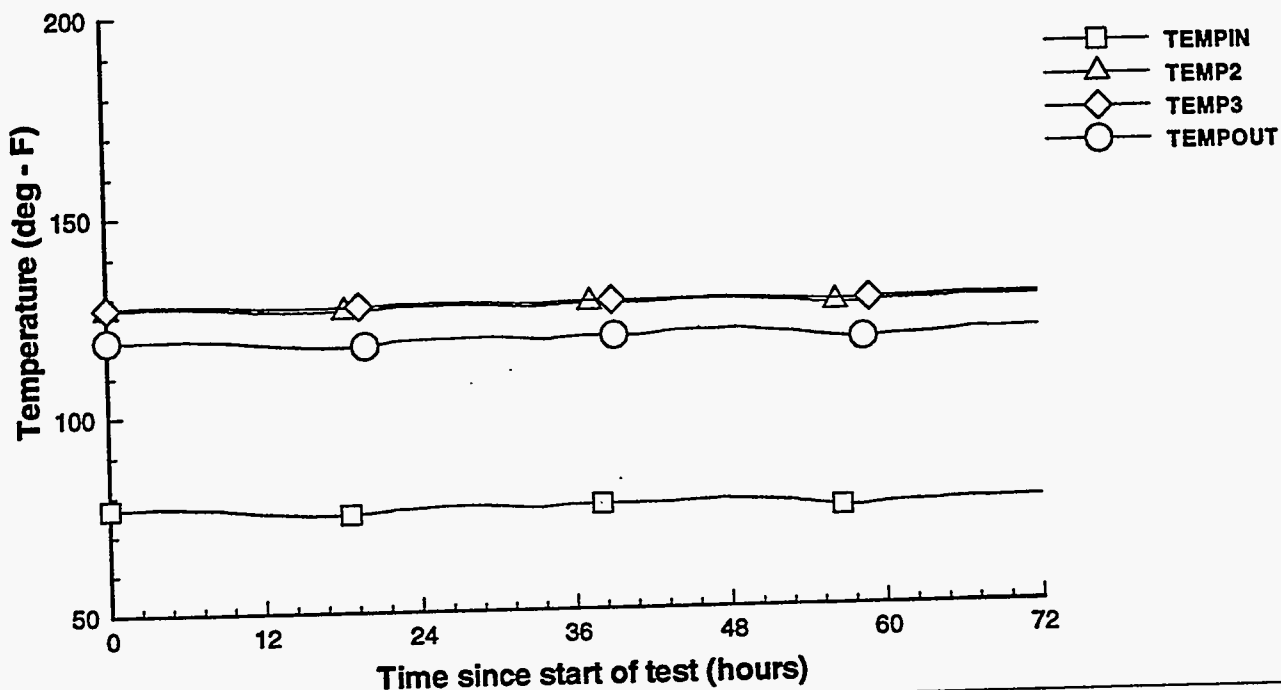


### Moisture Ratios (test 21)

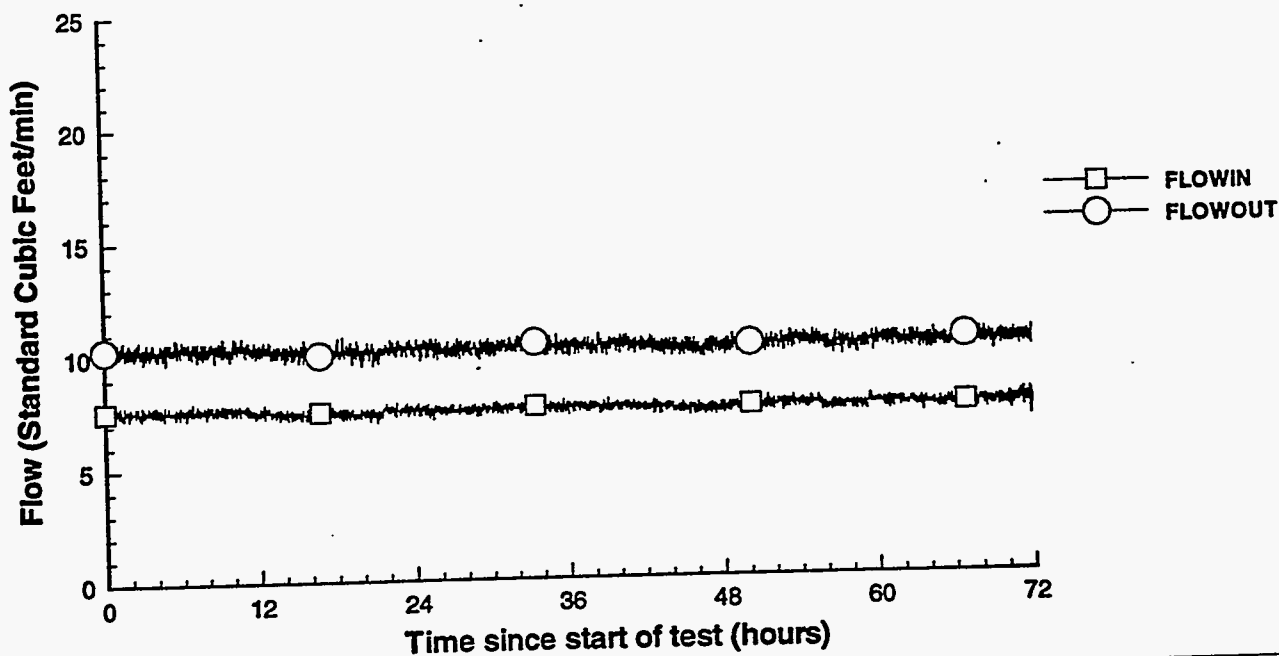


(2D) II Print II 17 Jun 1994 II test22.plt II TEST\_22\_DATA

### RTD Temperatures (test 22)

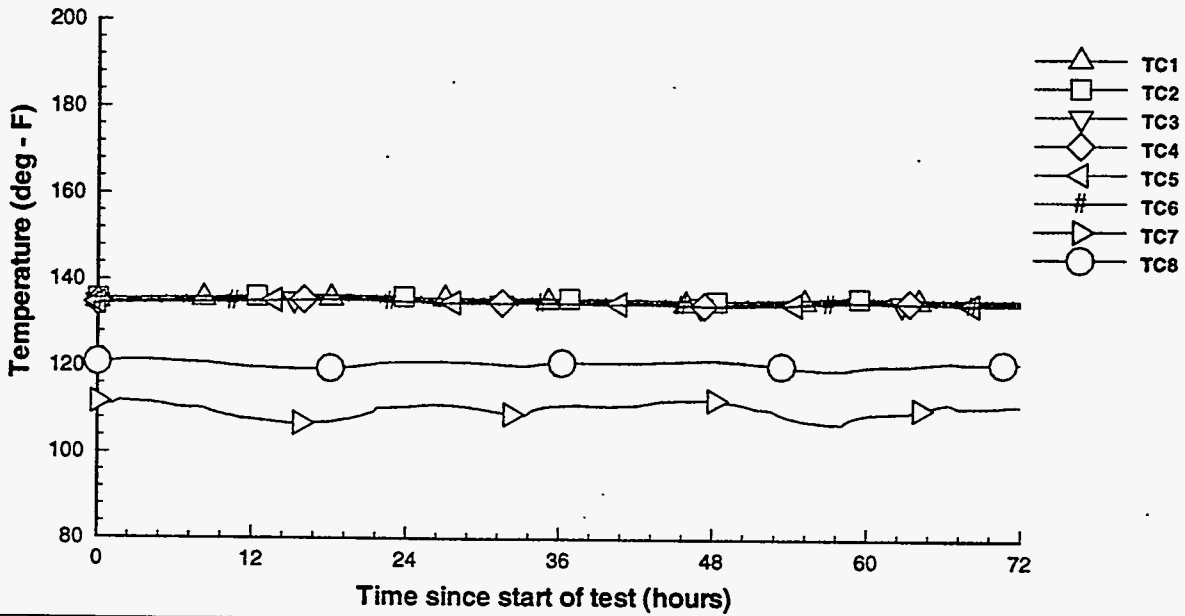


### Vapor Space Air Flow (test 22)

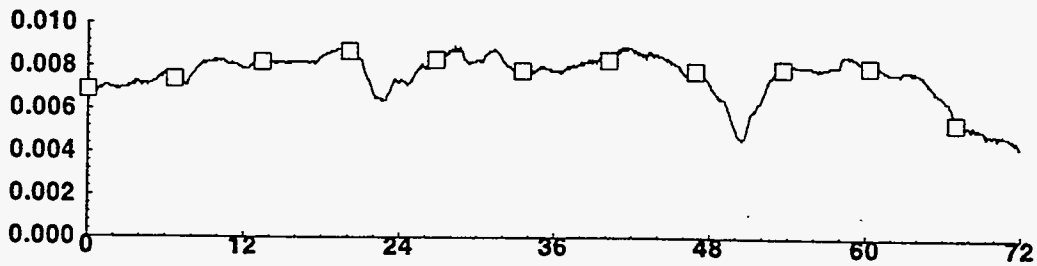
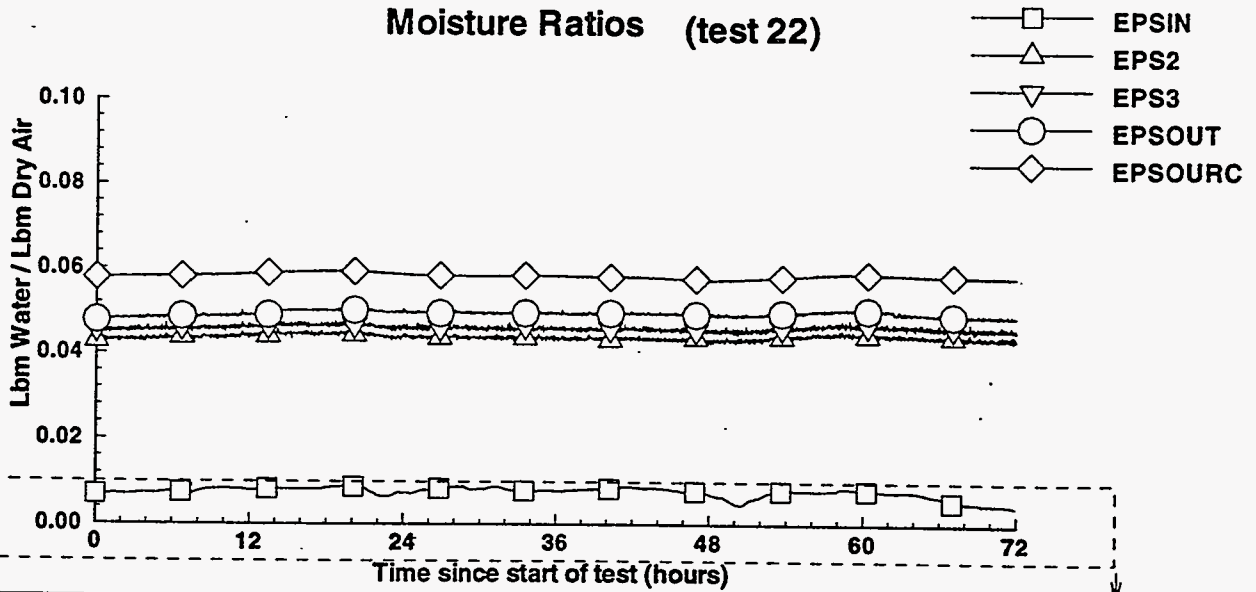


(2D) II Print II 19 Aug 1994 II test22.plt II TEST\_22\_DATA

### Thermocouple Temperatures (test 22)



### Moisture Ratios (test 22)



**Appendix D. Vapor Pressure Experiment on MWF Surrogate Solution.**

MAY 27 1993

Westinghouse  
Hanford CompanyInternal  
Memo

From: Chemical Engineering Laboratory 12130-93-043  
 Phone: 3-1102 S4-25  
 Date: May 26, 1993  
 Subject: RESULTS FROM VAPOR PRESSURE EXPERIMENT ON MWTF SURROGATE SOLUTIONS

To: C. A. Hinman H0-33

cc: C. J. Berglund S4-25  
 M. J. Kupfer H5-46  
 M. J. Schliebe S4-25  
 J. P. Sloughter T6-07  
 Project file 13.2  
 EJS file/LB

- References:
- (1) Internal Memo, P. J. Certa, J. R. Divine, and M. J. Kupfer, "Recommended Waste Composition Changes to the MWTF FDC," Dated February 25, 1993.
  - (2) Internal Memo, J. S. Garfield, "TWRS Systems Engineering Study Double Shell Tank Waste Inventories, Rev 1," Number 25900-92-29, Dated September 18, 1992.
  - (3) CRC - Handbook of Chemistry and Physics 62<sup>nd</sup> Edition, CRC Press, Inc, Boca Raton, Florida, 1981, pgs D-168 and 9.

The vapor pressures (VP) for two surrogate solutions of tank waste that will be stored in the Multiple Waste Tank Farm (MWTF) have been experimentally determined. The two solutions are expected to have the largest impact on VP due to their high salt concentrations and are, therefore, limiting. Data from this experiment is to be used to perform a thermodynamic balance around the tanks. The balance can be used to calculate such things as cooling requirements and water losses.

The experimental procedure and equipment for both solutions were nearly identical. Appropriate amounts of the reagents were weighed out, and demineralized water was added to make 700 mL of solution. The resulting solution was poured into a triple-necked flask, and the flask was placed in a heating mantle. In one neck of the flask, a mercury thermometer was placed (via a rubber stopper); in the second a thermocouple was placed (via a rubber stopper); and, in the third a condenser was placed. A cooling water line was attached to the condenser in order to condense the vapors exiting from the flask and, therefore, keep the solution at constant molarity. A tube connected the exit port of the condenser with a large Erlenmeyer flask via a rubber stopper. Also attached to the flask was a digital pressure gauge (absolute) and a vacuum pump. The bleed valve on the pump was manipulated to vary the systems pressure. The pump was then turned on, the lowest pressure set (~380 mm Hg), and then the heating mantle turned

C. A. Hinman  
Page 2  
May 26, 1993

12130-93-043

on. Once the solution started to boil and the thermocouple showed no temperature increase, the temperature from the thermometer was logged. Previous work showed that the thermocouple was calibrated incorrectly, so it was used solely as an indicator of when a steady state temperature was reached. After the temperature reading was taken, the pressure was increased and the process repeated.

The first solution was the maximum expected molarities listed in the MWTF Functional Design Criteria (Certa, 1993). In order to simplify the experiment, only the specifications for nitrate (5.1 M), nitrite (1.8 M), and hydroxide (6.9 M) were met. The sodium forms of the three anions were used in this experiment. The results follow:

Solution 1

Pressure (mm Hg)	Temperature (°C)
380.4	106.2
474.9	113.0
568.8	118.4
593.4	119.8
743.3	130.0

The tolerance on temperature and pressure readings are assumed to be less than +/- 0.5°C and +/- 0.5 mm Hg.

The second solution used the inventory of the DSS/DSSF waste listed in the TWRS Systems Engineering Study letter (Garfield, 1992). Any component less than 0.1 M and TOC (total organic carbon) were assumed to be inconsequential. For this solution, it was assumed that the  $Al^{+3}$  listed in the inventory was actually present as  $AlO_2^-$  (aluminate). In order to keep a charge balance, the amount of  $OH^-$  was decreased from ~8.7 M to 4.13 M. The chemical make-up of this surrogate is:

Solution 2

Chemical	Molarity
NaCl	0.17
NaOH	4.13
$NaAlO_2$	1.14
$NaNO_2$	1.80
$NaNO_3$	2.26
$KNO_3$	0.55

C. A. Hinman  
Page 3  
May 26, 1993

The result for solution 2, experiment 1 follow:

Solution 2 - Experiment 1

Pressure (mm Hg)	Temperature (°C)
380.3	96.1
569.9	107.6
745.6	119.7

Comparing these results with pure water VPs (CRC, 1981), the first solution decreases the VP by approximately 60% and the second solution by 47%. The attached figure (Figure 1) compares the data obtained from the two experimental runs with published data (CRC, 1981) on pure water. The 110°C line was used to calculate the VP depression for the two solutions. The values for the two solutions at 110°C were interpolated.

For solution 2, a second experiment was performed in order to obtain a larger array of data. The lower limit on pressure was decreased from 380 mm Hg to 83 mm Hg (the limit for the vacuum pump). The results follow:

Solution 2 - Experiment 2

Pressure (mm Hg)	Temperature (°C)
83.0	59.2
85.0	60.0
100.1	63.9
150.0	73.1
200.5	80.2
250.2	85.8
300.3	90.5
350.4	95.0
380.4	97.1
480.5	104.4
580.5	109.7
742.6	120.2

These values compare favorably with the numbers obtained from the first experiment. The slight variations can be attributed to possible water vaporation between runs (change in solution molarity) or experimenter error.




C. A. Hinman  
Page 3  
May 26, 1993

12130-93-043

Figure 2 compares the data for solution 1 from experiment 1 and 2 with literature data on pure water. As can be seen from the graph, solution 2 closely mimics the curvature of pure water. The average vapor pressure depression is approximately 44%. This agrees, within reason, with the factor obtain from the first experiment.

If you have any questions or comments, please contact me at 3-1102.

  
Eric J. Slaathaug, Engineer  
Chemical Engineering Laboratory

alh

Attachment (2)

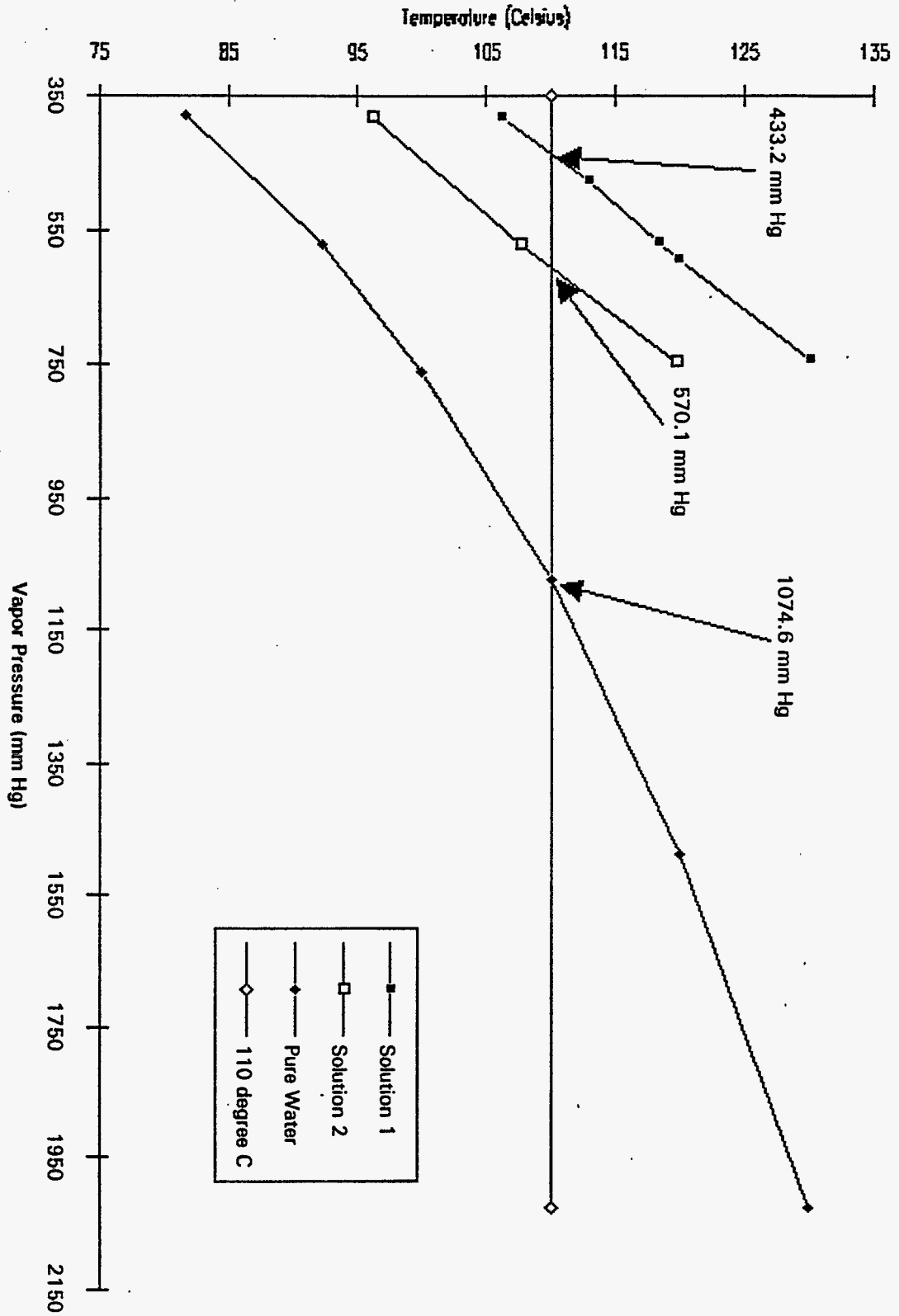


Figure 1 - Vapor Pressure Data for Solutions 1 and 2

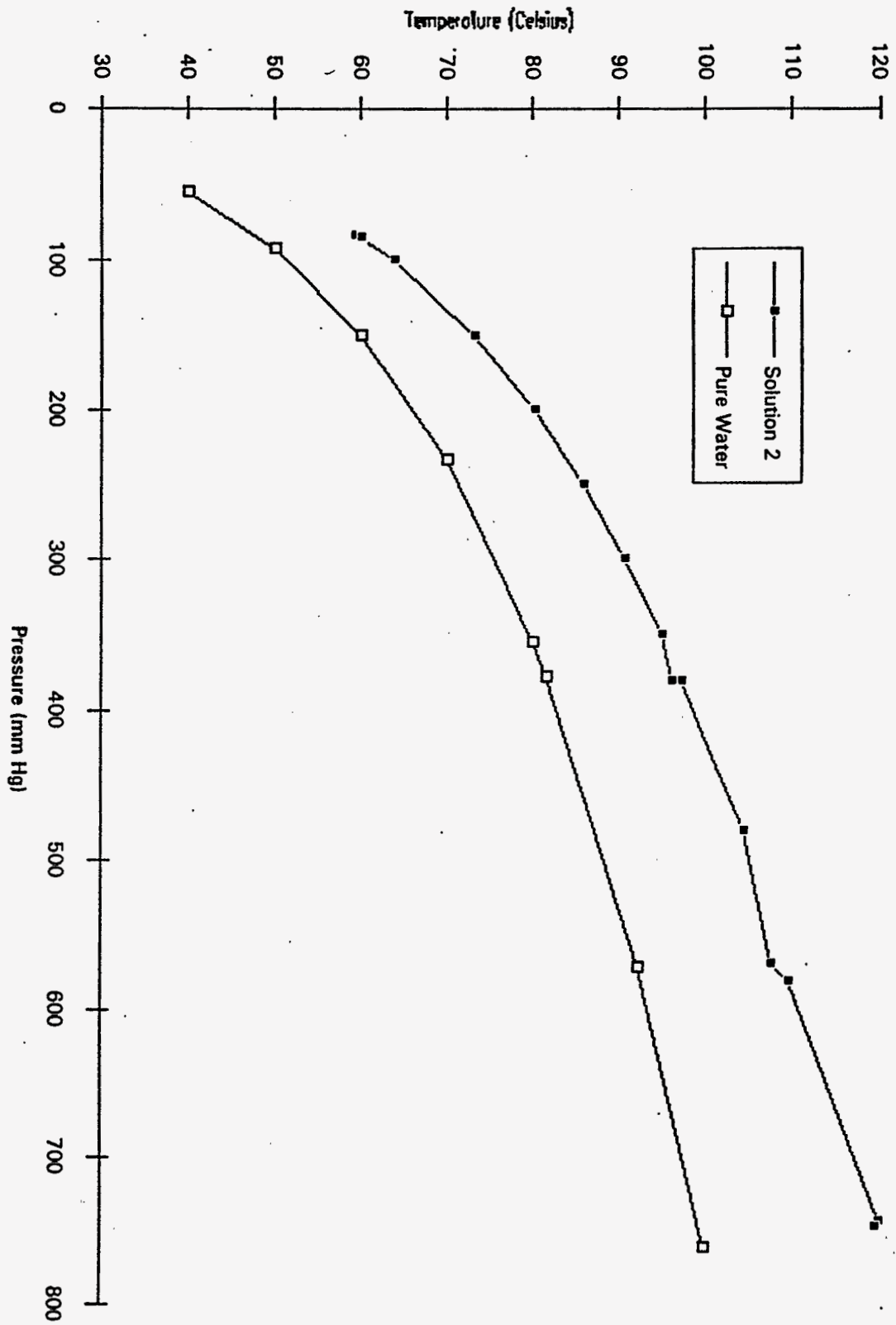


Figure 2 - Extended Vapor Pressure Data for Solution 2

**Appendix E. Literature Review.**

Literature Review on Evaporation Test

By Y. Lee

Extensive literature review on the evaporation of the water into still air has been performed, including the library data base search. Even though the interest on the process of evaporation begins from early 19th century, there are a limited number of literatures dealing with the evaporation of water into still air. Much of the previous research was focused on the evaporation of water into moving air.

Since earlier reports by Dalton<sup>1</sup>, Hinchley<sup>2</sup>, and Hinchley and Himus<sup>3</sup> have been discussed thoroughly in the paper by Pauker et al.<sup>4</sup>, they will not be repeated in this report. The most significant experimental report in this field was presented by Sharpley and Boelter<sup>5</sup>, and Boelter et al.<sup>6</sup> based on their measurement of evaporation rate from one-foot diameter pan into still air. Their reports cover the evaporation of distilled water within the temperature limit 63 and 200 F, into quiet air at 65 to 80 F. They, also, have established an empirical relationship to calculate the evaporation rate as a function of surface and bulk water vapor pressure as follows:

$$G = 0.067(P_s - P_b)^{1.22}$$

where, G       Evaporation rate (lb/ft<sup>2</sup>hr)  
P<sub>s</sub>       Water vapor pressure at surface (in Hg)  
P<sub>b</sub>       Water vapor pressure at bulk (in Hg)

Recently, Pauker et al.<sup>4</sup> have shown that the measurements of the evaporation rates for water at temperature ranging from 25 to 50 C into still air at 20 C using 47-inch diameter pan are close agreement with the results of Boelter et al.<sup>5</sup>, thus confirming the above relationship. These experiments, however, were limited to the lower air temperature ranges than the air temperature expected for the MWWF tank design, and it is questionable at best to extrapolate the above empirical relationship into the higher air temperature case for the design calculation.

As mentioned previously, there are a large number of studies reported on the evaporation of water into moving air representing the water loss at ponds or lakes<sup>7,8,9,10</sup>. In these studies, attempts were made to relate the water loss during moving air to the loss into still air assuming that the still air case is the limiting case for the moving air. Their results, however, are not as credible as the results from the experiments with still air. Adams et al.<sup>11</sup> have presented an excellent literature review on this subject. Also, Sparrow et al.<sup>12</sup> have reported the measurement of the evaporation rate in the system where the temperature of the water

layer is depressed relative in order to the air temperature to study the natural convection caused by the concentration difference alone.

A number of attempts have been made in order to develop the semi-empirical relationship to predict the evaporation rate. The relationship between temperature gradient and the strength of the natural convection for the horizontal plate has been expressed through the Rayleigh Number, and the relation between Rayleigh number and heat transfer coefficient has been well established for the wide range of the Rayleigh number<sup>13</sup>. Since the transfer of heat and mass are analogous, the relationship developed for the heat transfer can be applied to the mass transfer of water vapor between the interface and bulk phase during the evaporation. As pointed out by Eckert and Drake<sup>14</sup>, an equation for free convection heat transfer may be applied for free convection mass transfer simply by replacing the Nusselt number by the Sherwood number, and the Prandtl number by the Schmidt number. The driving force in the Rayleigh number, however, cannot be simply replaced by the concentration difference, since the evaporation system has not only the concentration difference but also the temperature difference. Somers<sup>15</sup> and Wilcox<sup>16</sup> solved the governing equations for simultaneous heat and mass transfer in laminar free convection from a vertical plate, and concluded that the effect on the natural convection due to temperature and concentration differences are additive for nearly equal the Prandtl and Schmidt numbers. It is clear from these studies that both differences will enhance the degree of natural convection more than a single difference. The exact magnitude of the contribution from one to another, however, is required for further study.

Assuming that the concentration gradient is the dominant driving force, Shah<sup>17</sup> has been developed the equation representing the evaporation rate from the heat and mass transfer analogy as follows:

where,	T	Water temperature (F)
	$\rho_b$	Density of bulk phase (lb/ft <sup>3</sup> )
	$\rho_i$	Density at interface (lb/ft <sup>3</sup> )
	$\rho$	Density of saturated air at water temperature (lb/ft <sup>3</sup> )
	$W_b$	Concentration of water vapor in bulk phase
	$W_i$	Concentration of water vapor at interface

Assuming that both driving forces, temperature and concentration differences, are additive, Paik and Henry<sup>18</sup> have suggested the following equation:

where, D Molecular diffusivity of diffusing gas in mixture (ft<sup>2</sup>/hr)  
 $\rho_o$  Density of mixture (lb/ft<sup>3</sup>)  
 $Y_i$  Interface mass fraction of diffusing gas  
 $Y_b$  Bulk phase mass fraction of diffusing gas  
 $\nu$  Kinematic viscosity of gas mixture (ft<sup>2</sup>/hr)  
g gravitational force (ft/hr<sup>2</sup>)  
 $T_i$  Temperature at interface (F)  
 $T_b$  Temperature at bulk phase (F)  
 $M_i$  Molecular weight of diffusing gas  
M Molecular weight of inert gas

Also, Adams et al.<sup>10</sup> suggested a similar but more complex equation. Since the predictions of these equations have not been validated by the experimental data for the water and air temperature ranges applicable to the MWTF design, the accuracy of these predictions is questionable at best for the temperature range covering the MWTF design. Also, it is worth stating that all literatures discussed in this section presented the study on the evaporation of pure water into still air while the waste water vapor pressure is much lower than that of the pure water due to the vapor pressure suppression. The effect of vapor suppression on the evaporation rate has never been addressed in the existing literature.

## References

1. Dalton, J., "Meteorological Observation and Essays," 2d Ed., 1834.
2. Hinchley, J. W., "The General Problem of Evaporation," J. Society of Chem. Industry, Vol. 41, pp. 242, 1922.
3. Hinchley, J. W. and G. W. Himus, "Evaporation in Currents of Air," Trans. Inst. Chem. Eng., Vol. 2, pp. 57, 1924.
4. Pauker, M. T., et. al., "A Novel Method for Measuring Water Evaporation into Still Air," ASHRAE Trans. Vol. 99, Pt. 1, pp. 297, 1993.
5. Sharpley, B. F. and L. M. K. Boelter, "Evaporation of Water into quit air from a One-foot-diameter Surface," Ind. Eng. Chem., Vol. 30, pp. 1125, 1938.
6. Boelter, L. M. K., et. al., "Free Evaporation into Air of Water from a Free Horizontal Quiet Surface," Ind. Eng. Chem., Vol. 38, pp. 596, 1946.
7. Carrier, W. H., "The Temperature of Evaporation," ASHVE Trans., Vol. 24, pp. 25, 1918.
8. Herbeck, G. E. and E. P. Anderson, "Water Loss Investigation: Vol. 1 - Lake Hefner Studies Technical Report," U.S. Geological Survey Paper 269, Washington, D.C., 1954.
9. Ryan, P. J., et. al., "Surface Heat Loss from Cooling Ponds," Water Resources Research, Vol. 10, pp. 930, 1974.
10. Adams, E. E., et. al., "Evaporation from Heated Water Bodies: Predicting Combined Forced Plus Free Convection," Water Resources Research, Vol. 26, pp. 425, 1990.
11. Adams, E. E., et. al., "Water and Energy Budget Analysis, Evaporation from Heated Waterbodies: Analysis of Data from the East Mesa and Savannah River Sites," Rep. CS-5171, EPRI, Palo Alto, Ca., 1987.
12. Sparrow, E. M., et. al., "Evaporation of Water from a Horizontal Surface by Natural convection," J. of Heat Transfer, Vol. 105, pp. 469, 1983.
13. Goldstein, R. J., et. al., "High-Rayleigh-Number Convection in a Horizontal Enclosure," J. Fluid Mech., Vol. 213, pp. 285, 1973.



14. Eckert, E. R. G., and R. M. Drake, "Analysis of Heat and Mass Transfer," pp. 731-733, McGraw-Hill, New York, 1972.
15. Somers, E. V., "Theoretical Consideration of Combined Thermal and Mass Transfer from a Vertical Flat plate," J. Apl. Mech., Vol. 23, pp. 295, 1956.
16. Wilcox, W. R., "Simultaneous Heat and Mass Transfer in Free Convection," Chem. Eng. Sci., Vol. 13, pp. 113, 1961.
17. Shah, M. M., "Estimating of Evaporation from Horizontal Surfaces," ASHRAE Trans., Vol. 87., Pt. 1, pp. 35, 1981.
18. Letter from M. A. Grolmes at Fauske & Associates, Inc. to D. Waters at Westinghouse Hanford Co., August 3, 1990.

**Appendix F. Scaling Discussion.**

May 1994

# Application of Small-Scale Evaporation Test to Full-Size Tank

---

*Multi-Function Waste Tank Facility  
Project W-236A*



Prepared by ICF Kaiser Hanford Company

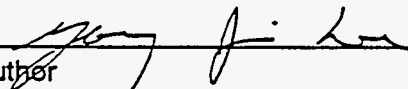
W236A-T1-TR12  
CR-9996

**KAISER ENGINEERS**  
**HANFORD**

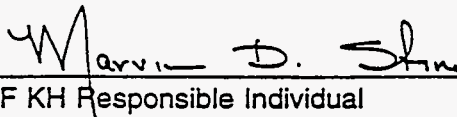
LETTER REPORT  
**Application of Small-Scale  
Evaporation Test to Full-Size Tank**

**Project W-236A**

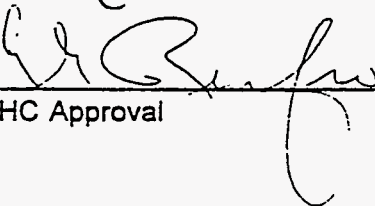
Prepared by  
**ICF Kaiser Hanford Company**  
for  
**Westinghouse Hanford Company**

  
\_\_\_\_\_  
Author

5.6.94  
Date

  
\_\_\_\_\_  
ICF KH Responsible Individual

5/6/94  
Date

  
\_\_\_\_\_  
WHC Approval

5/11/94  
Date

**CONTENTS**

1.0 Introduction ..... 1

2.0 Ra Number and Natural Convection ..... 2

3.0 Ra Number and Mass Transfer ..... 3

4.0 Ra Numbers for Test Configuration and Waste Tank ..... 5

    4.1 Characteristic Length ..... 5

    4.2 Driving Force ..... 6

    4.3 Physical Properties ..... 6

    4.4 Ra Numbers for Various Conditions ..... 7

    4.5 Mass Transfer Coefficients and Evaporation Rate ..... 7

5.0 Discussions and Conclusions ..... 8

6.0 References ..... 9

**FIGURES**

- Figure 1 Ra Number vs. Concentration Difference for Various Characteristic Lengths
- Figure 2 Ra Number vs. Temperature Difference for Various Characteristic Lengths
- Figure 3 Mass Transfer Coefficient vs. Concentration Difference
- Figure 4 Evaporation Rate vs. Mass Transfer Coefficient at 300 SCFM
- Figure 5 Evaporation Rate vs. Mass Transfer Coefficient at 1000 SCFM

# Application of Small-Scale Evaporation Test to Full-Size Tank

## 1.0 Introduction

In the current design of the MWTF tank, a large portion of the heat generated by the mixing pump and radioactive decay in the tank will be removed by the circulation of air through the primary vapor space of the tank. This circulating air will remove the heat from the waste, mainly by carrying away the vaporized water from the waste. The evaporation and removal of the water is dependent on the natural convection in the primary vapor area. Understanding the process of the evaporation and removal of the water from the waste is essential in determining the circulation rate of the air through the tank primary vapor area.

There are a number of experimental studies reported in the literature on the measurement of water evaporation into air at various conditions<sup>1,2,3</sup>. However, these data were obtained at lower water and air temperatures than the conditions expected in the MWTF waste tank. As part of the thermal/heat transfer analysis of the waste tank design, the thermal/hydraulics group at Westinghouse Hanford Company (WHC) has studied the natural convection and evaporation of the water in the primary vapor area using FIDAP, the finite element fluid dynamics code. The results are inconclusive at best. In general, the computational fluid dynamics codes are in the developmental stage for predicting the behavior of highly turbulent natural convection found in the tank primary vapor area. Therefore, experimental testing to determine the evaporation and removal rate of the water from the waste is required to ensure proper design of the cooling systems for the waste tanks. Presently, the thermal/hydraulics group at WHC is testing to determine heat removal rates by the evaporation and removal of water in the tank primary vapor area.

Since it is not practical to build a 75-foot-diameter full-size tank for this test, a 12-foot-diameter scale model tank was constructed for the test. As discussed previously, the evaporation and removal of the water from the waste will depend on the natural convection of the air in the primary vapor area. The degree of the natural convection is typically represented by the Rayleigh number ( $Ra$ ), a nondimensional parameter. The  $Ra$  number is proportional to the cube of the characteristic length of the system. The characteristic length is generally the size or diameter of the system itself. Since the size for the evaporation test is smaller than the actual tank, the  $Ra$  number for the test configuration is much smaller than that for the actual tank. In other words, the natural convection in the test configuration is less turbulent than that in the actual tank. Therefore, it is very important to understand how the test data can be related to the design of the waste tank heat removal system. This report will examine the problems, if any, in applying the small-scale evaporation test data to design the waste tank cooling system.

## 2.0 Ra Number and Natural Convection

The primary vapor region of the waste tank resembles a system enclosed by two horizontal surfaces with different temperatures, where the temperature of the bottom surface is higher than that of the top surface. In this system, the primary parameter describing the degree of the disturbance is the Ra number, as discussed previously. The Ra number is expressed as:

$$Ra = \frac{g\beta\Delta TL^3}{\nu\alpha} \quad \text{--- (1)}$$

Where, Ra — Rayleigh number  
 $\Delta T$  — Temperature difference between the bottom surface and the bulk  
 $g$  — Acceleration of gravity  
 $\beta$  — Coefficient of thermal volumetric expansion  
 $\nu$  — Kinematic viscosity  
 $\alpha$  — Thermal diffusivity  
 $L$  — Characteristic length

A similar relationship has been suggested for a system in which the fluid density is different at the bottom due to a concentration gradient as follows:

$$Ra = \frac{g\beta_m\Delta YL^3}{\nu D} \quad \text{--- (2)}$$

Where,  $\Delta Y$  — Mass fraction difference  
 $D$  — Molecular diffusivity of diffusing substance in gas mixture  
 $\beta_m$  — Concentration coefficient of volumetric expansion,  $(M_i - M)/M$   
 $M_i$  — Molecular weight of inert gas  
 $M$  — Molecular weight of diffusing gas

As shown in these equations, the Ra number represents the degree of natural convection and is a function of the driving force (density difference), a geometric constant, and physical properties. More precisely, the Ra number is proportional to the driving force and the cube of the characteristic length and is inversely proportional to the kinematic viscosity and diffusivity of

the fluid. As clearly demonstrated in this definition, higher Ra numbers will increase the disturbance in the system. Other nondimensional parameters affecting the natural convection are the Prandtl (Pr) and Schmidt (Sc) numbers, which represent the physical characteristics of the fluid. Since our system is used with an air and steam mixture, the Pr and Sc numbers are near 1.0. Only the cases with Pr and Sc numbers near 1.0 will be examined in this report.

A critical Ra number is defined as a value below which the transport of the heat is by conduction (or the transport of mass by diffusion), and the fluid is essentially motionless. Based on both theoretical analysis and experimental observation, this critical Ra for the onset of convection has a value of about 1703 and is independent of Pr or Sc numbers<sup>4</sup>. For Pr numbers less than 5, an increase in the Ra number beyond the critical value leads to a direct transition from steady two-dimensional flows to a time-dependent flow. The Ra number for this transition is an increasing function of the Pr number, ranging from below 2500 at Pr=0.01 to 20,000 at Pr=5<sup>5</sup>.

As the Ra is increased further, the flow becomes turbulent. There is no general agreement on when this transition occurs. One reference<sup>6</sup> has reported that this transition occurs at  $Ra=2 \times 10^7$  for air, while another reference<sup>5</sup> has presented that the transition occurs at  $Ra=10^4$  for a Pr number approaching unity. In other words, for the present system with the Pr number near 1, the natural circulation will be fully turbulent when the Ra number is between  $10^4$  and  $2 \times 10^7$ .

### 3.0 Ra Number and Mass Transfer

As discussed in the previous sections, the evaporation and removal of water from the waste in the tank depends on the degree of the natural convection, and the intensity of the natural convection can be expressed by the Ra number. Consequently, relationships have been developed to express the heat and mass transfer rate as a function of the Ra number. These relationships vary significantly depending on whether the natural convection is laminar or turbulent.

In the laminar region, the Nussel number (Nu) and Sherwood number (Sh), representing heat and mass transfer, respectively, become:

$$Nu = 0.54 Ra^{1/4} \quad \text{--- (3)}$$

and

$$Sh = 0.54 Ra^{1/4} \quad \text{--- (4)}$$



Where,  $Nu$  — Nussel number(=  $hL/k$ )  
 $h$  — Heat transfer coefficient  
 $k$  — Conductivity  
 $Sh$  — Sherwood number(=  $h_m L/D$ )  
 $h_m$  — Mass transfer coefficient

In the turbulent region, the relationships become:

$$Nu = 0.14 Ra^{1/3} \quad \text{--- (5)}$$

and

$$Sh = 0.14 Ra^{1/3} \quad \text{--- (6)}$$

As shown in these equations, the relationship is the same between the heat transfer phenomena and the Ra number, and between the mass transfer phenomena and the Ra number. Since our main interest in this study is the mass transfer phenomena, the discussion will be limited to the relationship between the mass transfer phenomena and the Ra number.

Introducing the definition of the Sh and Ra numbers, Equations (4) and (6) become:

$$h_m = 0.54 \left( \frac{g\beta_m \Delta Y D^3}{\nu L} \right)^{1/4} \quad \text{--- (7)}$$

for the laminar region, and

$$h_m = 0.14 \left( \frac{g\beta_m \Delta Y D^2}{\nu} \right)^{1/3} \quad \text{--- (8)}$$

for the turbulent region.

These relationships have been developed based on a large number of experiments conducted by various researchers. The constants in these equations vary somewhat depending on the experimental results, but the power relationships of 1/4 for the laminar flow and 1/3 for the turbulent flow is well accepted in this field. As shown in Equation 7, the mass transfer coefficient is inversely proportional to the 1/4 power of the characteristic length in the laminar flow regime, and is not a function of the characteristic length at all in the turbulent flow regime. In other words, the mass transfer rate between the interface and bulk phase is not influenced by the size of the equipment in the turbulent flow regime. This finding agrees well with the following explanation. In the turbulent flow regime, the natural convection will be presented by a

large number of small flow cells, which are much smaller than the test geometry and are not influenced by the test boundary. Since the mass transfer will be carried out by these flow cells, the mass transfer rate will not be a function of the equipment size.

#### 4.0 Ra Numbers for Test Configuration and Waste Tank

In the first step to compare the test configuration with the actual waste tank, the Ra numbers will be calculated for the test configuration and the actual waste tank. Before presenting the results of the calculation, it is worthwhile to discuss how each parameter affecting the Ra calculation is selected.

##### 4.1 Characteristic Length

The most significant difference between the test configuration and the waste tank will be the characteristic length representing the size. The size of the test tank will be 1/6.25 that of the waste tank. Since the Ra number is proportional to the cube of the characteristic length, as shown in Equation 1, the difference in the Ra numbers, due to the characteristic length, will be more than two orders of magnitude.

Also, there are a number of different definitions for the characteristic length. The most common definition is that the characteristic length is a dimension of the side for a square surface or 0.9 times of the diameter for a round surface<sup>6,7</sup>. On the other hand, Goldstein et. al.<sup>4</sup> and others<sup>8</sup> have used the height of the system as the characteristic length. Also, it has been suggested that the characteristic length should be defined as<sup>9</sup>:

$$\frac{1}{L} = \frac{1}{L_h} + \frac{1}{L_v}$$

Where,  $L_v$  — Vertical length  
 $L_h$  — Horizontal length

The objective of this report is not to settle the dispute on the proper definition of the characteristic length. Instead, it will show how the definition of the characteristic length will affect the use of the experimental data in the design of the waste tank. The characteristic length of the test geometry can vary from one foot (smallest height) to 10.8 feet (diameter x 0.9), while that of the actual waste tank can vary from a few feet to 67.5 feet. To maximize the effect of the characteristic length, the smallest possible characteristic length for the test configuration and the largest length for the tank are selected for this evaluation. In other words, the characteristic lengths of one foot and 67.5 feet are selected for the test configuration and the waste tank, respectively.

## 4.2 Driving Force

The Ra number is proportional to the driving force for the natural circulation, and the driving force is the difference in density between the interface and the bulk phase, caused by either the temperature or the concentration difference, or both. As shown in Equations 1 and 2, the Ra number is defined differently for the case with the temperature difference and for the case with the concentration difference. In the present system, both temperature and concentration differences will become the driving force for the natural convection. Most of the experimental and the analytical studies presented in the literature are based on only one of the differences as the driving force. A limited number of studies have been reported on natural convection caused by both differences. Somers<sup>10</sup> and Wilcox<sup>11</sup> solved the governing equations for simultaneous heat and mass transfer in laminar free convection from a vertical plate, and concluded that the effect on the natural convection due to temperature and concentration differences are additive for nearly equal Prandtl and Schmidt numbers. It is clear from these studies that both differences will enhance the degree of natural convection more than a single difference.

In this study, the Ra number will be evaluated for the wide range of concentration and temperature differences anticipated for the waste tank operations. However, the estimation of the evaporation rates for the experimental configuration and waste tank will be based solely on the concentration difference in order to be conservative in estimating the effect of the geometry. The concentration difference between the bulk and the interface will depend on the bulk phase concentration, since the interface concentration is constant. The bulk concentration will be balanced between the amount removed from the bulk phase and the amount transferred to the bulk phase from the interface. Therefore, the concentration difference becomes larger when more water vapor is removed from the bulk phase. Consequently the Ra number will be higher for the case in which a higher flow rate of air is introduced to the primary vapor area.

In the present design, the concentration difference expressed in mass fraction is expected to be 0.029 for 300 SCFM air flow at 77°F and 40% humidity inlet conditions, and 0.064 for the 1000 SCFM air flow rate. Both of these estimates are based on the empirical equation developed by Bolter, et. al.<sup>1</sup>. The FIDAP code calculates the approximate concentration difference of 0.1 at 300 SCFM inlet air flow rate. Since the empirical equation predicts lower concentration difference and a lower Ra number, only the concentration differences evaluated by the empirical equation will be considered in this study.

## 4.3 Physical Properties

Other factors affecting the Ra number are the physical properties, such as viscosity, thermal and molecular diffusivity, and density. These physical properties are not only a function of the

temperature, but are also dependent on the concentration. Since the physical properties are rather insensitive to these variables, the physical properties of air at 190°F were selected and used as constants in this study. It is expected that the Ra number calculated by these constant values of physical properties will be lower than other possible combinations of the physical property values. Therefore, the results of the analysis will be conservative.

#### 4.4 Ra Numbers for Various Conditions

The Ra numbers for the experimental configuration and waste tank were evaluated for various concentration differences, and the results are presented in Figure 1. Other parameters, including the characteristic length used in this evaluation, are selected conservatively as discussed above. The results show that natural convection in the waste tank will be turbulent for the range of the concentration difference of concern (0.01 - 0.1). The natural convection in the experimental configuration will be either laminar or turbulent, depending on whose definition we trust. In order to make this evaluation conservative, it will be assumed that the natural convection in the experimental configuration is laminar.

In Figure 1, the Ra numbers based on the maximum height (2.87 feet) of the experimental configuration and the minimum liquid-level height (13 feet) of the waste tank is presented to examine the degree of natural convection based on the selection of the characteristic length. Also, the Ra numbers calculated for various temperature differences and results are summarized in Figure 2. The magnitude of the Ra number based on the temperature differences in the range of interest (10° - 50°F) is similar to that due to concentration differences.

By examining the Ra numbers and the degree of natural convection, there may be difficulty in interpreting the data from the test to the actual waste tank design. As discussed above, we are not interested in the Ra number or the degree of natural convection. We are interested in the amount of mass transfer from the interface to the bulk phase, expressed as the mass transfer coefficient.

#### 4.5 Mass Transfer Coefficients and Evaporation Rate

Figure 3 shows the plot of the mass transfer coefficients as a function of concentration differences for the test configuration and the waste tank. For the test configuration, it is assumed that the characteristic length is one foot and the natural convection is laminar. As shown in this Figure, the mass transfer coefficient varies less than 15% between the experimental configuration and actual waste tank geometry for the concentration difference ranging from 0.01 to 0.1. This range of concentration differences will envelop the conditions created by the inlet air flow rate of 300 to 1000 SCFM. In particular, the error is expected to be 5% for the 300 SCFM flow

rate and 2% for the 1000 SCFM flow rate. It is important to note that the mass transfer coefficient at a laminar flow condition (test configuration) is higher than that at a turbulent flow condition for lower concentration differences according to Figure 3. This indicates that the present correlation to calculate the mass transfer coefficient from the Ra number needs further improvement. The mass transfer coefficient is strongly dependent on the concentration difference but is almost independent of the characteristic length for characteristic length larger than one foot.

The objective of this test is not to evaluate the mass transfer coefficient, but to determine the evaporation rate from the waste surface. The mass transfer coefficients can be converted into the evaporation rate by the following equation:

$$W_w = h_m \rho \left( C_i - \frac{W_w S + W_{wi}}{W_a + W_w S + W_{wi}} \right) \quad (10)$$

- Where,
- $W_w$  — Evaporation rate (lb/ft<sup>2</sup> hr)
  - $W_{wi}$  — Inlet water vapor flow rate (lb/hr)
  - $W_a$  — Air flow rate (lb/hr)
  - $\rho$  — Density
  - $C_i$  — Mass fraction at interface
  - $S$  — Waste surface area (ft<sup>2</sup>)

The evaporation rates corresponding to the various mass transfer coefficients are shown in Figures 4 and 5 for 300 and 1000 SCFM inlet air flow rates, respectively. Based on these Figures, the evaporation rate increases 22% for the 300 SCFM case and 57% for 1000 SCFM case, while the mass transfer coefficients increased by a factor of three from 20 to 60. This suggests that the error in mass transfer coefficients will be reduced to at least 80% when the mass transfer coefficient is converted to the evaporation rate. Therefore, the evaporation rate difference between the test configuration and the waste tank will be less than 3%, due to their size difference.

## 5.0 Discussions and Conclusions

The possible error induced by extending the experimental measurement of the evaporation rate from the small-sized test tank to the waste tank has been examined. The results indicate that the error will be less than 3%, even with the worst possible assumptions. These conservative assumptions include:

- Smallest characteristic length
- One driving force
- Conservative physical properties

It can be safely concluded that the evaporation data obtained from the test is directly applicable to the design of the waste tank cooling system.

One item of minor concern in this test is the difference in inlet air residence time. The volume of the vapor space in the test is  $(1/6.25)^3$  of that in the actual waste tank, but the interface area of the solution in the test is  $(1/6.25)^2$  of that in the waste tank. Since the flow rate of inlet air is proportional to the interface area, the residence time of the air in the test will be 1/6.25 of that in the waste tank. However, this residence time difference will not affect the evaporation rate as long as the inlet air does not disturb the interface and the air in the vapor space is well mixed. It is recommended, if readily achievable, that the inlet and outlet configuration be properly designed to achieve full mixing in the vapor space without disturbing the interface.

## 6.0 References

1. L. M. K. Boelter, et. al., *Free Evaporation into Air of Water from a Horizontal Quiet Surface*, Ind. and Eng. Chem., Vol. 38, pp. 596, 1946.
2. M. T. Pauker, et. al., *A Novel Method for Measuring Water Evaporation into Still Air*, ASHRAE Transactions, Vol. 99, Pt.1, pp. 297, 1993.
3. M. M. Shah, *Estimating of Evaporation from Horizontal Surfaces*, ASHRAE Transactions, Vol. 87, Pt. 1, 1981.
4. R. J. Goldstein et. al., *High-Rayleigh-Number Convection in a Horizontal Enclosure*, J. Fluid Mech. Vol. 213, pp. 111, 1990.
5. R. Krishnamurti, *Some Further Studies on the Transition to Turbulent Convection*, J. Fluid Mech., Vol. 60, pp. 285, 1973.
6. W. H. McAdams, *Heat Transmission*, 3rd Ed., pp. 180, McGraw-Hill, 1954..
7. F. Kreith, *Principles of Heat Transfer*, 2nd Ed., pp. 340, International Text Book, 1966.
8. K. C. Cheng and T. Kimura, *Observation of Convective Instability Phenomena in Slightly Inclined Air Layers Heated from Below: Effect of Air Layer Thickness*, HTD-Vol. 178, ASME, 1991.
9. M. Jacobs, *Heat Transfer, Vol. 1*, 8th Ed., pp. 532, Jonh Wiley & Sons, 1962.

10. E. V. Somers, *Theoretical Considerations of Combined Thermal and Mass Transfer from a Vertical Flat Plate*, J. Appl. Mech., Vol. 23, pp. 295, 1956.
11. W. R. Wilcox, *Simultaneous Heat and Mass Transfer in Free Convection*, Chem. Eng. Sci., Vol 13, pp. 113, 1961.

Figure 1. Ra Number vs. Concentration Difference for Various Characteristic Lengths

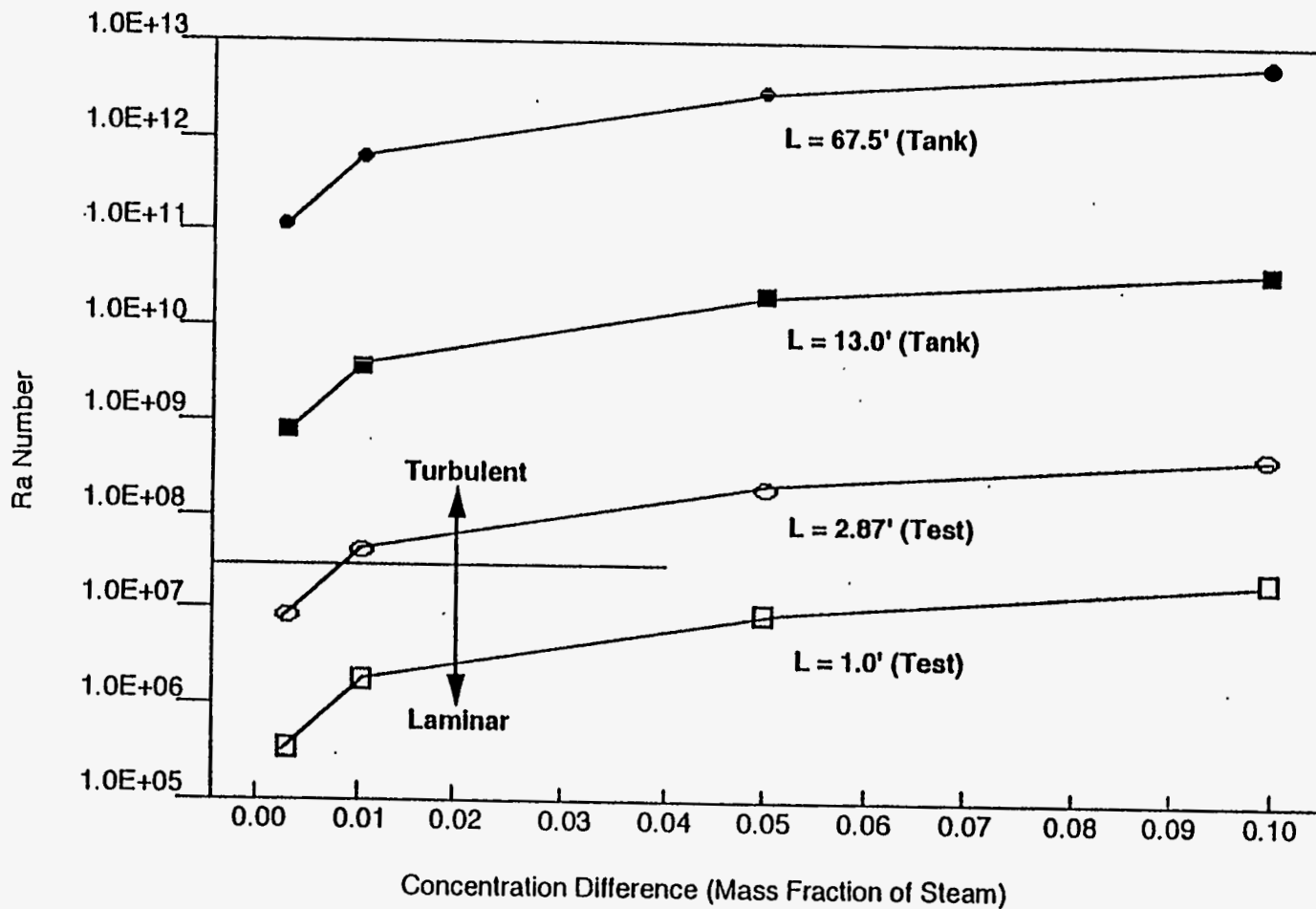




Figure 2. Ra Number vs. Temperature Difference for Various Characteristic Lengths

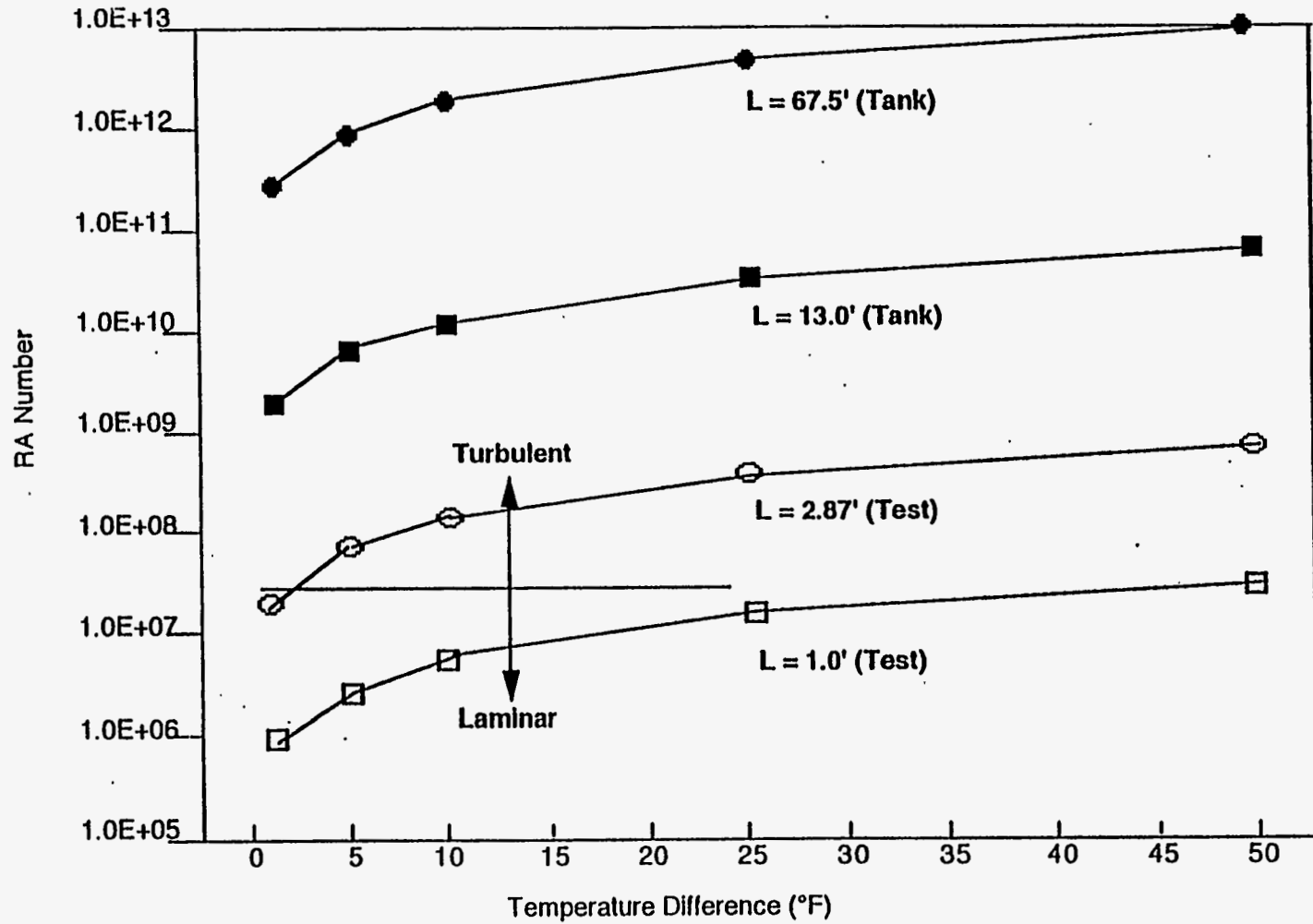


Figure 3. Mass Transfer Coefficient vs. Concentration Difference

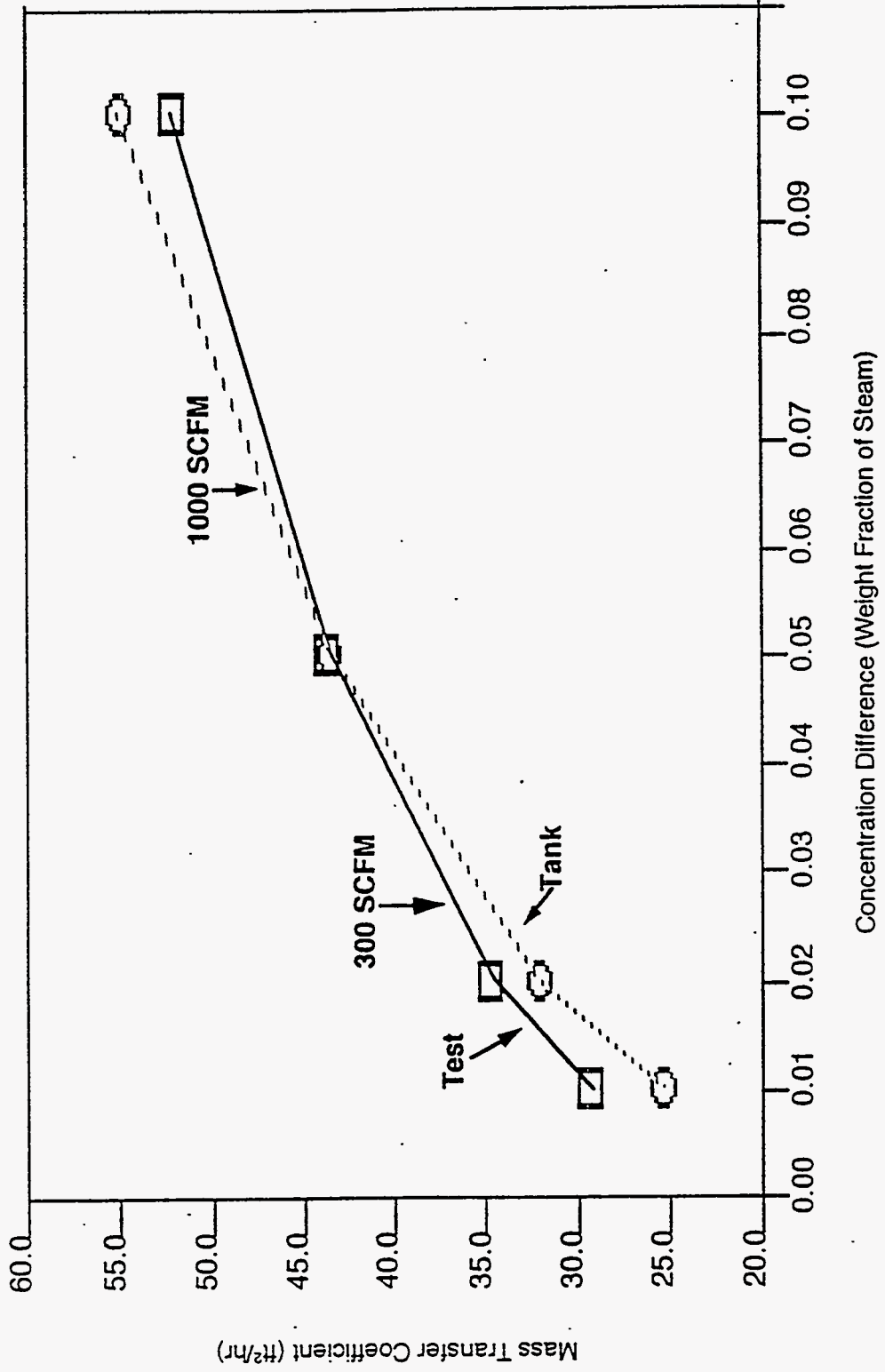


Figure 4. Evaporation Rate vs. Mass Transfer Coefficient at 300 SCFM

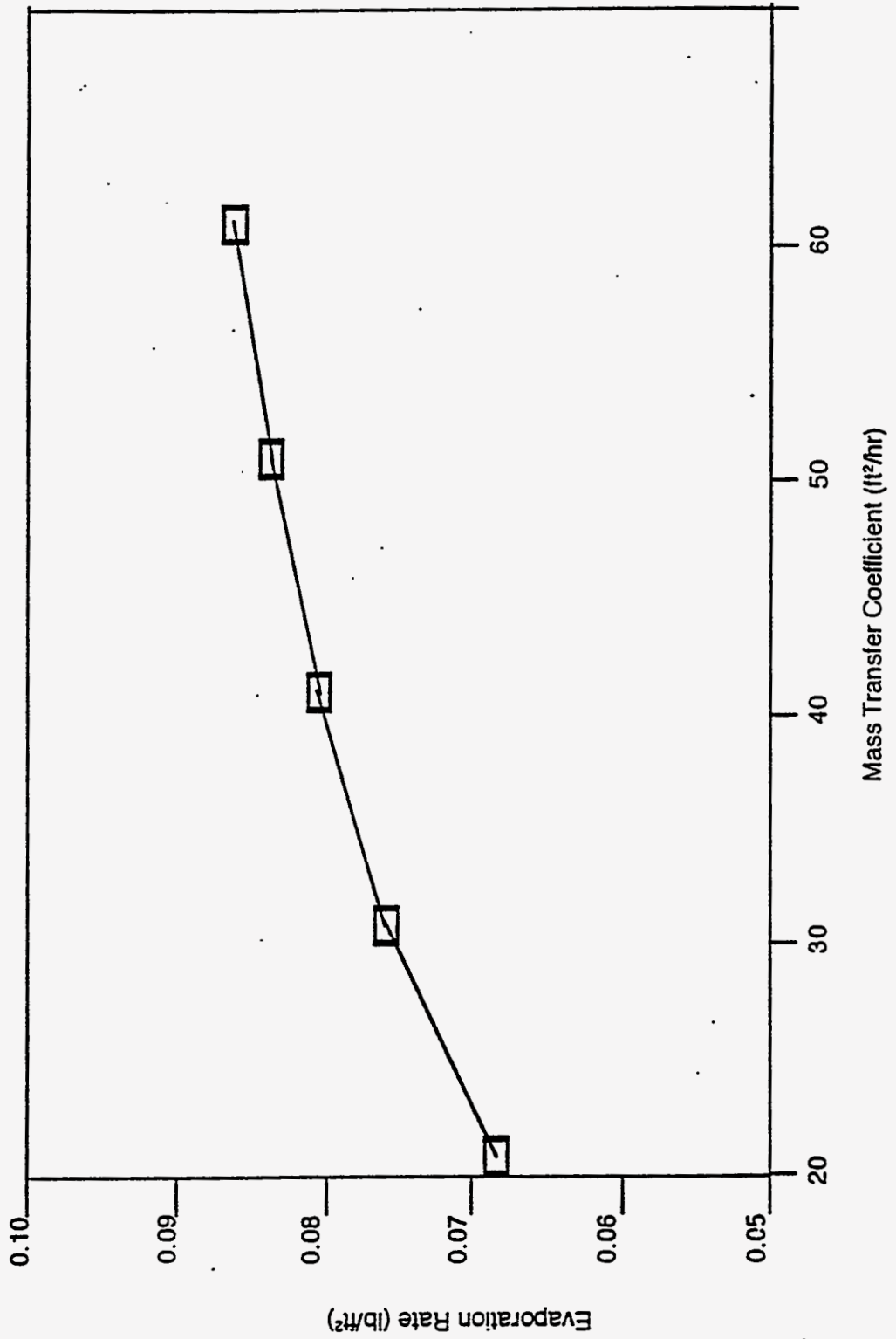


Figure 5. Evaporation Rate vs. Mass Transfer Coefficient at 1000 SCFM

